

University of South Bohemia in České Budějovice
Faculty of Science

**PHOTOTROPHIC MICROORGANISMS
IN EXTREME ENVIRONMENTS**

Ph.D. Thesis

Hana Medová

supervisor: Mgr. Michal Koblížek, Ph.D.

Institute of Microbiology CAS, Třeboň

scientific advisor: Doc. Libor Pechar, CSc.

University of South Bohemia. České Budějovice

Třeboň, Czech Republic 2013

This thesis should be cited as:

Medová H, 2013: Phototrophic microorganisms in extreme environments. Ph.D. Thesis Series, No. 1. University of South Bohemia, Faculty of Science, České Budějovice, Czech Republic, 123 pp.

Annotation

This thesis focuses on photosynthetic prokaryotes living in extreme saline, thermal, or acidic conditions. Their distribution and physiology was assessed by a range of physical and chemical techniques such as kinetic fluorometry, epifluorescence and light microscopy, emission spectroscopy, or high performance liquid chromatography.

Chapter 1 provides a brief overview of phototrophic organisms inhabiting various extreme environments and serves as a general introduction. Chapter 2 provides a field study of phototrophic communities inhabiting saline and soda lakes in the Great Steppe region. A small survey of bacterial phototrophic community in freshwater polar lakes on Svalbard (Spitsbergen) and James Ross Island, Antarctica is presented in Chapter 3. Further, a laboratory based study focusing on thermal stability of the anoxygenic reaction centers is presented in Chapter 4. The last Chapter 5 describes experiments studying the response of planktonic cyanobacteria to acidic post-mining waters.

Declaration (in Czech)

Prohlašuji, že svoji disertační práci jsem vypracoval/a samostatně pouze s použitím pramenů a literatury uvedených v seznamu citované literatury. Prohlašuji, že v souladu s § 47b zákona č. 111/1998 Sb. v platném znění souhlasím se zveřejněním své disertační práce, a to elektronickou cestou ve veřejně přístupné části databáze STAG provozované Jihočeskou univerzitou v Českých Budějovicích na jejích internetových stránkách, a to se zachováním mého autorského práva k odevzdanému textu této kvalifikační práce. Souhlasím dále s tím, aby toutéž elektronickou cestou byly v souladu s uvedeným ustanovením zákona č. 111/1998 Sb. zveřejněny posudky školitele a oponentů práce i záznam o průběhu a výsledku obhajoby kvalifikační práce. Rovněž souhlasím s porovnáním textu mé kvalifikační práce s databází kvalifikačních prací Theses.cz provozovanou Národním registrem vysokoškolských kvalifikačních prací a systémem na odhalování plagiátů.

V Třeboni dne 21.3. 2013

.....
Hana Medová

This thesis originated from a partnership of the Faculty of Science, the University of South Bohemia, and the Institute of Microbiology CAS, Třeboň, supporting doctoral studies in the biophysics study programme.



Přírodovědecká
fakulta
Faculty
of Science



Financial support

Grant Agency of CR No. P501/10/0221

Bilateral Czech-Russian Academy of Science exchange program No. 22

Research concepts of the Institute of Physical Biology, South Bohemia University No.
MSM6007665808

Research concept of the Institute of Microbiology ASCR No. AV0Z50200510

Project 'Czech Polar' of the Ministry of Education, Sports and Youth of CR
No. LM2010009

Grant Agency of ASCR No. IAA608170901

Project 'Algatech' of the Research, Development and Innovation program of the
Ministry of Education, Sports and Youth of CR No. CZ.1.05/2.1.00/03.0110

Research program of the Ministry of Education, Youth and Sport of CR No. 2B08006

Research, Development and Innovation program of the Ministry of Agriculture of CR
No. Qh82078

Acknowledgment (in Czech)

Ráda bych vyjádřila své poděkování všem lidem, kteří mě podporovali a provázeli po celou dobu mého studia. Mé nekonečné díky patří školiteli Michalu Koblížkovi, jenž mi umožnil studovat a pobývat v Třeboni. Vážím si jeho trpělivosti, přísnosti i vlídnosti. Cením si jeho rad, postřehů a doporučení, která se vždy ukázala jako přínosná a pravdivá. Skládám hold Ondřeji Prášilovi za vtisknutí přátelské, otevřené a podnětné atmosféry celému areálu Opatovického mlýna. Děkuji svým kolegům (Zuzce Bláhové, Jasonu Deanovi, Evě Kolářů) za veškeré jejich laskavé rady i pomoc, byli mi podporou, hromosvodem i vrbou. Ráda bych vyjádřila svůj vděk kolektivu laboratoře ENKI (Janě Šulcové, Lence Kröpfelové, Evě Chmelové, Zdeňce Benedové, Liborovi Pecharovi, Ivu Přikrylovi, Mirku Kosíkovi) za načerpání cenných a zajímavých zkušeností z treboňského i sokolovského terénu.

Děkuji svým rodičům za nekonečnou starost, lásku a pochopení a v neposlední řadě za pomoc s opatrováním mých dvou miláčků. Vážím si laskavosti Mišky Knížové, Helči Handrkové, Zuzičky Schwabové, Ondry Palkovského, Petry Hesslerové, Venduly Křinické, kteří mě slovy i beze slov dávali sílu vytrvat v mém treboňském studentském životě.

List of publications relevant to the thesis

Prášil O, Bína D, Medová H, Řeháková K, Zapomělová E, Veselá J, Oren A (2009) Emission spectroscopy and kinetic fluorometry studies of phototrophic microbial communities along a salinity gradient in solar saltern evaporation ponds of Eilat, Israel. *Aquat Microbial Ecology*, 56: 285-296

HM conducted kinetic fluorometry measurements and analyzed pigment composition of phototrophic community by HPLC, processed the data and revised the manuscript.

Řeháková K, Zapomělová E, Prášil O, Veselá J, Medová H, Oren A (2009) Composition changes of phototrophic microbial communities along the salinity gradient in the solar saltern evaporation ponds of Eilat, Israel. *Hydrobiologia*, 636: 77-88

HM conducted kinetic fluorometry measurements and analyzed pigment composition of phototrophic community by HPLC and analyzed recorded data.

Medová H, Boldareva EN, Hrouzek P, Borzenko SV, Namsaraev ZB, Gorlenko VM, Namsaraev BB, Koblížek M (2011) High abundance of aerobic anoxygenic phototrophs in saline steppe lakes. *FEMS Microbiol Ecol.*, 76: 393-400

HM performed epifluorescence microscopy and HPLC analyses of collected samples, processed the data and wrote the manuscript.

Medová H, Kaftan D, Koblížek M. Structural basis of thermostability in purple bacterial reaction centers. *in preparation*

HM cultivated the studied bacterial strains, performed fluorometric measurements, processed, and analyzed the data, and wrote the manuscript.

Medová H, Příkryl I, Zapomělová E, Pechar L (2013) Effect of post-mining waters on cyanobacterial photosynthesis. *Water Environ Res*, submitted

HM sampled the studied localities, conducted all the field and laboratory measurements, processed and analysed the fluorometric data and wrote the manuscript.

.

List of abbreviations

AAPs	aerobic anoxygenic phototrophs
AMD	acid mine drainage
APB	anoxygenic phototrophic bacteria
BChl	bacteriochlorophyll
Chl	chlorophyll
$rETR$	relative electron transport rate
FETR	forward electron transport rate
F_V/F_M	maximum photochemical yield
LH1	light-harvesting complex 1 (inner antenna)
LH2	light harvesting complex 2 (outer antenna)
PCA	principal canonical analysis
pH_{opt}	optimal growth pH value
RC	reaction center
RDA	redundancy analysis
RMSD	root mean square deviation
t_{opt}	optimal growth temperature

Content

1. Introduction to Extremophily	1
1.1 Phototrophic organisms	1
1.2 Definition of extremes and extremophiles	3
1.3 Main extremophilic groups	5
1.4 References	15
2. Anoxygenic Bacteria in Saline and Soda Lakes	21
2.1 Summary	21
2.1 Introduction	22
2.2 Methods	24
2.3 Results	28
2.4 Discussion	33
2.5 References	37
2.6 Supplements	42
3. Anoxygenic Phototrophic Bacteria in Polar Regions	45
3.1 Summary	45
3.2 Introduction	45
3.3 Methods	46
3.4 Results and discussion	52
3.5 Conclusions	56
3.6 References	57
4. Thermostability of Anoxygenic Reaction Centers	59
4.1 Summary	59
4.2 Introduction	60
4.3 Methods	62
4.4 Results	68
4.5 Discussion	75
4.6 References	79
4.7 Supplements	84
5. Effect of Post-mining Waters on Cyanobacterial Photosynthesis	93
5.1 Summary	93
5.2 Introduction	94
5.3 Material & Methods	96
5.4 Results	102
5.5 Discussion	110
5.6 References	113
5.7 Supplements	117
6. Thesis Summary	121
Curriculum vitae	122

1. Introduction to Extremophily

1.1 Phototrophic organisms

Phototrophic organisms use photosynthesis to convert light energy into chemical energy. Two fundamentally different forms of photosynthesis have been described in phototrophs: oxygenic photosynthesis (i.e. photosynthesis producing oxygen) and anoxygenic photosynthesis (i.e. not producing oxygen). Oxygenic photosynthetic organisms produce oxygen and generate an electrochemical gradient of protons and reducing equivalents in the form of NADPH for CO₂-fixation. Oxygenic photosynthesis is present in all photosynthetic eukaryotes (plants and algae) and in the prokaryotic cyanobacteria and Prochlorophyta. The only product of anoxygenic photosynthesis is the formation of an electrochemical gradient of protons across the photosynthetic membrane which may be used for ATP synthesis. Anoxygenic photosynthesis is restricted to five main phyla: Proteobacteria (purple phototrophic bacteria), Chlorobi (green sulfur bacteria), Chloroflexi (green nonsulfur bacteria), Heliobacteria and Acidobacteria (Blankenship 2010, Figure 1.1).

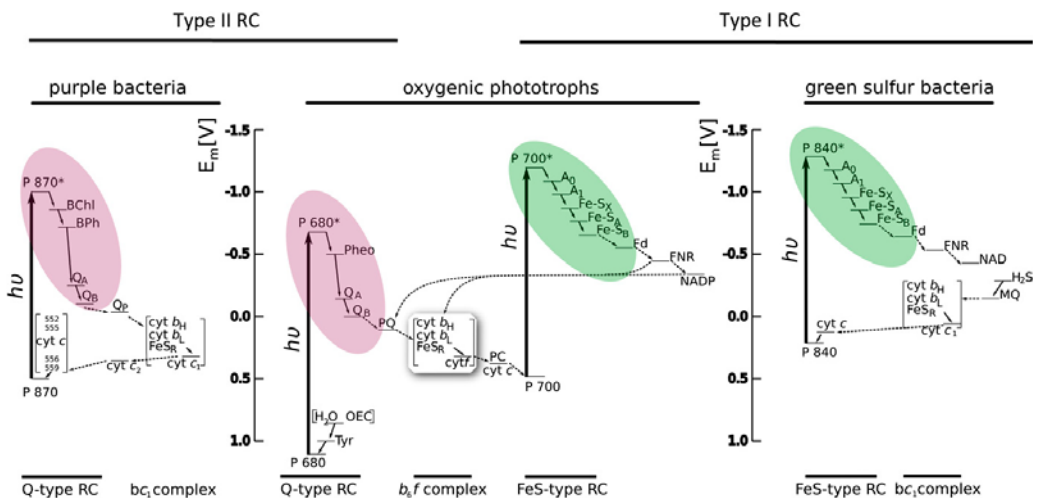


Figure 1.1 The diagram of electron transport in the reaction centers of type I (green coloured) and type II (purple coloured) found in photosynthetic organisms (adapted from Blankenship 2010).

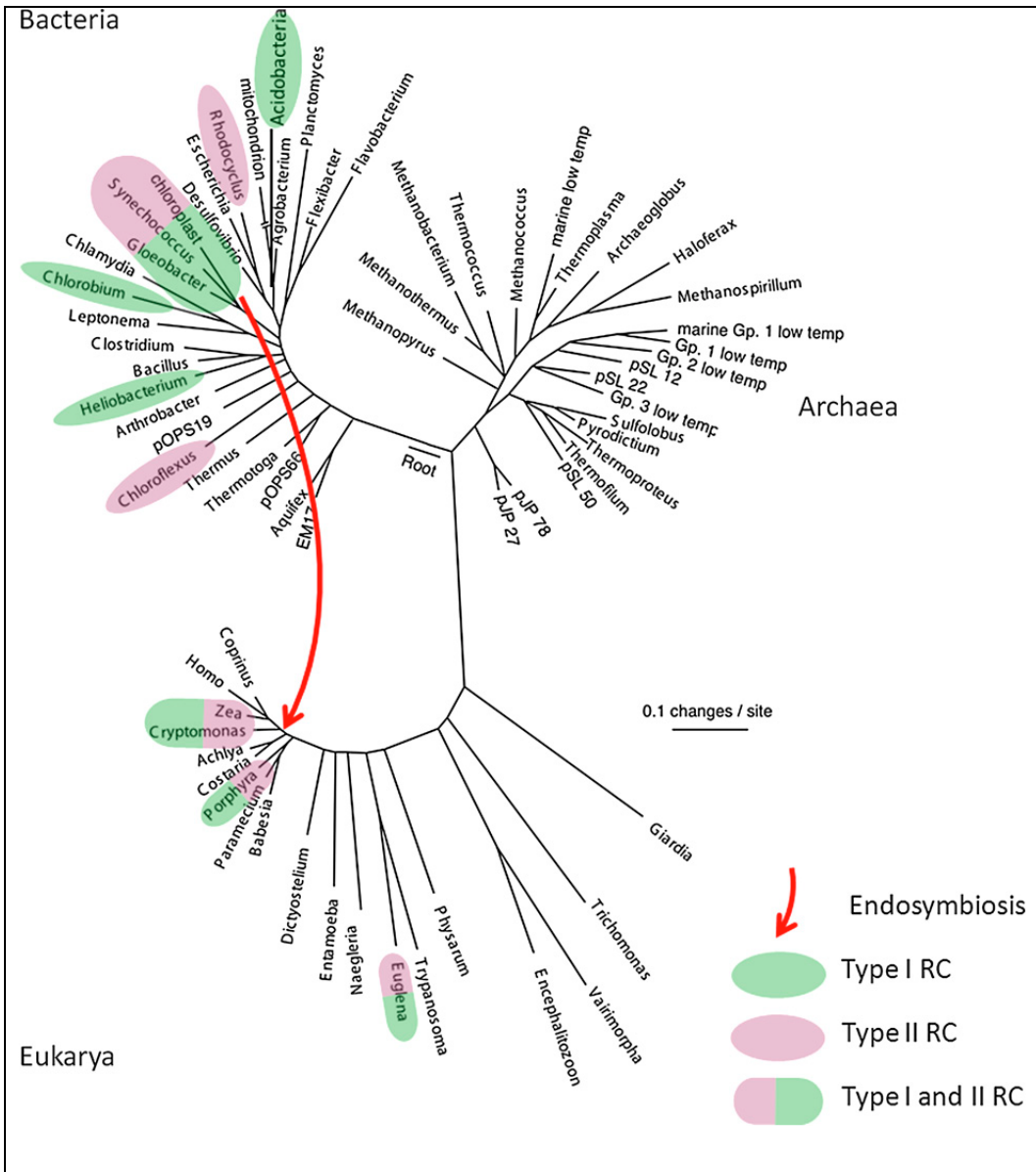


Figure 1.2 Universal phylogenetic tree based on SSU rRNA sequences (adapted from Blankenship 2010) showing the presence of reaction centers type I and II among phototrophic organisms.

The conversion of light energy is performed in pigment-protein complexes called reaction centers. The main photosynthetic pigment in oxygenic organisms, cyanobacteria, algae and higher plants, is chlorophyll *a* (Chl *a*). Anoxygenic

phototrophic organisms use various forms of bacteriochlorophylls (BChl). The mechanism of light-energy transduction in reaction centers follows the same principle in higher plants and algae, as in cyanobacteria and phototrophic bacteria (Björn and Govindjee 2009). Two types of reaction centers (RCs) have been detected in green algae and photosynthetic bacteria (Lengeler et al. 1999). The reaction centers of type I are present in green sulfur bacteria (Chlorobi), heliobacteria (firmicutes), cyanobacteria, algae and higher plants, the RC type II (in green algae and plants called photosystem II) in purple sulfur and purple non-sulfur bacteria (Proteobacteria), filamentous anoxygenic bacteria (green nonsulfur bacteria, Chloroflexi), cyanobacteria and eukaryotes (Blankenship 2010, Figure 1.2).

Photosynthesis has evolved to function in a broad range of environmental conditions. Extremophilic phototrophs have an important ecological function as primary producers and nitrogen-fixers in unfavorable habitats. For example, the phototrophic activity of *Thermochromatium tepidum* provides nutrients for the food chain of chemotrophic prokaryotes living together in microbial mats in Yellowstone hot springs (Madigan 2003). In soda lakes, the anoxygenic phototrophs are a major portion responsible for primary productivity where the bloom of haloalkaliphilic purple bacteria creates dense microbial mats (Jones et al. 1998). Extremophilic phototrophs represent new genetic resources for understanding the mechanisms of photosynthesis under extreme conditions (Madigan 2003).

1.2 Definition of extremes and extremophiles

Extremophiles are organisms that have adapted to grow optimally at or near extreme conditions (Hirokoshi 2011). Extremes¹ include physical (temperature, radiation or pressure), geochemical (desiccation, salinity, pH, oxygen species or redox potential), and chemical extremes (Rothschid and Machinelli 2001). On the other hand, ‘normal’ conditions are considered to be a pH of 5 – 8.5, temperature range 4 – 40°C, and salinity from freshwater to marine environment (0 – 3.5 g L⁻¹, Seckbach and Oren 2007).

¹ from *extremus* (lat.) superlative of *exter* = being outside

The typical understanding of the term “extreme environment” as an “objectively extreme” but stable environment (Elster 1999). This concept is usually followed with further categorization of extremophiles. Unstable ecosystems varying seasonally and diurnally in their conditions may represent another type of more energetically demanding and harsh extreme environment.

The word “extremophiles” for organisms inhabiting extreme environments was first used by MacElroy in 1974 in a paper “Some comments on the evolution of extremophiles”. A much larger collection of species is known tolerate extreme habitats, but grow poorly in them. These are called extremotrophs. An extremophile usually adapts to a plethora of unusual factors. In this case, a polyextremophile refers to an organism which has adapted to at least three extreme conditions.

In describing extremophilic and extremotrophic organisms, care must be taken to discriminate between the mere presence of an organism (or its phylogenetic signature) and those growing and being metabolically active in an extreme environment (Madigan 2003).

Most of the world’s main ecosystems - arid areas, oligotrophic regions, endorheic basins with highly saline lakes, the deep ocean - include potential extreme habitats which have evolved as a result of natural geological processes (Horikoshi 2011). The extreme thermal habitats are often associated with plate tectonic activity which gives rise to volcanoes, geothermal springs, and marine geothermal vent systems.

The extremophilic adaptations are assumed to have arisen in different periods of the geochemical-geophysical evolution of Earth. Assuming a thermophilic origin of life (Blankenship 2002, Nisbet and Sleep 2001), acidophily probably arose at an early stage, while alkaliphily could have evolved after certain mineral precipitated and a sufficient buffer concentration of CO₂ was established in the atmosphere (Horikoshi 2011). Alkalinity in nature may be the result of the local geology and climate, of industrial processes, or promoted by biological activities. The most stable alkaline environments on earth are the soda lakes and soda deserts distributed throughout the world. Halophily could have developed only after an arid climate was imposed on land and psychrophily only after a major temperature fall. Salinity was the major

determinant of microbial communities rather than extreme temperature, pH or other environmental factors. Because many modern extreme environments likely resemble habitats present on the early Earth, extremophilic species are particularly relevant models for the study of the evolution of photosynthetic systems (Madigan 2003).

New extreme ecosystems continue to be discovered. Nowadays, the greatest contributions to the current state of knowledge are expected from the investigations of the subsurface biosphere that exists in sub-floor sediments and in subterranean rock formations and deep-ocean hydrothermal volcanoes on the seafloor (Yurkov et al. 1999, Rathgeber et al. 2008).

1.3 Main extremophilic groups

The categorization of extremophiles is mainly based on one selected environmental parameter which is considering as being ‘extreme’ (Table 1.1).

1.3.1 Thermophiles

Thermophilic organisms have been described within all three domains of life Eukaryota, Bacteria, and Archea. The most thermophilic organisms are found among the domain Archea growing at temperatures above 80°C. The most extreme t_{opt} known to date is 113°C for the nitrate-reducing chemolithoautotroph *Pyrolobus fumarii* (Crenarchaeota; Horikoshi 2011). Among other groups, the upper growth limit for bacteria (95°C) contrasts with the upper limit for protists (62°C), multi-cellular eukaryotes (50°C), vascular plants (48°C), or fish (40°C).

The upper thermal limit for oxygenic photosynthesis is considered to be the upper growth temperature of *Synechococcus cf. lividus* (74°C) (Ward and Castenholz 2000, Madigan and Jung 2009). Chlorophyll molecules degrade above 75°C, excluding oxygenic photosynthesis above that temperature (Rothschild and Machinelli 2001). Anoxygenic photosynthesis has been proved to function up to a temperature of 70°C which is the upper growth limit of the green non-sulfur bacterium *Chloroflexus aurantiacus* (Madigan 2003).

Table 1.1 List of different groups of organisms relevant to their preferred living conditions (after Horikoshi 2011, modified). ¹⁾Wiegel 2011; ²⁾de la Haba et al.; 2011 ³⁾Helmke and Weyland 2004; ⁴⁾Antrakinian et al. 2005.

category of extremophiles	definition
acidophile	organism with a $\text{pH}_{\text{opt}} \leq 3 - 4$
alkalitolerant	growth at $\text{pH} < 9$ facultative alkaliphile: minimum $\text{pH} < 7.5$, maximum $\text{pH} \geq 10$, optimum > 8.5 obligative alkaliphile: minimum $\text{pH} \geq 7.5$, maximum $\text{pH} \geq 10$, optimum > 8.5
alkaliphile	growth at $\text{pH} \geq 8^1$
hyperalkaliphile	growth at $\text{pH} > 11$
halophile	requiring NaCl solution for growth slight halophiles ²⁾ requiring salinity of $12 - 30 \text{ g L}^{-1}$ moderate halophiles requiring salinity of $30 - 150 \text{ g L}^{-1}$ extreme halophiles requiring salinity of $> 150 \text{ g L}^{-1}$
metalotolerant	tolerating high levels of heavy metal ions such as Zn^{2+} , Co^{2+} , Cd^{2+} , As^{2+}
oligotroph	capable of growth in nutritionally depleted habitats
piezophile	optimally at hydrostatic pressures of $\geq 40 \text{ MPa}$
psychrophile	growth optimum of $\leq 10^\circ\text{C}$, maximum 20°C mild / moderate psychrophile ³⁾ : minimum $\leq 0^\circ\text{C}$, maximum $\leq 25^\circ\text{C}$,
thermophile	lives at elevated temperatures mild / moderate thermophile ⁴⁾ : optimum $50 - 60^\circ\text{C}$ extreme thermophile: optimum $60 - 80^\circ\text{C}$ hyperthermophile: optimum of $\leq 80^\circ\text{C}$
toxitolerant	withstand high levels of damaging agents, such as organic solvents
xerophile	growth at low water activity and resistant to high desiccation

The temperatures above the physiological limit of an organism denature proteins and nucleic acids, and increase the fluidity of membranes to lethal levels (Rothschild and Machinelli 2001). In thermophiles, proteins evolved to be less flexible at room temperatures by forming higher-order oligomers and decreasing surface area. Their electrostatic and hydrophobic interactions were optimized to increase internal hydrophobicity and helix propensity of α -helixes residues (Rothschild 2001). The solubility of gasses in water decreases with increasing temperature, resulting in lower availability of dissolved O_2 or CO_2 for aquatic organisms at high temperatures.

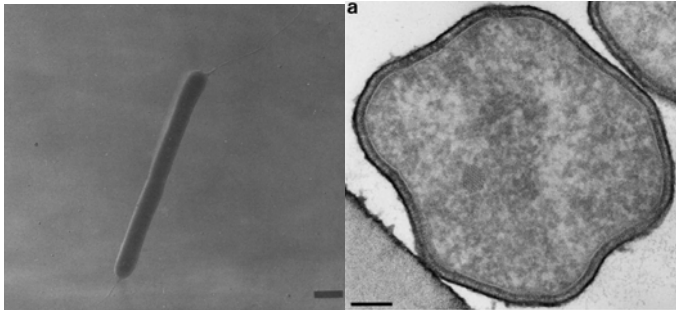


Figure 1.3
Electron micrographs of ultrathin sections of cells *Pyrolobus fumarii* (left) (bar = 200 nm, adapted from Blöchl et al. 1997).

Electron micrograph of *Thermus aquaticus* (right) (bar = 1 μ m, adapted from Brock and Freeze 1969).

Thermophilic anoxygenic phototrophic bacteria and cyanobacteria

Many recent anoxygenic bacteria evolved extremotolerance or extremophily to maximally enhance their fitness under suboptimal conditions. The green-nonsulfur bacterium *Chloroflexus aurantiacus* (family Chloroflexaceae) was the first thermophilic anoxygenic phototroph to be isolated (Madigan 2003). Its optimal growth temperature reaches up to 70°C. *Chloroflexus* possesses type II-RC which in contrast to the RC in purple bacteria lacks H protein subunit (Tang et al. 2011).

Chlorobium tepidum is a mildly thermophilic ($t_{\text{opt}} \sim 48^\circ\text{C}$) green sulfur bacterium (family Chlorobiaceae). This organism is capable of nitrogen fixation. It contains BChl *c* and uses thiosulfate as an electron donor. Strains of this organism have been isolated from relatively high sulfide (0.5 – 1 mM), acidic (pH 4 – 6) hot springs in New Zealand and Yellowstone National Park (Madigan 2003). *Heliobacterium modesticaldum* isolated from a hot spring in Yellowstone is the only known thermophilic species of Heliobacteria with $t_{\text{opt}} 52^\circ\text{C}$. It is capable of fixing nitrogen. Among Acidobacteria, one thermophilic photoheterotrophic bacterium *Candidatus Chloracidobacterium thermophilum* has been isolated from Yellowstone hot springs (Bryant et al. 2007). It synthesizes BChl *a* and BChl *c* under oxic conditions and possesses a type I RC.

Interestingly, purple bacteria lack truly thermophilic strains. In the 1980s, a mildly thermophilic bacterium named *Thermochromatium tepidum* was isolated. It grows up to 58°C, which is the highest observed temperature for purple sulfur bacteria ($t_{\text{opt}} 48 – 50^\circ\text{C}$, Nogi et al. 2000). *Thermochromatium* contains a novel LH1 which absorbs light in the infra-red region at 920 nm and transfers energy efficiently from the core

antenna to the reaction centre. Its RC is similar to that of other purple bacteria except that it has enhanced thermostability. Similarly, its RubisCO is stable up to 60°C (Madigan 2003).

Some mildly thermophilic purple nonsulfur bacteria ($t_{\text{opt}} \sim 40^\circ\text{C}$) have been isolated from hot spring microbial mats (e.g. *Rhodopseudomonas* sp. strain GI, *Rhodopseudomonas cryptolactis*, *Rhodospirillum centenum*) (Madigan and Jung 2009). Thermotolerant behaviour was observed for the mesophilic strains of *Rhodopseudomonas palustris*, *Blastochloris* (*Rhodopseudomonas*) *viridis* and *Rhodomicrobium vannielli*. They were detected in thermal springs with temperatures of 47°C. After cultivation in the laboratory, they show a typical mesophilic optimum 30 – 35°C (Castenholz and Pierson 1995). *Rhodospirillum centenum* found in thermal waters of 55°C, produces cysts tolerant to high heat and desiccation, which may explain its recovery under laboratory conditions.

The first freshwater thermotolerant species were isolated from Russian hot springs in 1990 (Yurkov and Beatty 1998). The sources were springs located in the Bol'shoi River Valley, Siberia, and the Neskuchninskii Spring on Southern Kuril Islands. The cyanobacterial mats of the thermal springs had a pH value of 8.0 – 9.4 and contained up to 10^6 cells of aerobic anoxygenic bacteria (AAPs). Despite the fact that the AAP strains were isolated from an environment of 40 or 54°C, in the laboratory they displayed mesophilic characteristics.

So far the only moderate thermophilic AAP species is *Porphyrobacter tepidarium* ($t_{\text{opt}} 40 - 48^\circ\text{C}$), which was isolated from Usami hot spring (Japan) which has a temperature of 42.5°C and a pH of 5.6 (Hanada et al. 1997).

The existence of thermophilic cyanobacteria was first documented in hot springs in Yellowstone National Park, Wyoming, USA (Seckbach and Oren 2007) and later in other geothermal areas around the world. The unicellular members of the genus *Synechococcus* (*Thermosynechococcus*) occurring at the temperatures of 73 – 74°C are the most thermophilic. Filamentous cyanobacteria (a.o. *Mastidogladus laminosus*, *Phormidium* and *Oscillatoria* species) are less thermotolerant; their upper temperature limit for growth is between 55 – 62°C.

1.3.2 Psychrophiles

Almost 80% of the Earth's biosphere is permanently below 5°C, giving the psychrophilic organisms an opportunity to proliferate (Antranikian et al. 2005). Active photosynthetic communities are found in and on ice, covering 10% of the Earth's surface in the form of sea ice, caps, sheets, glaciers, snowfields, and permafrost; in polar freshwater and saline lakes and streams; below and in rocks; in high-altitude mountain regions, and in the Arctic and Antarctic Oceans. Representatives of all main taxa were found to inhabit temperatures below 0°C (Rothschild and Matchinelli 2001). The lowest recorded temperature for active microbial communities is -18°C (Horikoshi 2011). Many microbes and cells can be preserved successfully at -196°C. However, not all organisms growing at low temperatures are psychrophiles. True psychrophilic organisms grow optimally below 10°C and do not survive temperatures above 20°C (Horikoshi 2011).

At low temperatures, water freezes and ice crystals can rip cell membranes. If the organism does not possess the capability of synthesizing cryoprotectants, the freezing of intracellular water is almost invariably lethal (Rothschild and Machinelli 2001). Psychrophilic cells must adjust the composition of their membrane lipids to maintain optimal membrane fluidity. A cold-adapted enzyme must have a higher specific activity and a high degree of conformational complementarity with its substrate than that of their mesophilic counterparts to decrease activation energy at low temperatures (Antranikian et al. 2005).

Psychrophilic photosynthetic organisms

Low temperatures appear to cause no apparent problems for the functioning of both anoxygenic and oxygenic photosynthesis. The diversity and primary production of phototrophic microorganisms in cold environments is surprisingly high (Seckbach and Oren 2007).

Four purple phototrophic bacterial strains from Antarctic environments have been isolated: *Roseovarius tolerans* (Labrenz 1999), *Staleyia guttiformis* (Labrenz 2000), *Rseisalinus antarcticus* (Labrenz 2005), and *Rhodoferox antarcticus* (Madigan 2000).

The first three strains were AAP species isolated from Ekho Lake in East Antarctica. The meromictic, hypersaline, heliothermal Ekho lake contains microflora of marine origin. The fourth organism, a purple non-sulfur bacterium *Rhodoferox antarcticus*, resided in algal microbial mats of an ice-covered pond near McMurdo and it grew phototrophically under anaerobic conditions. The growth temperature of *Staleyia guttiformis* (4 – 35°C), *Roseislainus antarcticus* (3 – 33.5°C), and *Roseovarius tolerans* (3 – 43.5°C, with an optimum of 8.5 – 33.5°C) classifies these bacteria among the psychrotolerants and not psychrophiles. *Rhodoferox antarcticus* is a moderate/mild psychrophile (did not grow above 25°C, t_{opt} 12 – 18°C).

1.3.3 Halophiles

A few physiological groups of organisms, including oxygenic and anoxygenic phototrophs, aerobically respiring archaea and bacteria, and denitrifiers, are able to live at salt concentrations of more than 300 g L⁻¹, while other groups like acetoclastic methanogens and autotrophic nitrite oxidizers seem to be unable to tolerate salinities much above those in seawater (Sørensen et al. 2004, Oren 2011b). The diversity of phototrophs growing at high salt concentrations is rather small (Oren 2011a).

To live at high salinities, an organism must be capable of energetically balancing the consequences of high osmotic pressure. Therefore, the main factor which determines whether an organism can survive at high salt concentrations is the amount of energy generated during its dissimilatory metabolism and the mode of osmotic adaptation used (Oren 1999; Oren 2011b). Photosynthetic life is generally not energy-limited, and oxidation of organic compounds with oxygen or nitrate as electron acceptors are highly exergonic dissimilatory processes, so enough energy is available to achieve osmotic equilibrium.

Osmotic pressure causes cellular dehydration and desiccation. Halophilic organisms have evolved two fundamentally different strategies to achieve osmotic balance. The first one is based on the accumulation of high ionic concentrations as was found in the domains *Archaea* and *Bacteria*. The extreme halophiles (e.g. *Halobacteriales* and *Haloanaerobiales*) prefer to accumulate K⁺ rather than Na⁺ in their cytoplasm. The

second more energetically demanding strategy is exclusion of salt and biosynthesis of organic 'compatible' solutes. Many microorganisms respond to an increase in osmolarity by accumulating osmotica in their cytosol. These compound include glycerol (found in *Dunaliella salina*), sucrose and trehalose (in slightly halophilic bacteria, slight halophiles of Cyanobacteria), glucosylglycerol (in mildly halophilic cyanobacteria), glycine betane (in halophilic anoxygenic bacteria, extremely halophilic cyanobacteria), and ectoine (in heterotrophic bacteria) (Oren 1999).

Halophiles among anoxygenic phototrophic bacteria

The orange or red pigmented Halobacteriaceae (Archea) are dominant in hypersaline waters up to the saturating salt concentrations² point (Antranikian 2005). *Halobacterium salinarium* is a photoheterotrophic organism which utilizes light energy to drive bacteriorhodopsin proton pumps and it requires an organic substrates such as carbon (Oren 2011b, Ng et al. 2000).

Organisms thriving in highly saline environments were found also among heliobacteria. Three alkaliphilic heliobacteria of the genus *Heliorestis* have been described (Asao and Madigan 2010). For example, *Heliorestis baculata* growing at pH_{opt} 8.5 – 9.5 has been isolated from Siberian soda lakes (Bryantseva et al. 2000).

The first extremophilic purple phototrophic bacteria were discovered in the 1960s and were either halophiles or acidophiles, including extremely halophilic species of the genus *Halorhodospira* (formerly *Ectorhodospira*) isolated from soda lakes in Wadi Natroun, Egypt, by Hans Georg Trüper and Johannes F. Imhoff (Madigan 2003). The purple sulfur bacterium *Halorhodospira halophila* is one of the most halophilic eubacterium known. It is capable to grow in a saturated solution of sodium chloride, however its growth optimum is only at 15 g L⁻¹ salt.

1.3.4 Alkaliphiles

Alkaliphiles that grow at high pH values are widely distributed throughout the world. The first true alkaliphilic aerobic bacterium *Sporosarcina pasteurii* was isolated in

² the salinity of saturated sodium chloride solution is 358 g L⁻¹ at 20°C

1889. Real interest started when the isolation of their alkaliphilic protease was attempted for the industrial application in laundry detergents. Up to now, the growth at the highest pH (11.3 – 11.4) has been described in *Bacillus firmus* and *Nirosomonas halophila*, which were grown in a pH-controlled chemostat (Sorokin 2005).

The upper pH limit for oxygenic photosynthesis lies near pH 10 (Boussiba et al. 2000). Anoxygenic photosynthesis has not been observed at pH greater than 10.5 (Bryantseva et al. 2000, Bryantseva et al. 1999, Madigan 2003).

The composition and structure of cell surface are essential for alkaliphility (Krulwich et al. 2011). Cell walls containing acidic polymers (teichuronic and poly-D-glutamic acid) function as a negatively charged matrix repulsing OH⁻ ions. Plasma membranes may also maintain pH homeostasis by using a Na⁺/H⁺ antiporter system, and ATPase-driven H⁺ expulsion. A metabolic strategy used for challenging an alkali environment is the upregulation of deaminases which produce cytoplasmatic acids and thus enhance the internal pH.

The optimal and maximal pH value for growth in polyextremophilic conditions are lower than those of simple alkaliphiles presumably due to the effect of additional stressors such as elevated temperature and salt concentrations. For example, an alkalithermophile *Thermococcus alkaliphilus* has an optimum growing temperature of 85°C and a pH of only 9, whereas the most alkaliphilic alkalithermophile *Clostridium paradoxum* has a pH_{opt} = 10.3 and a *t*_{opt} = 54 – 58°C (Wiegel, 2011).

Alkaliphilic anoxygenic and oxygenic phototrophs

Many alkaliphilic species exist in the group of purple nonsulfur bacteria. Among others, *Thioalkaliococcus limnaeus*, *Thiorhodospira sibirica* were isolated from Siberian lakes (Bryatseva et al. 1999; 2000). They grow up to pH 10.5 with an optimum of 9, and do not require sodium chloride for their growth. The aerobic anoxygenic bacterium *Roseinatronobacter thiooxidans* can grow at pH as high as 10.4 (Sorokin et al. 2000).

Oxygenic photosynthesis occurs up to salt saturation, but the diversity of phototrophs growing at high salt concentrations is rather small (Oren, 2011a). Only

few phytoplankton groups common in seawater have adjusted for life in concentrated brines. Diatoms are relatively well adapted and occur up to 100 – 150 g L⁻¹ salt. Cyanobacteria (mainly *Aphanothece halophytica*, *Microcoleus chthonoplastes*, *Halospirulina tapeticola*, *Phormidium* spp.) can grow up to the salinity of 200 – 250 g L⁻¹. The eukaryotic genus *Dunaliella* (green algae) frequently occurs up to the saturating salt concentrations

1.3.5 Acidophiles

Acidophiles living in pH < 4 are most widely distributed in the bacterial and Archaeal domains and contribute to numerous biogeochemical cycles including the iron and sulfur cycles. The most extreme acidophiles belong to the genus *Picrophilus*. *Picrophilus oshimae* and *Picrophilus torridus* and have been isolated from solfataric³ locations in Japan (Schleper 1995). They grow under aerobic conditions at temperatures of 45 – 65°C with a pH as low as 0 – 3.5 and a pH_{opt} of 0.7.

Several unicellular eukaryotes do live below pH 1 (Rothschild and Machinelli 2001). Three fungi (*Acontium cylatium*, *Cephalosporium* sp. and *Trichosporon cerebriae*) grow near pH 0. The red alga *Cyanidium caldarium*, which has been described in pH conditions⁴ as low as 0, has a sharp growth maximum at pH 1 (Seckbach 1999). Fish and cyanobacteria have not been found below pH 4, plants and insects below 2 – 3 (Table 1.2). Autotrophic anoxygenic life at pH 1.3 was reported for *Ferroplasma acidiphilum* (Golyshina 2000).

Low pH can impair processes such as DNA transcription, protein synthesis and enzyme activity (Baker-Austin and Dopson 2007). Acidophiles have a highly impermeable cell membrane to restrict proton influx into the cytoplasm.

Similar to neutralophiles, acidophiles require a neutral intraplasmatic pH. To grow at low pH, they must maintain a pH gradient of several pH units across their cellular membrane. Several mechanisms to control the pH homeostasis have evolved in acidophiles: the removal of excess protons from the cytoplasm, the reduction of the

³fumaroles that emit sulfurous gasses

⁴ corresponds to 1M solution of H₂SO₄

size and permeability of membrane channels, reduction of proton influx by the generation of an inside positive $\Delta\Psi$ (which is opposite to the inside negative $\Delta\Psi$ of neutralophiles) (Figure 1.4).

Table 1.2 The low limits of pH for the growth of given groups (after Seckbach 2000).

Organisms	The low grow limits of pH
Archea	0.06 – 5
Eubacteria	0 – 1
Cyanobacteria	4 – 5
Eukaryotic Algae	~ 0
Fungi	~ 0
Protozoa	< 2
Higher Plants	2 – 4
Invertebrates	< 2
Vertebrates	3.5 – 4

Acidophilic anoxygenic phototrophs

Only three acidophilic purple bacteria are known: *Rhodoblastus acidophilus* (formerly *Rhodopseudomonas acidophila*), *Rhodoblastus sphagnolica*, and *Rhodopila globiformis* (*Rhodopseudomonas globiformis*) isolated by Pfenning in 1930s (Madigan and Jung 2009). *Rhodoblastus acidophilus*, common in acidic lakes, marshes and bogs, showed a low growth limit at pH 4.8. *Rhodopila globiformis* was isolated from a hot acidic (pH 3.5 – 4) spring in the Yellowstone park.

The acidophily has been reported for the genera *Acidiphilium* and *Acidisphaera* that are capable of growth at pH 1.5 and 3.5 resp. (Yurkov and Beatty 1998). They have been isolated from acidic mineral environments, such as mine drainage and acidic soil. *Acidiphilium* species are obligatory acidophilic aerobic anoxygenic bacteria with major photopigment Zn-BChl *a* (Hiraishi and Shimada 2001). The advantage of performing photosynthesis with Zn-Bchl *a* may be the higher stability of Zn-porphyrin derivatives and higher availability of zinc ion under strongly acidic conditions.

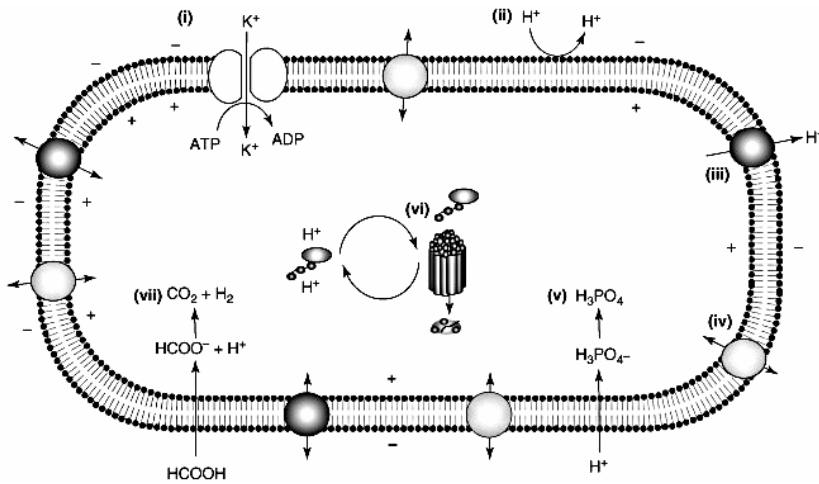


Figure 1.4 Processes associated with pH homeostasis in acidophiles: (i) acidophiles reverse the $\Delta\Psi$ to partially deflect the inward flow of protons; (ii) highly impermeable cell membranes to retard the influx of protons into the cell; (iii) ΔpH is maintained through active proton export by transporters; (iv) a higher proportion of secondary transporters than in neutralophiles; (v) the presence and availability of enzymes and chemicals capable of binding and sequestering protons (vi) larger proportion of DNA and protein repair systems (vii) organic acids that function as uncouplers (adapted from Baker-Austin and Dopson 2007).

1.4 References

- Antranikian G, Vorgias CE, Bertoldo C (2005) Extreme environments as a resource for microorganisms and novel biocatalysts. *Adv Biochem Eng Biotechnol* 96: 219-262
- Asao M, Madigan MT (2010) Taxonomy, phylogeny, and ecology of the heliobacteria. *Photosynth Res* 104: 103-111
- Baker-Austin C, Dopson M (2007) Life in acid: pH homeostasis in acidophiles. *Trends Microbiol* 15: 165-171
- Blankenship RE (2002) *Molecular mechanisms of photosynthesis*. Blackwell Science Ltd., Oxford, pp. 220-257
- Blankenship RE (2010) Early Evolution of Photosynthesis. *Plant Physiol* 154: 434-438
- Björn LO, Govindjee (2009) The evolution of photosynthesis and chloroplasts. *Curr Sci* 96: 1466-1474

- Blöchl E, Rachel R, Burggraf S, Hafenbrandl D, Jannasch HW, Stetter KO (1997) *Pyrolobus fumarii*, gen. and sp. nov., represents a novel group of Archaea, extending the upper temperature limit for life to 113°C. *Extremophiles* 1: 14-17
- Boussiba S, Wu X, Zarka A (2000) *Alkaliphilic cyanobacteria* in Seckbach J (ed.) *Journey to diverse microbial worlds*. Kluwer Academic Publishers, Netherland pp. 209-224
- Brock TD, Freeze H (1969) *Thermus aquaticus* gen. nov., sp. nov., a non-sporulating extreme thermophile. *J Bacteriol* 98: 289-297
- Bryant DA, Costas AMG, Maresca JA, Chew AGM, Klatt CG, Bateson MM, Tallon LJ, Hostetler J, Nelson WC, Heidelberg JF, Ward DM (2007) *Candidatus Chloracidobacterium thermophilum*: an aerobic phototrophic *Acidobacterium*. *Science* 137: 523-526
- Bryantseva IA, Gorlenko VM, Kompatseva EI, Imhoff JF, Suling J, Mityushina L (1999) *Thiorhodospira sibirica* gen. nov., sp. nov., a new alkaliphilic purple sulfur bacterium from a Siberian soda lake. *Int J Syst Evol Microbiol* 49: 697-703
- Bryantseva IA, Gorlenko VM, Kompatseva EI, Imhoff JF (2000) *Thioalkalicoccus limnaeus* gen. nov., sp. nov., a new alkaliphilic purple sulfur bacterium with bacteriochlorophyll *b*. *Int J Syst Evol Microbiol* 50: 2157-2163
- Bryantseva IA, Gorlenko VM, Kompatseva EI, Tourova TP, Kuznetsov BB, Osipov GA (2000) Alkaliphilic heliobacterium *Heliorestis baculata* sp. nov. and emended description of the genus *Heliorestis*. *Arch Microbiol* 174: 283-291
- Castenholz RW, Pierson BK (1995) *Ecology of thermophilic anoxygenic phototrophs* in Blankenship RE, Madigan MT, Bauer CE (eds.) *Anoxygenic photosynthetic Bacteria*. Kluwer Academic Publishers, Netherlands, pp. 31-47
- Elster J (1999) *Algal versatility in various extreme environments* in J. Seckbach (ed.) *Enigmatic Microorganisms and Life in Extreme Environments*. Kluwer Academic Publishers, Netherlands, pp. 215-227
- Golyshina OV, Pivovarova TA, Karavaiko GI, Kondrat'eva TF, Moore ERB, Abraham WR, Lünsdorf H, Timmis KN, Yakimov MM, Golyshin PN (2000) *Ferroplasma*

- acidiphilum* gen. nov., sp. nov., an acidophilic, autotrophic, ferrous-iron-oxidizing, cell-wall-lacking, mesophilic member of the *Ferroplasmaceae* fam. nov., comprising a distinct lineage of the Archaea. *Int J Syst Evol Microbiol* 50: 997-1006
- de la Haba RR, Sánchez-Porro C, Marquez MC, Ventosa A (2011) *Taxonomy of Halophiles* in Horikoshi K (ed.) *Extremophiles handbook*. Springer, Dordrecht, pp. 255-308
- Hanada S, Kawase Y, Hiraishi A, Takaichi S, Marsuura K, Shimada K, Nagashima KVP (1997) *Porphyrobacter tepidarius* sp. nov., a moderately thermophilic aerobic photosynthetic bacterium isolated from a hot spring. *Int J Syst Bact* 47: 408-419
- Helmke E, Weyland H (2004) Psychrophilic versus psychrotolerant bacteria – occurrence and significance in polar and temperate marine habitats. *Cell Mol Biol* 50: 553-561
- Hiraishi A, Shimada K (2001) Aerobic anoxygenic photosynthetic bacteria with zinc-bacteriochlorophyll. *J Gen App Microbiol* 47: 161-180
- Horikoshi K (2011) *Extremophiles Handbook*. Springer, Dordrecht, pp. 3-18
- Jones BE, Grant WD, Duckworth AW and Owenson GG (1998) Microbial diversity of soda lakes. *Extremophiles* 2: 191–200
- Krulwich TA, Liu J, Morino M, Fujisawa M, Ito M, Hicks DB (2011) *Adaptive mechanism of extreme alkaliphiles* in Horikoshi K (ed.) *Extremophiles handbook*. Springer, Dordrecht, pp. 119-140
- Labrenz M, Collins MD, Lawson PA, Tindall BJ, Schumann P, Hirsch P (1999) *Roseovarius tolerans* gen. nov., sp. nov., a budding bacterium with variable bacteriochlorophyll *a* production from hypersaline Ekho Lake. *Int J Syst Evol Microbiol* 49: 137-147
- Labrenz M, Tindall BJ, Lawson PA, Collins MD, Schumann P, Hirsch P (2000) *Staleyia guttiformis* gen. nov., sp. nov. and *Sulfitobacter brevis* sp. nov., α -3-*Proteobacteria* from hypersaline, heliothermal and meromictic antarctic Ekho Lake. *Int J Syst Evol Microbiol* 50: 303-313

- Labrenz M, Lawson PA, Tindall BJ, Collins MD, Hirsch P (2005) *Roseisalinus antarcticus* gen. nov., sp. nov., a novel aerobic bacteriochlorophyll a-producing α -proteobacterium isolated from hypersaline Ekho Lake, Antarctica. *Int J Syst Evol Microbiol* 55: 41-47
- Lengerer JW, Drews G, Schlegel HG (1999) *Biology of the Prokaryotes*. Georg Thieme Verlag, Stuttgart, pp. 327-340
- Madigan MT (2003) Anoxygenic phototrophic bacteria from extreme environments. *Photosynth Res* 76: 157-171
- Madigan MT (2006) *Anoxygenic phototrophic bacteria from extreme environments* in Govindjee, Beatty JT, Gest H, Allen JF (eds.) *Discoveries in Photosynthesis*. Springer, pp. 969-983
- Madigan MT, Jung DO (2009) *An overview of purple bacteria: systematics, physiology, and habitats* in Hunter CN, Daldal F, Thurnauer MC, Beatty JT (eds.) *The purple phototrophic bacteria*. Springer Science, pp. 1-15
- Madigan MT, Jung DO, Woese CR, Achenbach LA (2000) *Rhodoferrax antarcticus* sp. nov., a moderately psychrophilic purple nonsulfur bacterium isolated from an Antarctic microbial mat. *Arch Microbiol* 173: 269-277
- Nisbet EG, Sleep NH (2001) The habitat and nature of early life. *Nature* 409: 1083-1091
- Ng WV, Kennedy SP, Mahairas GG, Berquist B, Pan M et al. (2000) Genome sequence of *Halobacterium* species NRC-1. *Proc Natl Acad Sci* 97: 12176-12181
- Nogi T, Fathir I, Kobayashi M, Nozawa T, Miki K (2000) Crystal structure of photosynthetic reaction centre and high-potential iron-sulfur protein from *Thermochromatium tepidum*: Thermostability and electron transfer. *Proc Natl Acad Sci* 97: 13561-13566
- Oren A (1999) Bioenergetic aspects of halophilism. *Mol Biol Rev* 63(2): 334-348
- Oren A (2011a) *Diversity of halophiles* in Horikoshi K (ed.) *Extremophiles handbook*. Springer, Dordrecht, str. 310-325
- Oren A (2011b) Thermodynamics limits to microbial life at high salt concentrations.

Environ Microbiol 13: 1908-1923

- Rathgeber C, Lince MT, Alric J, Lang AS, Humphrey E, Blankenship RE, Verméglio A, Plumley FG, Van Dover CL, Beatty JT, Yurkov V (2008) Vertical distribution and characterization of aerobic phototrophic bacteria at the Juan de Fuca Ridge in the Pacific Ocean. *Photosynth Res* 97: 235-244
- Rothschild LJ, Macienelli RL (2001) Life in extreme environments. *Nature* 409: 1092-1101
- Schlepper Ch, Puehler G, Holz I, Gambacorta A, Janekovic D, Santarius U, Klenk H, Zillig W (1995) *Picrophilus* gen. nov., fam. nov.: a novel aerobic, heterotrophic, thermoacidophilic genus and family comprising Archaea capable of growth around pH 0. *J Bacteriol* 177: 7050-7059
- Seckbach J (1999) *The Cyanidiophyceae: hot spring acidophilic algae* in Seckbach J (ed.) *Enigmatic microorganisms and life in extreme environments*. Kluwer Academic Publishers, Dordrecht, pp. 425-435
- Seckbach J (2000) *Journey to diverse microbial worlds: adaptation to exotic environments*. Springer, pp. 109-116
- Seckbach J, Oren A (2007) *Oxygenic photosynthetic microorganisms in extreme environments* in Seckbach J (ed.) *Algae and cyanobacteria in extreme environments*. Springer, Dordrecht, Netherlands, pp. 3-25
- Sorokin DY, Tourova TP, Kuenen JG (2000) A new facultatively autotrophic hydrogen- and sulfur-oxidizing bacterium from an alkaline environment. *Extremophiles* 4: 237-245
- Sorokin DY (2005) Is there a limit for high-pH growth? *Int J Syst Evol Microbiol* 55: 1405-1406
- Tang KH, Barry K, Chertkov O, Dalin E, Han CS, Hauser LJ, Honchak BM, Karbach LE, Lamd ML, Lapidus A, Larimer FW, Mikhailova N, Pitluck S, Pierson BK, Blankenship RE (2011) Complete genome sequence of the filamentous anoxygenic phototrophic bacterium *Chloroflexus aurantiacus*. *BMC Genomics* 12: 334-355
- Waidner LA, Kirchman DL (2007) Aerobic anoxygenic phototrophic bacteria attached

to particles in turbid waters of the Delaware and Chesapeake Estuaries. *Appl Environ Microbiol* 73: 3936–3944

Wiegel J (2011) *Anaerobic alkaliphiles and alkaliphilic poly-extremophiles* in Horikoshi K (ed.) *Extremophiles Handbook*. Springer, Dordrecht, pp. 82-97

Yurkov V, Beatty (1998) Aerobic anoxygenic phototrophic bacteria. *Microbiol Mol Biol Rev* 62: 695-724

Yurkov V, Krieger S, Stackebrandt E, Beatty JT (1999) *Citromicrobium bathyomarinum*, a novel aerobic bacterium isolated from deep-sea hydrothermal vent plume waters that contains photosynthetic pigment-protein complexes. *J Bacteriol* 181: 4517-4525

2. Anoxygenic Bacteria in Saline and Soda Lakes

This chapter is based on the article:

High abundance of aerobic anoxygenic phototrophs in saline steppe lakes

Hana Medová^{1,2}, Ekaterina N. Boldareva^{1,2}, Pavel Hrouzek^{1,2}, Svetlana V. Borzenko³, Zorigto B. Namsaraev⁴, Vladimir M. Gorlenko⁴, Bair B. Namsaraev⁵, Michal Koblížek^{1,2} *FEMS Microbiol Ecol* (2011) 76: 393-400

2.1 Summary

We studied the distribution of anoxygenic phototrophs in 23 steppe lakes in Transbaikal region (Russia), in Uzbekistan (Central Asia) and Crimean peninsula (Ukraine). The lakes varied in their mineral content and composition (salinities from 0.2 to 300 g L⁻¹). The Transbaikal lakes were alkaline (pH > 9) with high amounts of soda. The Uzbek and Crimean lakes were more pH neutral frequently with high amount of sulfates. The presence of anoxygenic phototrophs was registered by infra-red epifluorescence microscopy, infra-red fluorometry and pigment analyses. In mostly shallow, fully oxic lakes, the anoxygenic phototrophs represented 7% to 65% of total Prokaryotes with the maxima observed in Transbaikal soda lakes Gorbunka (32%), Khilganta (65%), Zanday (58%) and Zun-Kholbo (46%). Some of the lakes contained over 1 µg bacteriochlorophyll L⁻¹. In contrast, only small amount of anoxygenic phototrophs were registered in highly mineralized lakes (>100 g total salts L⁻¹) Borzinskoe, Tsagan-Nur (Transbaikal), Staroe (Crimea) and in the residual part of the southwest Aral Sea (Uzbekistan). The oxic environment and observed specific diurnal changes of bacteriochlorophyll concentration suggest that the phototrophic community

¹Institute of Microbiology CAS, Třeboň, Czech Republic; ²University of South Bohemia, Faculty of Science, České Budějovice, Czech Republic; ³Institute of Natural Resources, Ecology, and Cryology, Siberian Division RAS, Chita, Russia; ⁴Winogradsky Institute of Microbiology RAS, Moscow, Russia; ⁵Institute of General and Experimental Biology RAS, Ulan-Ude, Russia

was mostly composed of aerobic anoxygenic phototrophs. The reported abundances and bacteriochlorophyll concentrations are about two to three orders of magnitude higher than numbers reported from the marine environments, which signalize an important role of aerobic anoxygenic phototrophs in the studied habitats.

2.1 Introduction

Anoxygenic phototrophic bacteria (APB) are one of the oldest life forms on Earth. They evolved long before the oxidation of Earth's atmosphere, thus, most of them grow and photosynthesize only under anoxic conditions (Yurkov and Csotonyi 2009). Under current aerobic conditions, these organisms are restricted to marginal ecological niches, such as anoxic zones of lakes or sulfide springs. However, some groups of anoxygenic phototrophs have adapted to aerobic conditions and employed facultative or strictly aerobic life styles. Facultative aerobic growth is frequent for purple nonsulfur bacteria, whereas it has been documented only in a few species of purple sulfur bacteria. A recently discovered group of aerobic anoxygenic phototrophs (AAPs) is formed by obligatory aerobic and facultatively phototrophic species (Yurkov and Csotonyi 2009). The AAPs are photoheterotrophic organisms, they lack capacity to fix inorganic carbon. AAPs require a supply of organic substrates for respiration and growth, but they are able to derive a significant portion of their energy requirements from light (Koblížek et al. 2010).

AAPs were shown to play an important role in the microbial community in the ocean (Kolber et al. 2001, Jiao et al 2007, Koblížek et al. 2007, Yutin et al. 2007), shelf seas (Koblížek et al. 2005, Mašín et al. 2006) and river estuaries (Waidner and Kirchman 2007, Cottrell et al. 2010). AAPs have also recently been reported in freshwater lakes (Mašín et al. 2008, Eiler et al. 2009). Their abundance and importance for ecosystem of various terrestrial brakish and salty lakes is less clear. The presence of AAPs in brakish and saline lakes was demonstrated by several culture-work studies from Clifton and Heyward lake, Australia (Shiba et al 1991), Ekho Lake, Antarctica (Labrenz et al. 1999) or Mahoney Lake, Canada (Yurkova et al. 2002). The presence of AAPs has been reported from high altitude brakish lakes in Tibet (Jiang et al. 2008).

Steppes are important geographical regions occupying large parts of Eurasia and Americas (Hammer 1986). The world's largest steppe zone, often referred to as "the Great Steppe" stretches over large part of Eurasia from Ukraine and southern Russia to Mongolia, East Siberia and northern China. The climate in this region is typically continental with extreme differences between summer and winter temperatures. The steppes are semiarid grasslands with only a small number of lakes or rivers. The steppe lakes are typically shallow and the extreme climatic conditions lead to large changes of water during the season. Due to the dry conditions many steppe lakes have an elevated content of salts and other minerals.

Some of the largest steppe lakes are located in Uzbekistan, Central Asia. The Aral Sea used to be the fourth largest lake on Earth, with an area of over 65,000 km². Starting from 1961, the lake has been continuously retreating due to the restricted inflow of fresh water from Amudarya and Syrdarya rivers. Both these rivers have been drained by numerous irrigation channels supplying the surrounding fields. Presently, the Aral area has shrunk to about 10% of its original size and it has fragmented into several residual lakes. Concomitantly, the salinity of the formerly brackish lake increased by more than an order of magnitude, now exceeding 100 g L⁻¹ (Zavialov et al. 2009). On the other hand the Amudarya irrigating system formed some new lakes, some of them also sampled within this study (Ashat, Athakara, Shor-Shor lakes). A similar scenario occurred in Lake Aydar where the building of an irrigation dam on Syrdarya River led to an increase of water level in the adjacent Kyzyl Kum depression. Aydar has been rising in size since the 1960's from mostly saline marshland to the present size of 3,000 km².

There are a number of soda lakes in the Transbaikal region (East Siberia) of Russia. These lakes represent a specific type of salt lake, which contain a relatively high amount of sodium carbonate among other, pH-neutral, salts. Despite their high salinity and alkalinity, many shallow soda lakes are highly productive caused by an almost infinite supply of CO₂ in these habitats.

The composition of the microbial community in the sediments (Gorlenko et al. 1999) and microbial mats in lake Khilganta was studied in the 1990's (Kompantseva et

al. 2005), however, only little is known about the planktonic bacterial community in these lakes. The presence of photosynthetic bacteria in these lakes has been indicated in previous work of Bryantseva et al. (1999), Kompantseva et al. (2005, 2007) and Boldareva et al. (2008, 2009a, 2009b), which isolated a number of new species of APB from these environments. However, more detailed information about the abundance and activity of phototrophs in such environments is missing. Therefore, in the presented study we examined the distribution of phototrophic bacteria in 23 steppe lakes in the Transbaikal region (Russia), Uzbekistan and Crimean Peninsula (Ukraine). The APB were registered using infra-red kinetic fluorometry and infra-red epifluorescence microscopy.

2.2 Methods

2.2.1 Sampling

13 steppe lakes in the Transbaikal region, East Siberia, Russia (see Table 2.1) were sampled during an expedition in August and September 2008. The samples from eight lakes in Uzbekistan (Central Asia) and two lakes in Crimea, Ukraine (see Table 2.1) were taken in August and September 2009. The water samples were collected from the fully oxic planktonic zone at approx. 0.2 m depth. The pH was recorded with a HANNA portable pH meter and the temperature with a VWR digital thermometer. The chemical composition of the water and salinity (total mineralization) was determined by anion chromatography. Total alkalinity was determined by the titration with 0.05 N HCl. Samples for infra-red microscopy were collected into sterile, plastic test tubes, fixed with 2% formaldehyde and stored at 4°C. The samples for infrared fluorometry were processed immediately.

2.2.2 Fluorometry

Bacteriochlorophyll *a* fluorescence was recorded by a single channel infra-red kinetic fluorometer modified from a commercially available instrument AOM (Photon Systems Instruments Ltd., Brno, Czech Republic). The standard blue and red flashing

units were replaced with two blue-green Luxeon Rebel diodes (505 nm) and the emission filter replaced with a RG850 Schott glass filter. A DC/DC convertor was used to power the instrument and notebook computer from a standard 12V car battery. To separate the chlorophyll and bacteriochlorophyll signal we used the herbicide diuron (DCMU, 3-(3,4-dichlorophenyl)-1,1-dimethylurea) as described earlier (Koblížek et al. 2005). To increase the sensitivity by accumulating more signal, the BChl *a* concentration was estimated from the area above the BChl *a* fluorescence induction curve. The measurement was repeated 10 times and the mean value has been calculated. The instrument was calibrated prior to the expedition using a diluted culture of *Roseobacter* strain COL2P where the BChl *a* content was determined spectroscopically in acetone:methanol 7:2 (*vol:vol*) pigment extracts (Koblížek et al. 2010). The detection limit of the portable fluorometer was approx. 5 ng BChl *a* L⁻¹.

2.2.3 Epifluorescence microscopy

The composition of the planktonic community was analyzed by epifluorescence microscopy as described previously (Mašín et al. 2006). Briefly, the 2% formaldehyde fixed water samples were collected onto 0.2 µm polycarbonate filters, dried, and stained with 4',6-diamidino-2-phenylindole (DAPI). The DAPI was dissolved in a 3:1 mixture of Citifluor™ AF1 and Vectashield® at a final concentration of 1 µg mL⁻¹. First, the total DAPI-stained bacteria were recorded in the blue part of the spectrum (200 ms exposure). Then, red Chl autofluorescence was recorded to identify Chl-containing organisms (500 ms exposure) and, finally, an infrared emission (>850 nm) image was captured, showing both APB and phytoplankton (20 s to 35 s exposure). The acquired images were saved and semi-manually analyzed with the aid of AnalySiS software (Soft Imaging Systems) to distinguish the number of heterotrophic bacteria, picocyanobacteria and APB for each sample. For each individual sample, 10 to 12 frames were recorded and analyzed (~400 to 600 DAPI cells).

Table 2.1 General characteristics of the studied lakes. Due to strong evaporation some lakes vary largely in depth and size. The reported values represent lake status at the time of sampling in August and September 2008 and September 2009 (* data from year 2006).

Lake	Region	Latitude (N)	Longitude (E)	Depth (m)	Area (km ²)
Alvakhon	Transbaikal	50°39.6'	115°04.1'	<0.5	0.02
Babye	Transbaikal	50°18.0'	116°23.1'	<0.5	0.38
Borzinskoe	Transbaikal	50°15.1'	116°16.8'	<0.5	0.84
Doroninskoe	Transbaikal	51°14.4'	112°14.4'	6.5	5.10
Gorbunka	Transbaikal	50°39.6'	115°04.1'	<0.5	0.01
Chep-Check 2	Transbaikal	51°15.2'	112°16.3'	1.25	0.18
Chep-Check 3	Transbaikal	51°14.7'	112°15.6'	1.0	0.17
Khilganta	Transbaikal	50°42.5'	115°06.1'	<0.5	0.13
Torom	Transbaikal	51°15.6'	112°16.4'	1.8	1.75
Tsagan-Nur	Transbaikal	50°13.2'	116°15.7'	<0.5	1.43
Zanday	Transbaikal	50°03.3'	116°03.4'	<0.5	0.74
Zun-Kholvo	Transbaikal	50°43.2'	115°08.3'	<0.5	0.85
Zun-Torey	Transbaikal	50°06.4'	115°41.6'	6.5	220,00
SW Aral Sea	Uzbekistan	44°30.2'	58°13.9'	41*	~3,300*
Ashat	Uzbekistan	41°18.4'	60°20.7'	2	3.25
Atakhara	Uzbekistan	41°21.0'	60°26.7'	2	0.28
Aydar	Uzbekistan	40°51.5'	66°46.7'	10	~3,000
Aydar lagoon	Uzbekistan	40°51.4'	66°46.7'	1.5	0.11
Hog	Uzbekistan	41°24.8'	60°23.3'	20	1.28
Shor-shor	Uzbekistan	41°17.6'	60°27.1'	3	0.50
Sudocheskoe	Uzbekistan	43°35.2'	58°32.6'	5	496
lagoon Crimea	Crimea	45°12.2'	33°24.6'	2	1.99
Staroe	Crimea	45°58.4'	33°45.9'	n.d.	6.95

Table 2.2 Physio-chemical properties of Transbaikal lakes sampled in September 2008. BChl *a* concentration (value \pm SD) was estimated from the fluorometric data. n.d. = no data.

Lake	Salinity (g L ⁻¹)	CO ₃ / HCO ₃ ⁻ (g L ⁻¹)	SO ₄ ²⁻ (g L ⁻¹)	Cl ⁻ (g L ⁻¹)	pH	BChl <i>a</i> (ng L ⁻¹)	Chl <i>a</i> (μ g L ⁻¹)	Temperature (°C)
Alvakhon	1.5	0.2 / 1.1	n.d.	n.d.	9.6	1554 \pm 16.5	180.7	17.8
Babye	35.0	0.0 / 0.1	4.2	17.5	9.9	177 \pm 4.0	7.2	n.d.
Borzinskoe	305.8	4.3 / 4.0	44.4	137.7	9.9	0	20.1	16.1
Doroninskoe	24.3	5.5 / 5.6	0.2	4.0	9.9	9 \pm 2.3	n.d.	15.0
Gorbunka	41.3	0.0 / 0.4	6.4	19.0	9.3	612 \pm 28.7	n.d.	19.4
Chep-Check 2	21.0	0.6 / 5.5	1.1	6.1	9.9	293 \pm 73.6	2.7	19.0
Chep-Check 3	6.9	0.2 / 3.3	0.5	0.8	9.8	58 \pm 8.9	15.0	22.4
Khilganta	17.0	0.0 / 0.2	4.1	6.8	9.4	185 \pm 4.1	11.4	15.0
Torom	21.3	0.5 / 4.8	0.9	7.0	9.6	51 \pm 5.4	8.4	15.8
Tsaga-Nur	174.1	5.0 / 4.4	30.3	69.4	9.7	4 \pm 4.2	36.8	13.8
Zanday	19.0	0.5 / 1.8	n.d.	n.d.	10.0	52 \pm 4.7	n.d.	n.d.
Zun-Kholvo	25.0	n.d.	n.d.	n.d.	9.9	1255 \pm 49.1	8.5	19.8
Zun-Torey	5.1	0.5 / 1.4	0.4	1.0	10.4	30 \pm 4.2	1.3	17.2

Table 2.3 Physio-chemical properties of Uzbek and Crimean lakes sampled in September 2009.

Lake	Salinity (g L ⁻¹)	HCO ₃ ⁻ (g L ⁻¹)	SO ₄ ²⁻ (g L ⁻¹)	Cl ⁻ (g L ⁻¹)	pH	Temperature (°C)
SW Aral Sea	121.4	1.7	29.0	46.5	8.2	15
Ashat	7.5	1.8	2.3	1.4	7.9	20
Atakhara	2.5	1.0	0.6	0.4	7.2	23
Aydar	10.0	0.4	4.8	1.5	7.9	20
Aydar lagoon	16.2	1.7	6.7	2.8	7.5	22
Hog	2.4	0.4	0.8	0.5	7.8	20
Shor-shor	3.7	1.3	0.9	0.6	7.7	18
Sudocheskoe	1.8	0.2	0.7	0.4	7.4	18
lagoon Crimea	0.6	0.3	0.1	0.1	6.6	20
Staroe	>300	2.9	60.0	238.0	6.3	20

2.2.4 High-performance liquid chromatography (HPLC)

Water samples for pigment analyses were filtered through 13 mm GF/F filters. The filters were placed in 3.5 mL of 7:2 acetone/methanol mixture and stored at 4°C in the dark. In the laboratory, the filters were homogenized and the obtained suspensions were centrifuged at 10,000×g for 10 min. The obtained extracts were injected (50 µL) into an Agilent Technologies 1200 series HPLC as described previously (Koblížek et al. 2010). Chl *a* was detected at 660 nm, BChl *a* was detected at 770 nm. The detection limit for Chl *a* was approximately 50 pg per injection.

2.3 Results

2.3.1 Survey of Transbaikal lakes

Thirteen alkaline steppe lakes (see Table 2.1) located in the Transbaikal region, Russia were surveyed in September 2008. Most of the studied lakes had an elevated content of soda and other salts (see Table 2.2). The largest visited lakes were Zun-Torey (~220 km²) and Doroninskoe (~5 km²). The rest of the lakes were mostly small and shallow water bodies. Some of the lakes (Khilganta) were only temporal (ephemeric) due to strong evaporation. The lakes differed in their trophic status from the large oligotrophic lakes Zun-Torey and Doroninskoe to the eutrophic Alvakhon Lake. Phytoplankton in the lakes with a salinity lower than 100 g L⁻¹ were dominated by diatoms belonging to the genera *Nitzschia* and *Surirella*, green algae belonging to genera *Euglena* and *Chlorella*, and cyanobacteria of the genus *Synechococcus*. Filamentous cyanobacteria were found also in planktonic phase belonging to genera *Oscillatoria*, *Nodularia*, *Phormidium* and *Spirulina* that dominated the cyanobacterial mats on a bottom of lakes. Highly saline lakes Borzinskoe and Tsagan-Nur were dominated by unicellular halophilic green algae *Dunaliella salina*.

During the expedition the presence of APB species was surveyed using a portable infra-red fluorometer. BChl *a* signal was registered in almost all lakes, except the most mineralized (above 100 g L⁻¹) Borzinskoe and Tsaga-Nur lakes (Table 2.2). The highest signals indicating BChl *a* concentrations above 0.6 µg L⁻¹ were registered

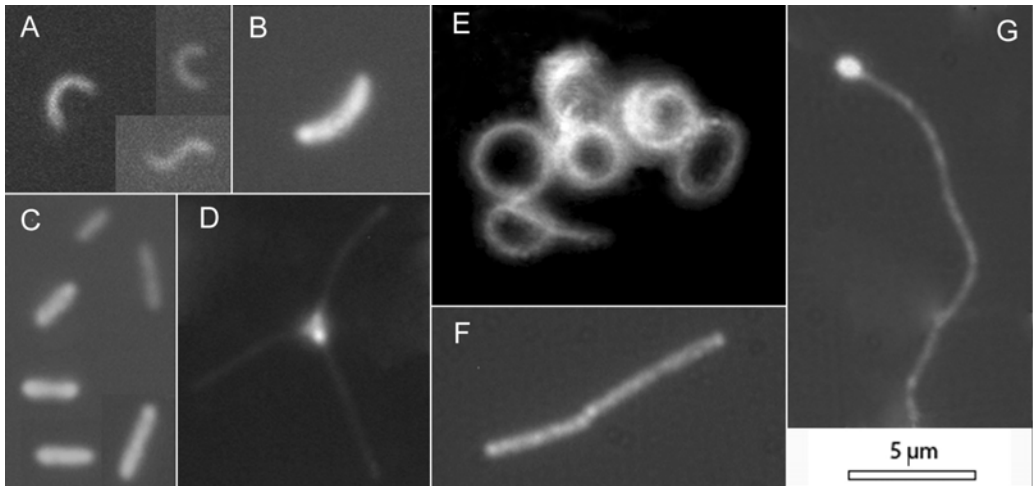


Figure 2.1. Images of APB obtained by the infra-red epifluorescence microscopy. The displayed morphotypes were found in lakes: A – Zun-Torey, B – Doroninskoe, C – Khilganta, D – Alvakhon, E – Hog, F – Aydar-kol, G – Sudocheskoe

in lakes Gorbunka, Zun-Kholvo and Alvakhon (Table 2.2). The BChl *a*/Chl *a* ratios varied from 0 to 0.14, with the highest number observed in lake Zun-Kholvo which indicates a high proportion of APB in this lake.

The presence of anoxygenic phototrophs in the lakes were further examined by infra-red microscopy. The collected samples contained APB of various morphology (Figure 2.1). Common morphotypes were short rods 1 – 2 µm long and ovoid cells with a diameter smaller than 1 µm, which dominated in lakes Gorbunka, Khilganta, and Zanday. Less frequent were long rods up to 10 µm and various vibrio or sickle-shape bacteria. Unusual star-like morphotypes with three to four filamentous arms (5 – 6.5 µm long) were observed in Lake Alvakhon (Figure 2.1D).

The content of APB varied strongly between the studied lakes ranging from 0.2% to 65% of total prokaryotes (Figure 2.2). The highest abundances of APB were found in lake Alvakhon (16.8×10^6 cells mL⁻¹), which is in good agreement with the high BChl *a* content estimated from the fluorometric data. The highest proportion was observed in lakes Gorbunka, Khilganta, Zanday, Zun-Kholvo and Alvakhon where APB represented between 20 and 65% of total prokaryotes. Smaller percentages were observed in lakes Babye (15.2%), Chep-check 2, Chep-check 3 and Zun-Torey (5 –

10%). The lowest abundance was found in lake Borzinskoe (6.6×10^4 cells mL⁻¹), here, APB formed only 0.2% of total prokaryotes.

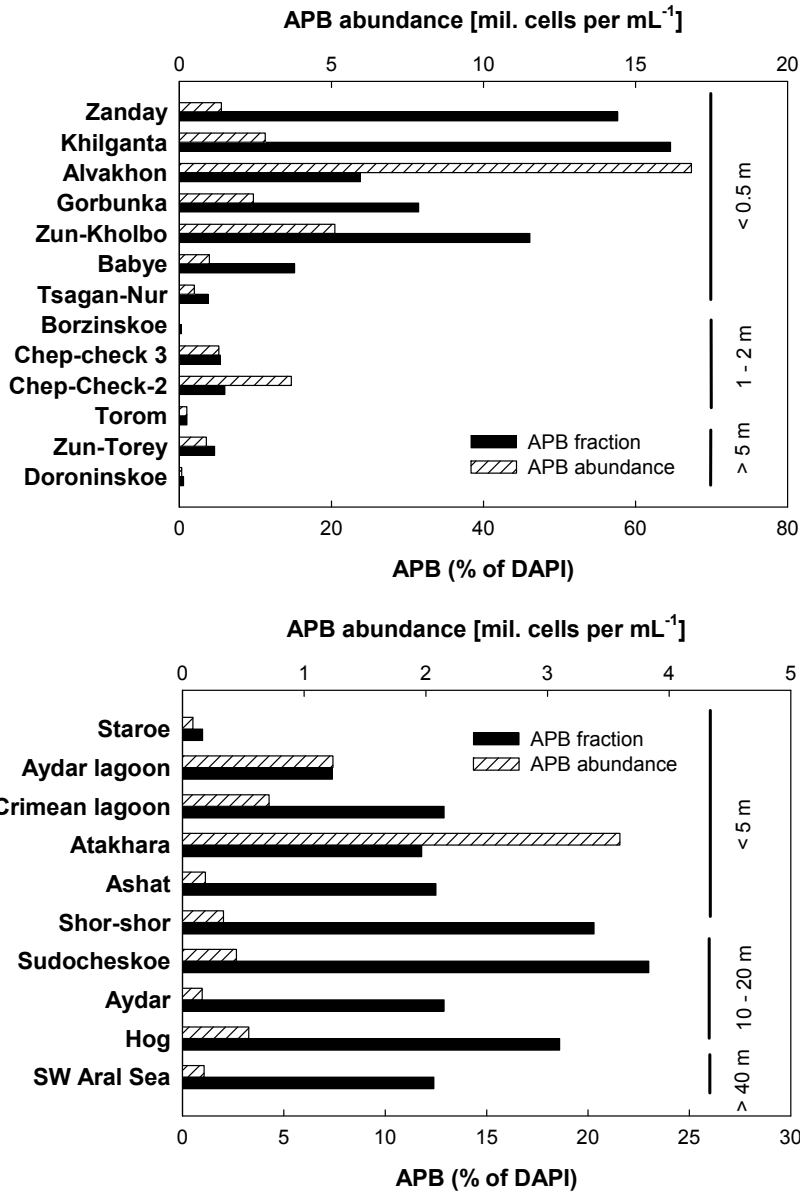


Figure 2.2 Abundance of APB bacteria in the studied lakes given as cell counts (slashed bars) and as the percentages of total DAPI (filled bars). Upper panel: lakes of Transbaikal region sampled in August and September 2008. The lakes are divided into three groups according to their total depth. Lower panel: lakes in Uzbekistan and Crimea sampled in September 2009.

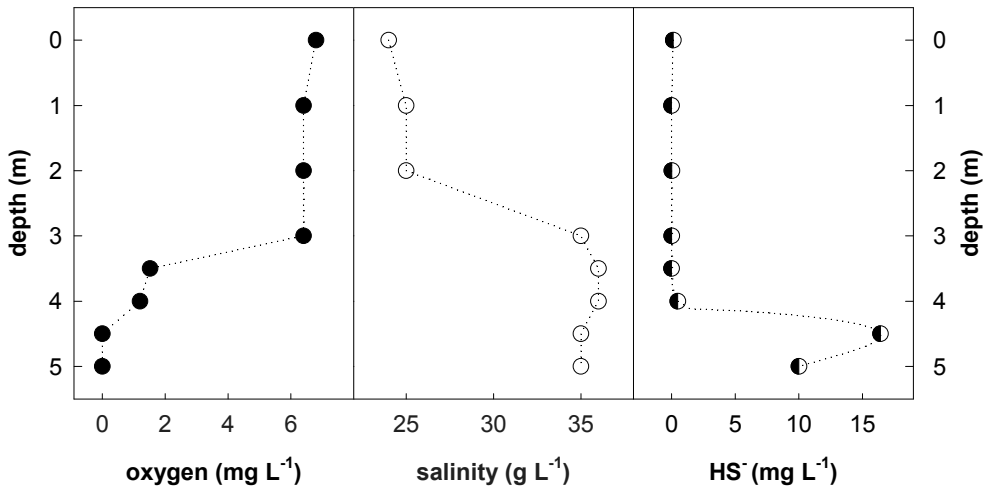


Figure 2.3 The deep profile oxygen, salinity and temperature in lake Doroninskoe. The steeply changing value at the depth of 4 m indicated the presence of the chemocline.

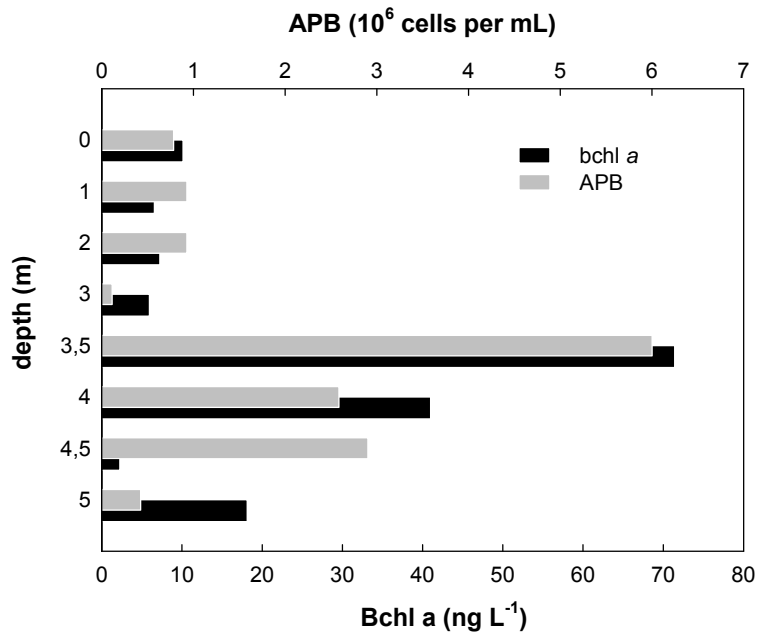


Figure 2.4 The deep profile of Bchl *a* concentration and abundance of APB bacteria in Lake Doroninskoe sampled in August 2008. The maximum of Bchl *a* and highest abundance were detected at the depth of 3.5 – 5 m where the chemocline was found. Both aerobic and anaerobic bacteria may create the prokaryotic community found in this layer.

2.3.3 BChl *a* diurnal changes

The highest proportion of phototrophic bacteria was observed in Lake Khilganta ($1.1 - 2.8 \times 10^6$ cells mL^{-1} which represented 52 – 65% of total prokaryotes). The diurnal changes of BChl *a* fluorescence signal were followed in this lake for 36 hours. The fluorescence exhibited strong diurnal changes with the maxima recorded in the early morning. Then, the BChl *a* signals exponentially decreased during the day-light period and recovered at night (Figure 2.5). As suggested previously the BChl *a* decay measurement can be used for determination of AAP mortality rates (Koblížek et al. 2005). For this reason the observed BChl *a* decay has been analyzed by exponential fitting providing the rate of $2.9 \pm 0.2 \text{ day}^{-1}$.

Lake Doroninskoe represents an exception among the studied lakes, which are holomictic and fully aerobic, as it regularly develops seasonal stratification lasting from spring till late summer (Figure 2.3, Gorlenko et al. 2010). The diurnal changes of BChl *a* fluorescence signal were followed at the aerobic surface layer for 42 hours. Similarly to lake Khilganta the signal exhibited strong diurnal changes with the maxima recorded in the early morning and the minima in the evening (Figure 2.5B). The BChl *a* decay rate was determined to be $3.2 \pm 0.6 \text{ day}^{-1}$ by exponential fitting.

2.3.4 Uzbek and Crimean lakes

In September 2009, BChl *a*-containing bacteria were surveyed in 8 steppe lakes in Uzbekistan and 2 lakes in Crimea. The two most important lakes in this area were the southwestern (SW) part of the former Aral Sea (approximately $3,300 \text{ km}^2$, depth of 41 m) and Lake Aydar ($1,050 \text{ km}^2$, 10 m deep). Another large water body was brakish lake Sudocheskoe, another remnant of the former Aral, which is still supplied by freshwater from the Amudarya river (Table 2.1 and 2.3). The mineralization of the lakes was medium $0.2 - 15.5 \text{ g L}^{-1}$, the only two highly mineralized lakes were the SW part of the former Aral Sea ($\sim 120 \text{ g L}^{-1}$) and lake Staroe on Crimea ($>300 \text{ g L}^{-1}$). Most of the Uzbek lakes were characterized by a relatively high content of sulfates ($0.6 - 30 \text{ g L}^{-1}$). In contrast to Transbaikal soda lakes the Uzbek and Crimean lakes contained smaller amount of carbonates, resulting in a lower pH, 7.2 – 8.3 for Uzbek lakes and

6.3 – 6.6 for Crimean lakes.

The presence of APB was surveyed by IR epifluorescence microscopy. APB were observed in all the studied lakes and exhibited a wide diversity of morphotypes (ovoids, short rods, vibrios, spiral or stalk bacteria). The star-like morphotypes were found in lake Atachara where various coccal cyanobacteria were present in a significant amount. The abundance of APB ranged from 8.5×10^4 to 3.6×10^6 cells mL^{-1} , whereas their percentage varied between 1.0 – 23.0% (Figure 2.2). The highest proportion of APB was found in lakes Sudocheskoe (23.0%), Shor-shor (20.3%), and Hog (18.6%). Only smaller APB abundances were registered in highly mineralized lakes (>100 g L^{-1}) Staroe (8.5×10^4 cells mL^{-1}) and in the SW part of former Aral Sea (1.8×10^5 cells mL^{-1}).

2.4 Discussion

In the study presented, we have identified APB in all the studied lakes, though in different numbers (Figure 2.2). The highest percentages of APB have been observed in shallow saline lakes such as Khilganta or Zanday where phototrophs represented more than one half of total bacteria. Such high numbers were previously only reported in some freshwater mountain lakes in the Czech Republic (Mašín et al. 2008). The concentrations of BChl *a* observed in lakes Alvakhon ($1.6 \mu\text{g L}^{-1}$), Zun-Kholvo ($1.3 \mu\text{g L}^{-1}$) or Gorbunka ($0.6 \mu\text{g L}^{-1}$) are the highest numbers ever reported in an aerobic environment.

An important question which arises from the performed study is whether the observed BChl *a*-containing cells can be classified as purple non-sulfur bacteria or AAPs. According to the current definition, AAPs are aerobic organisms, which both grow and express BChl *a* under fully aerobic conditions. Moreover, in the strict sense, AAPs should not grow under anaerobic conditions. In reality the discrimination of whether a particular organism is a purple non-sulfur or an AAP bacterium is rather difficult, as a number of species exists, which can thrive under both conditions. An example of such ambiguous organism is *Rhodobaca barguzinensis*, a phototrophic organism isolated from a Siberian soda lake, which was classified as a purple non-

sulfur bacterium only after thorough laboratory investigation. These alkalophilic species of APB are tolerant to oxygen and show positive aerotaxis (Boldareva et al. 2008).

Nevertheless, there is evidence indicating that the majority of observed BChl *a*-containing cells were indeed AAPs. Firstly, the water column of the studied lakes was aerobic and contained various forms of oxygenic phytoplankton. The oxic conditions were also documented by high levels of sulfates registered in most of the studied lakes. The only exception was the meromictic Lake Doroninskoe, but even there the density stratification separated aerobic epilimnion from anoxic hypolimnion preventing mixing of the different microbial communities (Figure 2.3 and 2.4).

Secondly, the BChl *a* cellular quotas determined for Transbaikal lakes average at 127 ± 81 ag BChl *a* per cell. This number is very similar to values obtained previously in both AAP cultures and field studies in marine environment (Koblížek et al. 2010). This suggests that observed APB cells are indeed AAPs as the pigment content in anaerobic species are significantly higher.

Finally, a typical feature of AAPs is that they restrict BChl *a* synthesis to periods of darkness (Iba and Takamiya 1989). This physiological behavior together with concoming mortality of the cells leads to large diurnal oscillations in the BChl *a* content (Koblížek et al. 2005, Koblížek et al. 2007). The observation of the same phenomenon in the Khilganta and epilimnion of Doroninskoe lake strongly suggests that the observed phototrophic communities are dominated by AAPs or at least by organisms with very similar physiology to AAPs.

The majority of the studied lakes are terminal lakes of water catchment areas. These lakes have a high input of allochthonous organic matter in the form of plant residuals of steppe vegetation. Carbon isotope fractionation measurements performed previously in Transbaikal lakes indicated the dominant role of allochthonous organic matter recycling in the lakes' carbon cycle (Namsaraev and Namsaraev 2007). This supports the hypothesis that the local phototrophic community lives mainly photoheterotrophically by recycling organic matter rather than photoautotrophically by conducting CO₂ fixation.

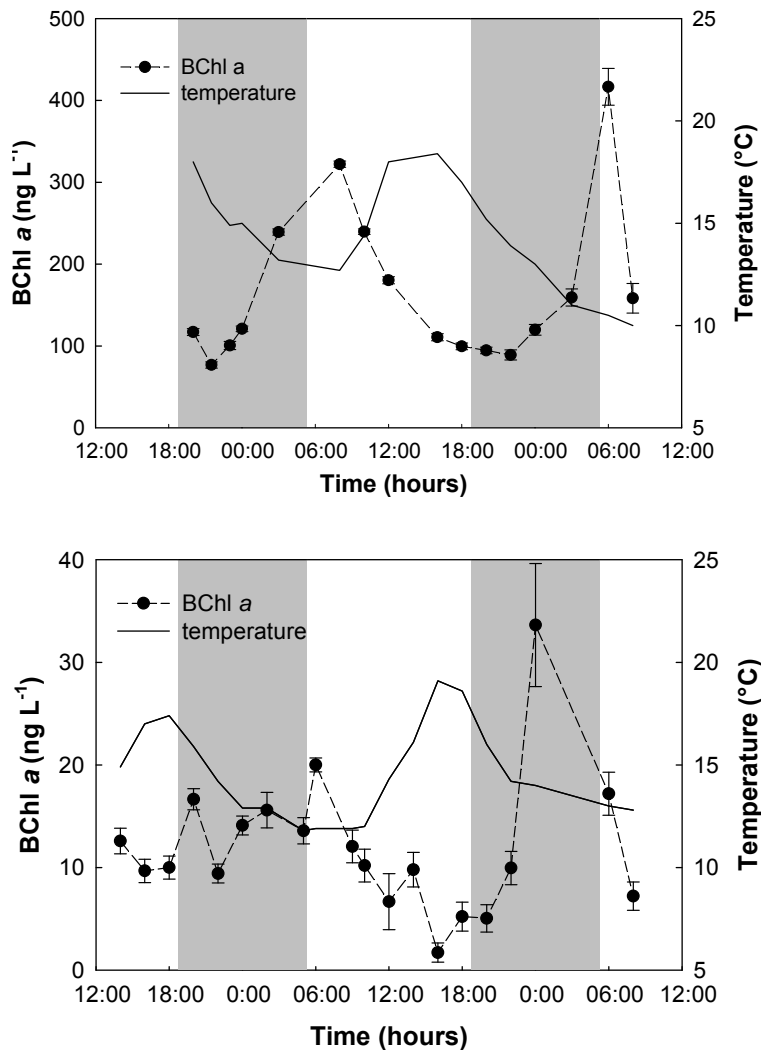


Figure 2.5 Diurnal dynamics of BChl *a* fluorescence signal and water temperature recorded in Khilganta on Aug. 28th – 30th, 2008 (upper panel) and in Doroninskoe lake on Sept. 1st – 3rd 2008 (lower panel).

The correlation analysis performed between the abundance of observed APB and various physio-chemical and biological variables showed no significant linear correlation was found between the mineral composition of lakes and the percentage or abundance of APB. No relationship was found between temperature and APB abundance. However, there was a strong positive correlation between the Chl *a* and APB abundance (see Table 2.4). This is consistent with similar data reported from

the marine environment (Mašín et al. 2006, Sieracki et al. 2006, Jiao et al. 2009). The obvious correlation between BChl *a* content and APB count reflects the fact that BChl *a* is a natural tracer of APB.

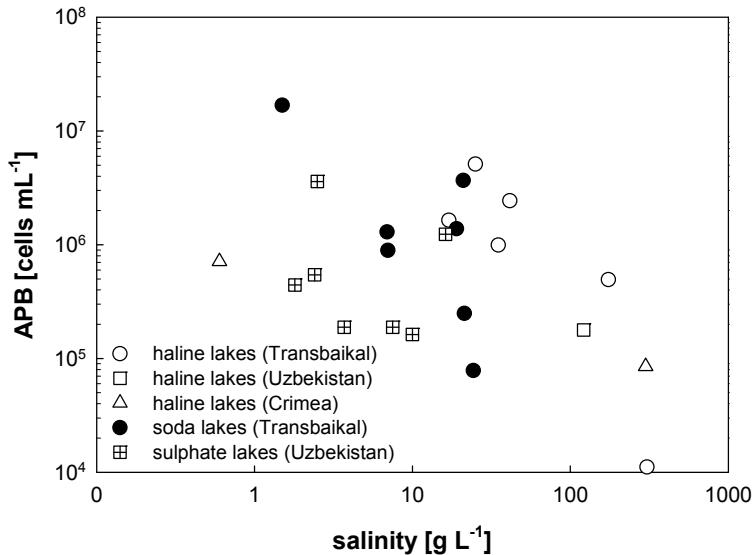


Figure 2.6 The abundance of APB in differently mineralized lakes of Transbaikal region, Central Asia and Crimea. The prevailing compound contributed to the salinity (total mineralization) is depicted.

Another pronounced trend is the smaller amount of APB observed in highly mineralized lakes (100 g L⁻¹) Aral, Tsagan-Nur, Borzinskoe and Staroe. Here APB numbers decrease with increasing mineralization (Figure 2.6). Similar influence of salinity on BChl *a* content has already been reported from saltern ponds in Eilat, Israel (Prášil et al. 2009). We assume that lower oxygen concentration in highly saline lakes may be one of the reasons for considerable lower AAP numbers when compared to the moderately saline waters. A decrease in oxygen content is a fundamental physico-chemical feature of saline waters (Williams 1998). The equilibrium concentration of oxygen at 100 g L⁻¹ salinity is about 55% of the concentration in fresh water while it is about 20% at 300 g L⁻¹. The hypothesis that AAP growth may be suppressed by lower oxygen tension might also be supported by the observation of BChl *a* changes in lake Gorbunka. The lake was sampled twice during the expedition in September 2008.

During the first sampling the lake was almost dry with a mineralization of 164 g L⁻¹,

and the BChl *a* signal was low, corresponding to 38 µg BChl *a* L⁻¹. The second sample was taken 9 days later after heavy rains, which caused a decrease of mineralization to 41.3 g L⁻¹. This change caused more than a 16 times increase of BChl *a* concentration, up to 612 µg L⁻¹. A similar effect has been observed during a simple experiment conducted at lake Borzinskoe. Here, the dilution (3x) of highly saline water sample with distilled water induced a rapid increase in BChl *a* content (not shown).

In conclusion, the AAPs were found in all the studied steppe lakes. The highest numbers were observed in shallow alkaline soda lakes in Transbaikal region, Russia. This fact together with high BChl *a* turnover rates indicates an important role of AAPs in these environments.

Table 2.4 Linear correlation analysis of obtained data for Transbaikal, Uzbek and Crimean lakes. The regression analysis was performed by SigmaPlot for Windows Version 10.0. The table provides the multiple correlation coefficients *R*, the *p* value and number of samples *n*. The significant correlation is marked in bold letters.

Variables	APB abundance			% APB		
	<i>R</i>	<i>p</i>	<i>n</i>	<i>R</i>	<i>p</i>	<i>n</i>
salinity	0.252	0.243	23	0.334	0.111	24
carbonates	0.078	0.722	23	0.030	0.891	24
chlorides	0.320	0.167	20	0.295	0.195	21
sulfates	0.345	0.091	20	0.279	0.220	21
pH	0.215	0.317	22	0.171	0.425	24
BChl <i>a</i>	0.882	<0.0001	13	0.345	0.249	13
Chl <i>a</i>	0.909	<0.0001	11	0.076	0.835	10
total depth	0.230	0.290	23	0.140	0.513	24
temperature	0.265	0.222	21	0.109	0.631	22

2.5 References

- Boldareva EN, Akimov VN, Boychenko VA, Stadnichuk IN, Moskalenko AA, Makhneva ZK, Gorlenko VM (2008) *Rhodobaca barguzinensis* sp nov., a new alkaliphilic purple nonsulfur bacterium isolated from a soda lake of the Barguzin Valley (Buryat Republic, Eastern Siberia). *Mikrobiologiya (engl. trans.)* 77: 206–218

- Boldareva EN, Tourova TP, Kolganova TV, Moskalenko AA, Makhneva ZK, Gorlenko VM (2009a) *Roseococcus suduntuyensis* sp nov., a new aerobic bacteriochlorophyll *a*-containing bacterium isolated from a low-mineralized soda lake of Eastern Siberia. *Mikrobiologiya (engl. trans.)* 78: 92–101
- Boldareva EN, Tourova TP, Kolganova TV, Tourova TP, Kolganova TV, Gorlenko VM (2009b) *Rubribacterium polymorphum* gen. nov., sp nov., a novel alkaliphilic nonsulfur purple bacterium from an Eastern Siberian soda lake. *Mikrobiologiya (engl. trans.)* 78(1): 92–101
- Bryantseva IA, Gorlenko VM, Kompantseva EI, Achenbach LA, Madigan MT (1999) *Heliorestis daurensis*, gen. nov. sp. nov., an alkaliphilic rod-to-coiled-shaped phototrophic heliobacterium from a Siberian soda lake. *Arch Microbiol* 172: 167–174
- Cottrell MT, Ras J, Kirchman DL (2010) Bacteriochlorophyll and community structure of aerobic anoxygenic phototrophic bacteria in a particle-rich estuary. *ISME J*, 4: 945-954
- Eiler A, Beier S, Säwström C, Karlsson J, Bertilsson S (2009) High ratio of bacteriochlorophyll biosynthesis genes to chlorophyll biosynthesis genes in bacteria of humic lakes. *Appl Environ Microbiol* 75: 7221–7228.
- Gorlenko VM, Namsaraev BB, Kulzrova AV, Zavarzina DG, Zhilina TN (1999) The Activity of Sulfate-reducing Bacteria in Bottom Sediments of Soda Lakes of the Southeastern Transbaikal Region. *Mikrobiologiya (engl. trans.)* 68: 580–585
- Gorlenko VM, Buryukhaev SP, Matyugina EB, Borzenko SV, Namsaraev ZB, Bryantseva IA, Boldareva EN, Sorokina DY, Namsaraev BB (2010) Microbial Communities of the Stratified Soda Lake Doroninskoe (Transbaikal Region). *Mikrobiologiya (engl. trans.)* 79: 390–401.
- Grant WD, Sorokin DY (2011) *Distribution and diversity of soda lake alkaliphiles* in Horikoshi K (ed.) *Extremophiles Handbook*, Springer, Dordrecht, pp. 27-54
- Hammer T (1986) *Saline lake ecosystems of the world*. Dr. W. Junk Publishers, Dordrecht, pp. 16–60
- Iba K, Takamiya K (1989) Action spectra for inhibition by light of accumulation of

- bacteriochlorophyll and carotenoid during aerobic growth of photosynthetic bacteria. *Plant Cell Physiol* 30: 471–477
- Jiang H, Dong H, Yu B, Lv G, Deng S, Wu Z, Dai M, Jiao N (2009) Abundance and diversity of aerobic anoxygenic phototrophic bacteria in saline lakes on the Tibetan plateau. *FEMS Microbiol Ecol* 67: 268–278
- Jiao N, Zhang Y, Zeng Y, Hong N, Liu R, Chen F, Wang P (2007) Distinct distribution pattern of abundance and diversity of aerobic anoxygenic phototrophic bacteria in the global ocean. *Environ Microbiol* 9: 3091–3099
- Jones BE, Grant WD, Duckworth AW, Owenson GG (1998) Microbial diversity of soda lakes. *Extremophiles* 2: 191–200
- Koblížek M, Ston-Egiert J, Sagan S, Kolber ZS (2005) Diel changes in bacteriochlorophyll *a* concentration suggest rapid bacterioplankton cycling in the Baltic Sea. *FEMS Microbiol Ecol* 51: 353–361
- Koblížek M, Mašín M, Ras J, Poulton AJ, Prášil O (2007) Rapid growth rates of aerobic anoxygenic phototrophs in the ocean. *Environ Microbiol* 9: 2401–2406
- Koblížek M, Mlčoušková J, Kolber Z, Kopecký J (2010) On the photosynthetic properties of marine bacterium COL2P belonging to *Roseobacter* clade. *Arch Microbiol* 192: 41–49
- Kolber ZS, Plumley FG, Lang AS, Beatty JT, Blankenship RE, VanDover CL, Vetriani C, Koblizek M, Rathgeber C, Falkowski PG (2001) Contribution of aerobic photoheterotrophic bacteria to the carbon cycle in the ocean. *Science* 292: 2492–2495
- Kompantseva EI, Sorokin DYu, Gorlenko VM, Namsaraev BB (2005) The Phototrophic Community Found in Lake Khilganta (an Alkaline Saline Lake Located in the Southeastern Transbaikal Region). *Mikrobiologiya (engl. trans.)* 74: 352–361
- Kompantseva EI, Bryantseva IA, Komova AV, Namsaraev BB (2007) The structure of phototrophic communities of soda lakes of the southeastern transbaikal region. *Mikrobiologiya (engl. trans.)* 76: 211–219
- Labrenz M, Lawson PA, Tindall BJ, Collins MD, Hirsch P (2005) *Roseisalinus*

antarcticus gen. nov., sp. nov., a novel aerobic bacteriochlorophyll a-producing α -proteobacterium isolated from hypersaline Ekho Lake, Antarctica. *Int J Syst Evol Microbiol* 55: 41-47

Mašín M, Zdun A, Stoń-Egiert J, Nausch M, Labrenz M, Moulisová V, Koblížek M (2006) Seasonal changes and diversity of aerobic anoxygenic phototrophs in the Baltic Sea. *Aquat Microbial Ecol* 45: 247–254

Mašín M, Nedoma J, Pechar L, Koblížek M (2008) Distribution of aerobic anoxygenic phototrophs in temperate freshwater systems. *Environ Microbiol* 10: 1988–1996

Namsaraev BB, Namsaraev ZB (2007) *Ecological Features and Microbial Processes of Carbon and Sulfur Cycles in Alkaline Lakes of Mongolia and Transbaikal region* in Galchenko VF (ed.) *Proceedings of Winogradsky Institute of Microbiology*. Nauka, Moscow, pp. 218-237.

Oren A, Pri-El N, Shapiro O, Siboni N (2006) The buoyancy studies in natural communities of square gas-vacuolate archaea in saltern crystallizer ponds. *Saline Systems* 2: 4

Prášil O, Bína D, Medová H, Řeháková K, Zapomělová E, Veselá J, Oren A (2009) Emission spectroscopy and kinetic fluorometry studies of phototrophic microbial communities along a salinity gradient in solar saltern evaporation ponds of Eilat, Israel. *Aquat Microbial Ecol* 56: 285–296

Řeháková K, Zapomělová E, Prášil O, Veselá J, Medová H, Oren A (2009) Composition changes of phototrophic microbial communities along the salinity gradient in the solar saltern evaporation ponds of Eilat, Israel. *Hydrobiologia*, 636(1): 77-88

Shiba T, Shioi Y, Takamiya K, Sutton DC, Wilkinson CR (1991) Distribution and physiology of aerobic bacteria containing bacteriochlorophyll *a* on the east and west coasts of Australia. *Appl Environ Microbiol* 57: 295–300

Sieracki ME, Gilg IC, Thier EC, Poulton NJ, Goericke R (2006) Distribution of planctonic aerobic anoxygenic photoheterotrophic bacteria in the northwest Atlantic. *Limnology and Oceanography* 51(1): 38-46

Sørensen K, Canfield DE, Oren A (2004) Salinity Responses of Benthic Microbial

- Communities in a Solar Saltern (Eilat, Israel). *Appl Env Microbiol* 70: 1608-1616
- Waidner LA, Kirchman DL (2007) Aerobic Anoxygenic Phototrophic Bacteria Attached to Particles in Turbid Waters of the Delaware and Chesapeake Estuaries. *Appl Environ Microbiol* 73: 3936–3944
- Williams WD (1998) Management of inland saline waters. Guidelines of Lake Management, Vol. 6, ILEC/UNEP, Kusatsu, p.23
- Yurkov VV, Csotonyi JT (2009) *New light on aerobic anoxygenic phototroph* in Hunter CN, Daldal F, Thurnauer MC, Beatty JT (eds.) *The purple phototrophic bacteria*. Springer Verlag, New York, pp. 31–55
- Yurkova N, Rathgeber C, Swiderski J, Stackebrandt E, Beatty JT, Hall KJ, Yurkov V (2002) Diversity, distribution and physiology of the aerobic phototrophic bacteria in the mixolimnion of a meromictic lake. *FEMS Microbiol Ecol* 40: 191–204
- Yutin N, Suzuki MT, Teeling H, Weber M, Venter JC, Rusch DB, Béjà O (2007) Assessing diversity and biogeography of aerobic anoxygenic phototrophic bacteria in surface waters of the Atlantic and Pacific Oceans using the Global Ocean Sampling expedition metagenomes. *Environ Microbiol* 9: 1464–1475
- Zavialov PO, Ni AA, Kudyshkin TV, Ishniazov DP, Tomashevskaya IG, Mukhamedzhanova D (2009) Ongoing changes of ionic composition and dissolved gases in the Aral Sea. *Aquatic Geochem* 15: 263–275

2.6 Supplements

2.6.1 Mat and planktonic communities of Siberian steppe lakes

Table S2.1 The ratio of APB and cyanobacteria in mat prokaryotic communities. The lakes are located in the Great Steppe in Transbaikal Region, Russia and Mongolia. Samples were taken by Dr. Ekaterina Boldareva in August 2009 during the expedition organised by prof. Gorlenko, Institute of Microbiology RAS, Moscow. (n.d. = not detected).

lakes	region	APB	cyanobacteria	pH	mineralization	temperature
		(%)	(%)		(g L ⁻¹)	(°C)
Doroninskoe	Transbaikal	57.4	2	n.d.	28	9.7
Galuuta Nuur	Mongolia	90.6	0	9.7	50	21.2
Gorbunka	Transbaikal	28.5	0	8.2	200	n.d.
Khilganta	Transbaikal	27.3	0.76	n.d.	n.d.	n.d.
Zun-Kholvo	Transbaikal	20.4	0.43	n.d.	n.d.	n.d.
Zun-Torei	Transbaikal	25.7	1.05	9.5	7	n.d.

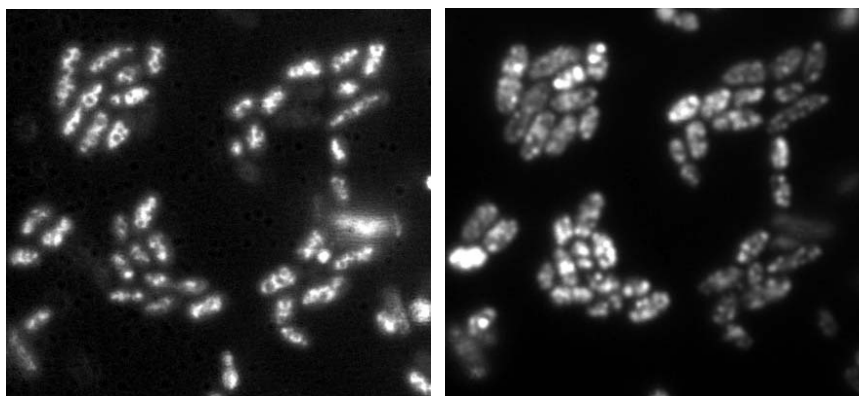


Figure S2.1 The phototrophic bacteria present in Galuuta Nuur. The water sample were intensively pink coloured. The phototrophic bacteria created 91% of prokaryotic community here. The images were recorded in DAPI (left) and IR channel (right).

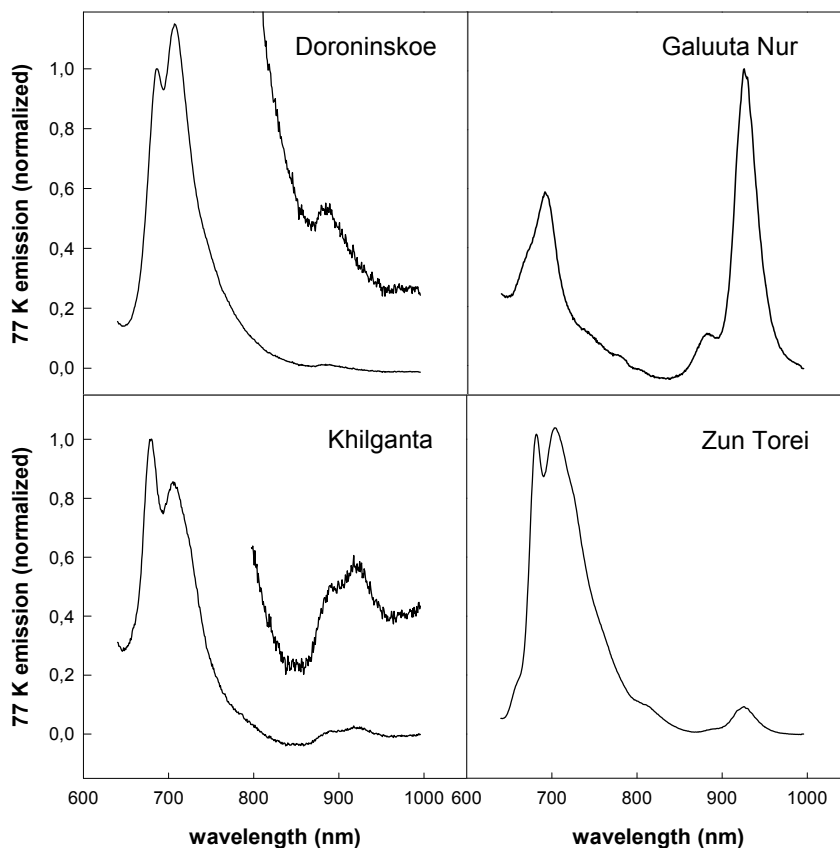


Figure S2.2 The low temperature (77K) emission spectra of the mat (Doroninskoe, Khilganta, Zun-Torei) and planktonic (Galuuta Nur) communities of Siberian lakes. The samples were taken in August 2009. The spectra were obtained after excitation by a 455 nm light-emitting diode. They are normalized to 680 nm. In the plankton of Galuuta Nur, 18×10^6 BChl *a*-containing cells per mL were found. (Figure S2.1). In mats, the APB represented 20.4 – 90.6% of the prokaryotic community (Table S2.1). The emission peaks at 890 nm in Doroninskoe, 885 and 925 nm in Galuuta Nur, 891 and 925 nm in Khilganta, and 776 and 925 nm in Zun-Torei indicated the presence of phototrophic bacteria in the studied lakes.

2.6.2 Saltern ponds in Eilat, Israel

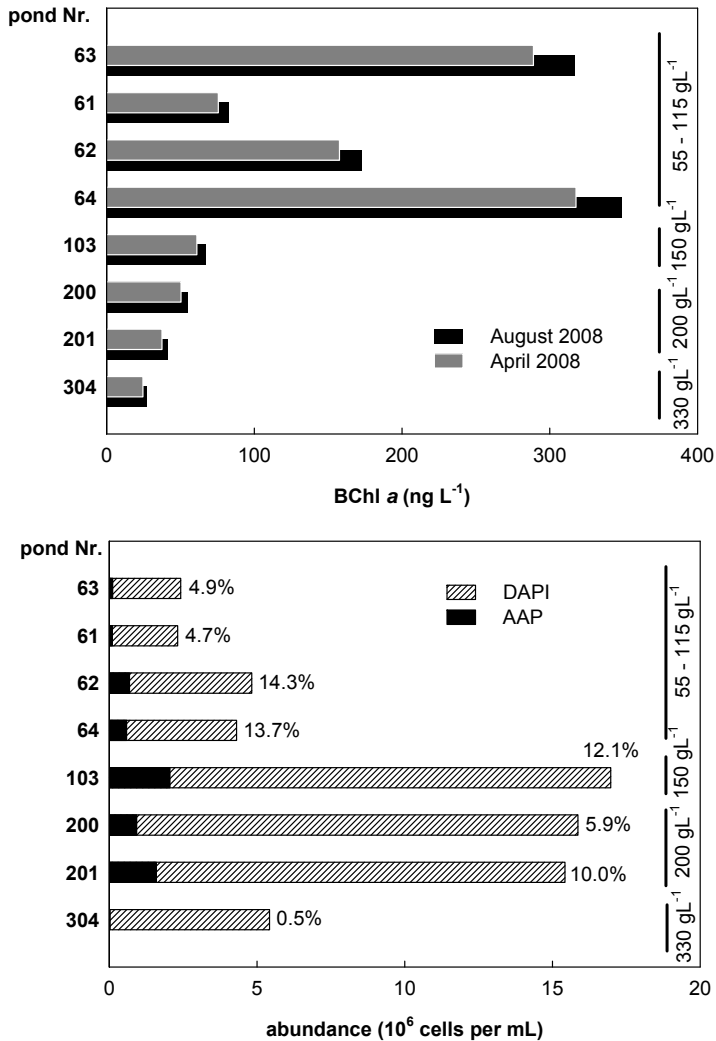


Figure S2.3 Eight saltern evaporation ponds located near to Eilat, Israel were surveyed in April and August 2008. The site description and chemical parameters of studied sites are described in Prášil et al. 2009 and Řeháková et al. 2009. Generally, the BChl *a* concentration detected by kinetic fluorometry (upper panel) decreased with increasing salinity. The BChl *a* concentration was slightly higher in August (27 – 349 ng L⁻¹) than in April (24 – 317 ng L⁻¹). The maximum signals were observed in the pond with a salinity at 114 (94 g L⁻¹) in August, whereas the minimum was found in the most saline pond which almost corresponded to a crystallized brine. The lower panel shows the abundance and ratio of APB in eight saltern ponds in August 2008. The shape and size of cells in pond Nr. 304 with salinity reaching a brine (330 g L⁻¹), their intensive BChl *a* pigmentation and the low amount of dissolved oxygen indicated that these bacteria belong to anaerobic groups of anoxygenic phototrophs. The presence of APB in this pond was earlier described in Oren et al. (2006) in total amount of $2.4 \pm 0.3 \times 10^7$ cells per mL.

3. Anoxygenic Phototrophic Bacteria in Polar Regions

3.1 Summary

The distribution of AAPs was studied in polar freshwater lakes on Svalbard and James Ross Island, in the maritime Antarctica using kinetic fluorometry and epifluorescence microscopy methods. AAPs were found in two thirds of studied lakes. Their abundance amounted to 1.7×10^5 (Arctic) and to 7.9×10^6 (Antarctica) cells per mL. In Svalbard lakes, the phototrophic as well as heterotrophic bacterial community seemed to be limited by nitrogen. Lake water temperature can reach up to 11°C during the polar summer, which has been proved to be sufficient for the AAP growth. Water temperature under 5°C limited the AAP abundance.

3.2 Introduction

The majority of studies on AAPs have been conducted in tropical and temperate regions. Little is known about AAP bacteria from polar regions. The presence of AAPs in polar lakes was first documented by Labrenz et al. (2005) who isolated four AAP strains from the meromictic Ekho Lake and microbial mats (Labrenz et al. 2005). In the same year, Schwalbach and Fuhrman (2005) attempted to enumerate AAPs in marine Antarctic samples using the qPCR. Based on the analyses targeting *pufM* gene they suggested that the abundance of AAPs in the sea water was very low (0.01- 0.06%). The *pufM* gene was also used to describe the distribution of AAPs in ice-covered regions of the Ross Sea, Antarctica, where AAPs were found more abundant in the open water than in the ice (Koh et al. 2011).

The study of the composition of the prokaryotic community in the Chukchi Sea (Arctic) reported AAP abundance of 0.13×10^6 cells per mL in the summer decreasing four fold between the seasons (Cottrell et al. 2009). Interestingly, the contribution of AAP bacteria to the total prokaryotic community did not change during the year and made up 5 to 8% of the prokaryotes. Surprisingly, AAPs appeared to compete successfully with heterotrophic bacteria during the Arctic winter darkness below the ice. The *pufM* genes identified in the Arctic Ocean are phylogenetically distinct from

genes seen in lower-latitude waters and also from those in Antarctic Lake Fryxell with a highest similarity of 83% (Cottrell et al. 2009).

Freshwater AAPs have been found in a spring in the Canadian high Arctic (Perreault et al. 2008). The total microbial numbers were lower than in the nearby Arctic Ocean (10^7 cells per mL). The sequence analysis of *pufM* genes indicated that these AAPs were distinct from those found in marine systems.

In this study we describe the bacterial composition of polar lakes on Svalbard (Spitsbergen) and James Ross Island (Antarctica) to enlarge the knowledge about planktonic communities in polar regions.

3.3 Methods

3.3.1 Sampling

The Arctic sampling sites were located in Petuniabukta (Billefjorden, Svalbard). The annual mean temperature is -5.8°C ($+6.2^{\circ}\text{C}$ in July) and precipitation 200 mm. Seventeen lakes with different geologies were studied in the Arctic high-season in July 2011 (Table 3.1). Different types of lakes have been identified in the area with a predominance of small lakes on recently deglaciated moraines (Nordenskiöld 1–5, Sven 1–5). Some older lakes with a high amount of organic matter sedimentation were found as well (Brucebyen, Ebba). The artificial water body Pyramiden 1 and 2 served as a local water source. Lakes Mathiesundalen 1–3 evolved in the area with anhydrite and gyps bedrock formation. At the time of sampling, the lakes were neutral or slightly alkaline with a temperature of $5.1 - 11.2^{\circ}\text{C}$.

The Antarctic lakes chosen for our study are situated on James Ross Island, near the Antarctic Peninsula, maritime Antarctica (Table 3.3). Sampling was done during the Antarctic summer in January and February 2009. Most of the localities were stable and shallow lakes. The water temperature spanned between $0.3 - 9.2^{\circ}\text{C}$.

The surface water layer was sampled and found to be fully oxygenated (86 – 110% and 86 – 180% oxygen saturation in Svalbard and James Ross Island lakes resp.). Samples for infra-red microscopy were collected in sterile, plastic test tubes, fixed with

2% formaldehyde. All samples were stored at 4°C. Basic physico-chemical parameters were measured in the field (Table 3.1 and 3.3). The nutrient analysis was performed within one month in the laboratory (Table 3.2 and 3.4).

3.3.2 Fluorometry

BChl *a* concentration was measured in the field with a portable fluorometer (AOM 2800, prototype MUF, P.S.I. Brno). The photodiode detector was protected by a Schott glass RG850 filter. The fluorescence transient was induced using two Luxeon light emitting-diodes with a wavelength of 505 nm. The volume of the cylindrical measuring cuvette is 50 mL. Before starting the measurement, diuron (3-(3,4-dichlorophenyl)-1,1-dimethylurea) was added to samples to inhibit the Chl-containing phytoplankton. The BChl *a* concentration was estimated from the area under the induction curve. The total duration of the protocol was 200 ms. In total, 30 measurements were averaged to get the actual BChl *a* concentration. The device was calibrated using a diluted culture of *Rubrivivax gelatinosus*.

3.3.3 Epifluorescence microscopy

The composition of the Antarctic planktonic community was analyzed using the epifluorescence microscopy technique as described in Chapter 2, section 2.2.2. The Svalbard lakes samples were analysed using a Zeiss Axio Imager.D2 microscope equipped with a Plan-Apochromat 63x/1.46 Oil Corr objective and a Hamamatsu EM CCD camera C9100-02.

The DAPI was dissolved in a 3:1 mixture of Citifluor AF1 and Vectashield with a final concentration of 1 µg mL⁻¹. The total DAPI stained bacteria were recorded and enumerated in the blue part of the spectrum (5 – 10 ms exposure). Red chlorophyll *a* autofluorescence was then recorded to identify Chl *a*-containing organisms (5 – 10 ms exposure), followed by the capture of an infrared emission (> 850 nm) image, showing both anoxygenic phototrophs and Chl *a*-containing objects (100 – 200 ms exposure). The acquired images were saved and analysed semi-manually with the aid of AxioVison software to distinguish the number of heterotrophic bacteria, cyanobacteria

Table 3.1 The geographical and physico-chemical parameters of studied Svalbard lakes. (the Chl α concentration was estimated using the HPLC analysis, the BChl α one from fluorometric data; n.d. = no data).

Lake	Latitude (S)	Longitude (W)	Altitude (m)	Type of lake	Temp. (°C)	pH	Conductivity (mS m ⁻¹)	O ₂ (mg L ⁻¹)	Chl α (μ g L ⁻¹)	BChl α (ng L ⁻¹)
Brucebyen	78°38.28'	16°44.15'	8	organogenic	10.3	6.8	85	13.0	24.0	67.1
Ebba	78°44.59'	16°36.84'	10	organogenic	9.6	8.9	20	11.8	4.6	14.7
Mathiesondalen 1	78°33.80'	16°34.36'		karst	5.1	8.2	142	n.d.	0.4	2.5
Mathiesondalen 2	78°33.77'	16°35.29'	35	karst	10.2	8.4	55	n.d.	1.2	16.6
Mathiesondalen 3	78°33.58'	16°36.31'		karst	11.0	8.7	20	n.d.	2.1	4.2
Nordenskiöld 1	78°38.32'	16°49.60'		moraine	9.5	8.5	25	11.5	n.d.	n.d.
Nordenskiöld 2	78°38.32'	16°49.69'		moraine	8.5	8.6	16	12.4	10.8	11.9
Nordenskiöld 3	78°38.30'	16°49.96'		moraine	10.2	8.4	41	11.8	n.d.	n.d.
Nordenskiöld 4	78°38.31'	16°49.06'		moraine	6.0	8.3	39	14.0	1.3	1.2
Nordenskiöld 5	78°38.28'	16°50.33'		moraine	9.6	8.7	19	11.7	n.d.	n.d.
Pyramiden 1	78°39.25'	16°11.97'	111	antropogenic	7.0	8.2	12	13.1	2.3	1.2
Pyramiden 2	78°39.00'	16°11.03'	130	antropogenic	8.9	8.3	9	12.2	1.7	0
Sven1	78°43.79'	16°24.57'		moraine	8.0	8.5	18	10.3	1.7	0
Sven2	78°43.61'	16°24.46'		moraine	8.5	8.6	30	10.5	1.8	0
Sven3	78°43.61'	16°24.86'		moraine	11.2	8.6	44	9.9	4.0	6.6
Sven4	78°43.63'	16°24.02'		moraine	9.6	8.5	45	n.d.	1.6	0
Sven5	78°43.68'	6°24.45'		moraine	8.5	8.5	30	n.d.	0.1	0

Table 3.2 The geographical and physico-chemical parameters of Svalbard lakes.

Lake	N-NO ₂ (µg L ⁻¹)	N-NO ₃ (µg L ⁻¹)	TN (µg L ⁻¹)	P-PO ₄ (µg L ⁻¹)	TP (µg L ⁻¹)	Cl ⁻ (µg L ⁻¹)
Ebba	<0.11	<0.23	604	16.2	37.8	16.0
Mathiesondalen 1	<0.11	7.48	254	20.1	56.1	6.1
Mathiesondalen 2	1.69	3.83	170	17.5	42.0	3.4
Mathiesondalen 3	<0.11	3.85	227	12.6	34.8	7.9
Nordenskiöld 2	0.11	0.23	142	12.1	29.3	10.5
Nordenskiöld 4	<0.11	<0.23	271	12.7	32.8	4.9
Pyramiden 1	<0.11	<0.23	154	10.2	32.1	2.6
Pyramiden 2	<0.11	<0.23	176	10.3	22.7	5.1
Sven 1	2.13	3.14	127	12.1	29.1	2.7
Sven 2	0.17	3.31	104	27.0	47.3	5.1
Sven 4	<0.11	2.37	206	20.1	49.6	7.0
Sven 5	<0.11	<0.23	172	18.8	43.2	4.2

and anoxygenic phototrophs for each sample. For each individual sample, 10 – 12 frames were recorded and analysed (~1000 – 1200 DAPI-stained cells).

3.3.4 Data analysis

The analysis was carried out using the program CANOCO for Windows, version 4.56 (Lepš and Šmilauer 2003). The plots were made using the program CanoDraw distributed with the CANOCO software. Principal component analysis (PCA) and redundancy analysis (RDA) were chosen for these data sets. The data was log transformed, centred and standardized by species. 999 permutations in the Monte Carlo test were used to test the significance of the first axis and/or all axes.

For the principal component analysis, the measured environmental characteristics were chosen as the ‘species‘ in CANOCO for Windows 4.0 terminology, and abundances of aerobic phototrophic and heterotrophic bacteria were passively plotted into the diagram. The abundance of both heterotrophic and phototrophic bacteria and the measured physio-chemical parameters were used in the redundancy analysis as species and environmental variables respectively. The linear correlation analysis was done using SigmaPlot 10.0.

Table 3.3 The geographical and physico-chemical parameters of James Ross Island lakes (n.d. = no data).

Lake	Latitude (S)	Longitude (W)	Altitude (m)	Type of the lake	Temperature (°C)	pH	Conductivity (mS m ⁻¹)	O ₂ (mg L ⁻¹)	Chl <i>a</i> (µg L ⁻¹)
Black	63°57'58"	57°52'60"	224	stable shallow	8.3	7.89	13	12.0	1.5
Blue-green	63°54'54"	57°57'25"	201	thermokarst	5.5	7.81	9	16.4	2.6
Clearwater 1	64°01'36"	57°42'13"	245	stable shallow	6.8	8.68	98	11.6	1.1
Clearwater 2	64°01'33"	57°42'48"	245	stable shallow	8.0	8.9	54	11.2	0.6
Clearwater 3	64°01'48"	57°42'59"	245	stable shallow	9.2	8.32	48	10.7	0.7
Clearwater 4	64°01'58"	57°43'41"	250	stable shallow	5.0	8.56	400	10.9	0.9
Cyanobacterial	63°57'56"	57°54'25"	199	stable shallow	7.1	8.72	10	13.2	5.9
Federico	63°56'17"	57°58'50"	414	cirque	0.3	9.53	8	23.0	6.7
Ginger	63°52'29"	57°48'10"	275	seasonal	n.d.	7.18	3	11.5	0.5
Noodle	64°02'02"	57°41'00"	170	stable shallow	7.2	8.5	109	11.2	3.7
Omega 1	62°51'40"	57°48'50"	250	thermokarst	n.d.	7.73	7	11.3	4.1
Vondra 1	63°58'41"	57°54'10"	238	stable shallow	7.9	7.65	6	12.5	6.6
Vondra 2	63°57'36"	57°54'23"	239	stable shallow	7.4	7.71	5	12.9	7.1
Vondra 3	63°57'33"	57°54'08"	239	stable shallow	7.7	7.98	7	12.5	1.9
Vondra 4	63°57'37"	57°53'55"	238	stable shallow	6.8	7.43	6	12.5	2.5

Table 3.4 The nutrient analysis of James Ross Island lakes.

Lake	N-NO ₂ (µg L ⁻¹)	N-NO ₃ (µg L ⁻¹)	TN (mg L ⁻¹)	SRP (µg L ⁻¹)	TP (µg L ⁻¹)	DOC (mg L ⁻¹)	TC (mg L ⁻¹)	Cl ⁻ (mg L ⁻¹)	SO ₄ ²⁻ (mg L ⁻¹)
Black	0.20	0.062	0.6	3.6	13.6	5.1	17.8	14.8	2.5
Blue-green	0.40	0.023	0.2	54.5	78.9	0.8	11.3	4.1	2.6
Clearwater 1	0.30	0.02	1.2	5.8	30.4	9.1	42.2	181.4	7.3
Clearwater 2	0.20	0.04	0.6	4.8	15.1	5.2	25.6	103.7	17.1
Clearwater 3	0.10	0.01	0.6	4.4	12.1	4.5	22.2	104.0	15.2
Clearwater 4	0.20	0.00	1.0	4.0	17.9	7.4	66.2	1128.8	104.4
Cyanobacterial	0.50	0.04	0.3	54.9	85.8	1.3	13.9	3.5	2.5
Federico	1.50	0.02	0.3	64.2	94.6	1.7	8.3	7.0	3.2
Ginger	0.10	0.04	0.2	63.0	88.1	0.7	8.0	3.3	1.1
Noodle	0.10	0.003	1.3	8.5	52.8	7.6	41.1	230.2	22.5
Omega 1	0.10	0.01	0.3	113.4	125.7	0.7	8.7	7.5	2.1
Vondra 1	0.20	0.02	0.4	4.6	25.5	2.8	10.5	3.6	1.4
Vondra 2	0.30	0.03	0.2	17.6	36.1	1.3	7.0	4.2	1.7
Vondra 3	0.04	0.08	0.2	4.3	11.3	1.3	9.7	4.1	1.5
Vondra 4	0.20	0.03	0.2	36.4	80.7	0.9	6.4	3.4	5.3

3.4 Results and discussion

3.4.1 The abundance of anoxygenic phototrophic and heterotrophic bacteria

Anoxygenic phototrophic bacteria (APB) were registered in eleven of seventeen lakes on Svalbard and in fourteen of seventeen studied lakes on James Ross Island using epifluorescence microscopy (Figure 3.1). The bacterial morphotypes were rods of varying length (typically 1 – 3 μm). Their abundance amounted to 1.7×10^5 cells per mL which was 0 – 29.2% (median 0.3%) of the prokaryotic community. Surprisingly, the APB were observed in eight moraine Arctic lakes in orders 10^3 – 10^5 . These lakes were located in a deglaciated area formed approx. 100 – 150 years ago.

The heterotrophic bacteria were observed in sixteen from seventeen studied Svalbard lakes with a highest abundance of 2.5×10^6 (median 2.2×10^5).

The *in situ* measured BChl *a* concentration measured in Svalbard lakes ranged from 0 – 67 ng L^{-1} with the maximum found in the organogenic lakes in Brucebyen. A positive BChl *a* signal was detected in nine of seventeen studied lakes. The highest BChl *a* concentration was comparable to that found in mesotrophic mountain lakes of Central Europe (Mašin et al. 2008).

APB were observed in fourteen of fifteen studied lakes on James Ross Island (Figure 3.1). Their highest abundance was found in Lake Vondra 1 in 7.9×10^5 cells per mL. They represented 0 to 21.4% (median 1.6%) of prokaryotic community. The occurrence of phototrophic bacteria in the Antarctic was predominantly in stable shallow lakes.

In the lakes on James Ross Island, heterotrophic cells were found in fifteen lake water samples in maximal abundances of one order higher than in Svalbard lakes (0 – 36.9×10^6 cells per mL, median 1.2×10^6 cells per mL). The most common morphotypes of heterotrophic bacteria were rods (1 – 5 μm), and filamentous bacteria (up to 12 μm). Further, some sickle-shape forms were recorded.

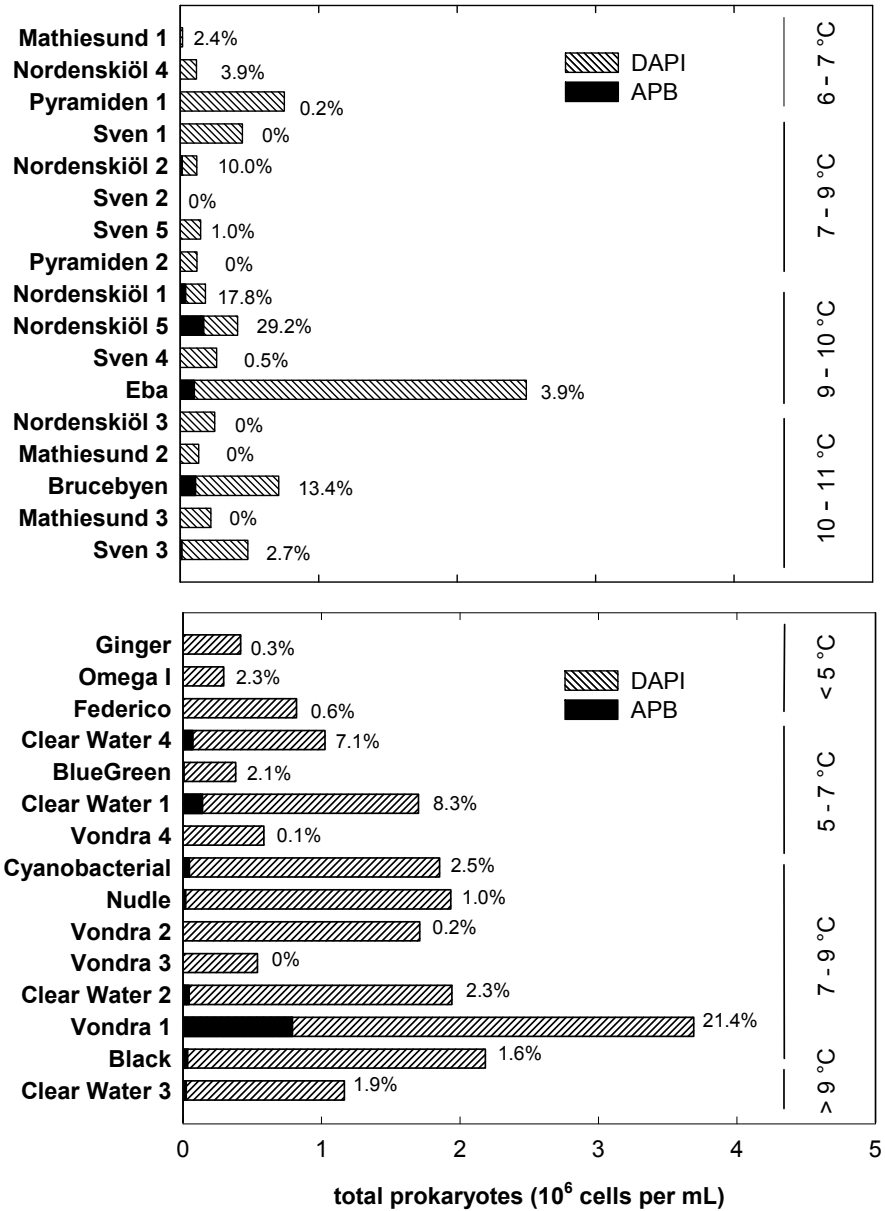


Figure 3.1 The abundances of heterotrophic bacteria (DAPI, hatched column) and anoxygenic phototrophic bacteria (APB, black column) found in Svalbard (upper panel) and Antarctic freshwater lakes on James Ross Island (lower panel) are plotted here. The percentage expresses the fraction of phototrophs in the planktonic prokaryotic community. The lakes are ordered according to increasing water temperature.

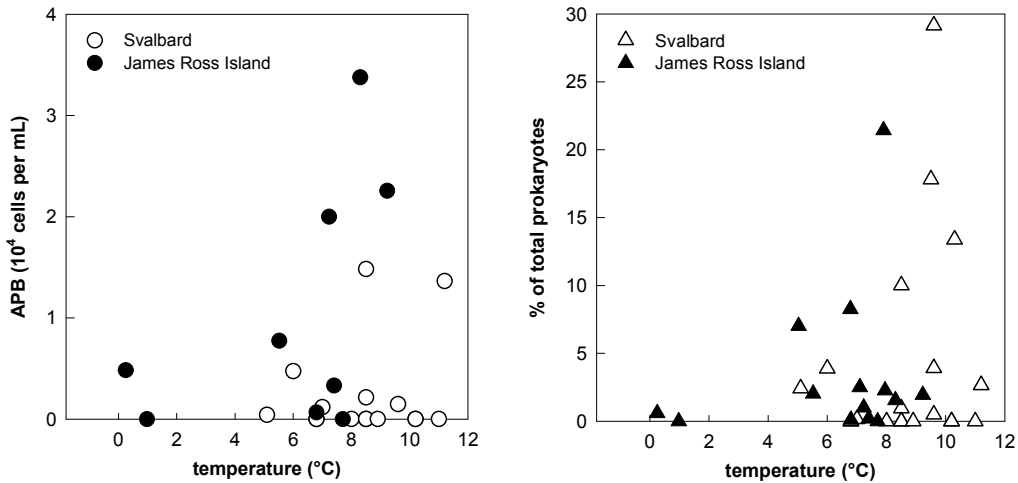


Figure 3.2 The abundance of phototrophic anoxygenic bacteria (left) and their ratio (right) in prokaryotic community vs temperature of Svalbard lakes (white circles) and lakes on James Ross Island (black circles). The abundance of APB restricted in the colder conditions ($<4^{\circ}\text{C}$).

The numbers of APB bacteria in orders 10^5 cells per mL found in Svalbard and James Ross Island lakes are similar to data reported from oligotrophic parts of the southern Pacific Ocean (Kolber et al. 2001), euphotic zones of the Atlantic Ocean (Koblížek et al. 2007), and from the Arctic Ocean (Cottrell et al. 2009).

The abundance of APB bacteria seems affected by temperature (Figure 3.2). APB were more abundant in warmer water, under 5°C , their abundance was only minimal.

3.4.2 Statistical analyses

The linear correlation analysis suggested that the bacterial community in the Svalbard lakes was limited by nitrogen concentration. The abundance of phototrophic as well as heterotrophic bacteria were positively linearly correlated with the TN:TP ratio and total nitrogen concentration in the studied Svalbard lakes (Table 3.5). The APB abundance and their ratio in prokaryotic community increased with increasing chlorophyll *a* concentration ($R=0.732$, $p<0.001$; $R=0.744$, $p<0.001$ resp.). This is in accordance with studies (see Chapter 2, Section 2.3) reporting that higher temperature and higher Chl *a* concentration implied a higher AAP abundance. In contrast, in James Ross Island lakes the only significant correlation ($R = 0.557$, $p < 0.031$) was found between soluble

reactive phosphorus concentration and heterotrophic abundance (DAPI).

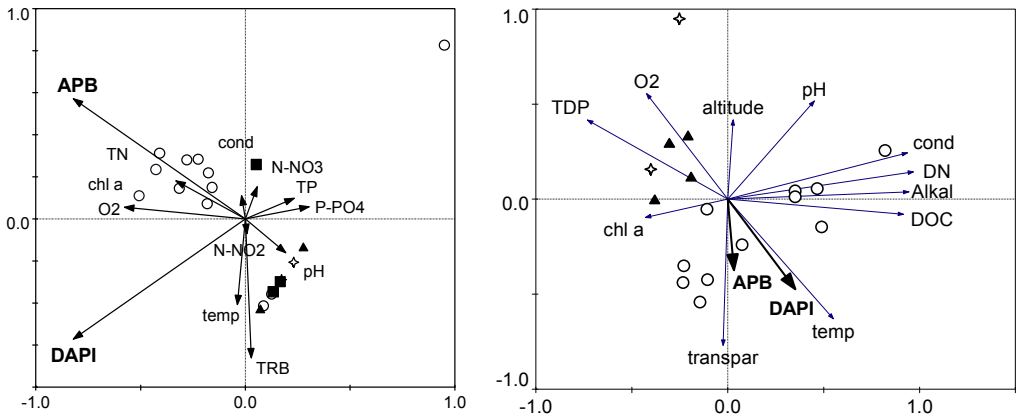


Figure 3.3 Principal component analysis (PCA) on correlation matrix. The triplot shows the relationship among measured environmental variables taken as ‘species’ in the analysis. The abundance of aerobic phototrophic bacteria (AAP) and heterotrophic bacteria (DAPI) is passively projected into the diagram. The circles represent the sample scores of the basic type of (A) Svalbard lakes, the Arctic (moraine - circles, antropogenic - triangles, anhydride - squares, organogenic - stars) and (B) James Ross Island lakes, the Antarctica (thermokarst – black triangles, stable shallow – circles, cirque – stars).

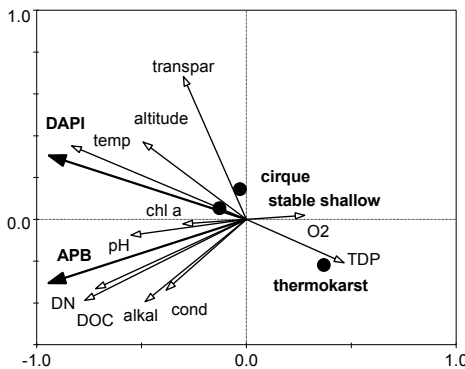


Figure 3.4 Redundancy analysis of James Ross Island lakes data set. The phototrophic bacteria (APB) and heterotrophic bacteria (DAPI) (in analysis represented species) are shown here together with measured environmental variables and basic type of lakes.

The observed relationships were further studied using principal component analysis. The Svalbard moraine lakes were characterised by higher total nitrogen, chloride, chlorophyll *a*, and oxygen concentrations than organogenic and antropogenic lakes (Figure 3.3A). These parameters were positively correlated with APB abundance.

In the PCA analysis of James Ross Island lakes, the first axis may be interpreted as

amount of dissolved ions. The thermokarst type of lake is positively correlated with oxygen and total dissolved phosphorus concentration (Figure 3.3B). The bacterial abundances may be influenced by water transparency and temperature. Higher bacterial numbers should be expected in stable shallow lakes.

In RDA of Antarctic lakes data set, the first axis explained 89% of variance and its permutation test was significant ($F = 7.929$, $p = 0.007$, Figure 3.4). This might suggest that the RDA model may be performed with our data, although only two species were used in the analysis. The abundance of heterotrophic bacteria is positively correlated with temperature, whereas the abundance of APB was influenced by more environmental factors, such as dissolved carbon concentration, dissolved nitrogen concentration, pH, and conductivity. To find out which variable could explain the highest portion of Antarctic data set variability, we used the manual forward selection of environmental variables (the type of lakes coded by dummy variables was not used in the analysis) where temperature ($p = 0.024$) and the altitude ($p = 0.036$) together explained 46% of variability. In the case of the Svalbard lakes data set, the permutation test of first axis in redundancy analysis was not significant.

3.5 Conclusions

APB were found in two thirds of studied polar lakes of Svalbard and James Ross Island. In some of the lakes their abundance reached up to 7.9×10^5 (median 1.5×10^4) and they represented up to 21% of the prokaryotic community. They were more abundant in lakes with a higher total nitrogen, chlorophyll *a*, oxygen concentration, and temperature. Their numbers were limited in the lakes with a temperature lower than 5°C. Based on the fact that the observed organisms originated from fully aerobic lakes we assume that they were mostly AAP bacteria. Thus, AAPs appear to have adapted to the conditions present in the polar environments.

Table 3.5 The linear correlation analysis of studied lakes. Only the significant correlation is shown here (DAPI/APB - abundance of heterotrophic/APB bacteria in cells per mL; %APB - ratio of APB of total prokaryotes; R - correlation coefficient; n - number of samples).

Lakes	x	y	R	p	n
Svalbard lakes	DAPI	TN	0.711	0.0064	12
	DAPI	AAP	0.456	0.0214	24
	DAPI	TN:TP	0.713	<0.0001	12
	APB	TN	0.748	<0.0001	12
	APB	chl _a	0.732	<0.0001	21
	APB	TN:TP	0.706	<0.0001	12
	%APB	TN	0.925	<0.0001	12
	%APB	chl _a	0.744	<0.0001	21
	%APB	TN:TP	0.876	<0.0001	12
James Ross Island lakes	DAPI	SRP	0.557	0.031	15

Acknowledgements I would like to express my thanks to Linda Nedbalová (Faculty of Science, Department of Ecology, Charles University in Prague; Institute of Botany, CAS, Třeboň) for providing the fixed samples from Antarctic lakes, their basic physio-chemical parameters, and results from nutrient analysis and for her kindly supervising in the field polar course in Spitsbergen. The sampling of Arctic lakes was supported by the research project of the Ministry of Education, Sports and Youth of the Czech Republic – LM2010009 CzechPolar.

3.6 References

- Cottrell MT, Kirchman DL (2009) Photoheterotrophic microbes in the Arctic Ocean in summer and winter. *Appl Environ Microbiol* 75: 4958-4966
- Koblížek M, Mašín M, Ras J, Poulton AJ, Prášil O (2007) Rapid growth rates of aerobic anoxygenic phototrophs in the ocean. *Environ Microbiol* 9: 2401–2406
- Koh EY, Phua W, Ryan KG (2011) Aerobic anoxygenic phototrophic bacteria in Antarctic sea ice and seawater. *Environ Microbiol Reports* 3: 710-716
- Kolber ZS, Plumley FG, Lang AS, Beatty JT, Blankenship RE, VanDover CL, Vetriani C, Koblížek M, Rathgeber C, Falkowski PG (2001) Contribution of aerobic photoheterotrophic bacteria to the carbon cycle in the ocean. *Science* 292: 2492–

- Labrenz M, Lawson PA, Tindall BJ, Collins MD, Hirsch P (2005) *Roseisalinus antarcticus* gen. nov., sp. nov., a novel aerobic bacteriochlorophyll a-producing α -proteobacterium isolated from hypersaline Ekho Lake, Antarctica. *Int J Syst Evol Microbiol* 55: 41-47
- Lepš J, Šmilauer P (2003) *Multivariate Analysis of Ecological Data using CANOCO*. University Press, Cambridge
- Mašín M, Zdun A, Stoń-Egiert J, Nausch M, Labrenz M, Moulisová V, Koblížek M (2006) Seasonal changes and diversity of aerobic anoxygenic phototrophs in the Baltic Sea. *Aquat Microbial Ecol* 45: 247–254
- Perreault NN, Greer CW, Andersen DT, Tille S, Lacrampe-Couloume G, Lollar BS, Whyte LG (2008) Heterotrophic and autotrophic microbial populations in cold perennial springs of the high Arctic. *Appl Environ Microbiol* 74: 6898-6907
- Schwalbach MS, Fuhrman JA (2005) Wide-ranging abundances of aerobic anoxygenic phototrophic bacteria in the world ocean revealed by epifluorescence microscopy and quantitative PCR. *Limnol Oceanogr* 50: 620–628

4. Thermostability of Anoxygenic Reaction Centers

This chapter is based on the manuscript:

Structural basis of thermostability in purple bacterial reaction centers

Hana Medová^{1,2}, David Kaftan¹, Michal Koblížek^{1,2}

4.1 Summary

Anoxygenic phototrophic bacteria are one of the oldest life forms on Earth. During their long evolution these organisms had to adapt to diverse environmental conditions including a wide span of ambient temperatures. Here we investigated the thermal stability of photosynthetic reaction centers in purple phototrophic bacteria using infrared kinetic fluorometry and computer modeling. It was found that purple reaction centers had their forward electron transport optima between 40 – 75°C, approximately 20°C above their optimum growth temperature. Moreover, their reaction centers exhibited a remarkable stability of charge separation which stayed functional up to at least 50°C. Molecular dynamics simulations revealed that in spite of general structural similarity between purple bacterial reaction center and Photosystem II reaction center, the structural basis of their thermal stability significantly differ. While the thermophilic cyanobacteria rely on reaction center stabilization using interhelical hydrogen bonds (sequence-based stabilization), the purple reaction center stability largely depend on tertiary structure stabilization through weak interhelical van der Waals interactions (structure-based stabilization). The bulky molecular design of their reaction centers seems to represent an example of an evolutionary constraint, which prevents the evolution of truly psychrophilic or hyperthermophilic species.

¹University of South Bohemia, Faculty of Science, České Budějovice, Czech Republic;

²Institute of Microbiology CAS, Třeboň, Czech Republic

4.2 Introduction

Phototrophic organisms represent one of the oldest life forms on Earth. During their over three billion year long evolution (Björn and Govidjee 2009, Nisbet and Sleep 2001), the phototrophic bacteria have had to adapt to various environmental conditions including physical (temperature, radiation or pressure) and chemical extremes (desiccation, salinity, pH, oxygen species or redox potential; Rothshild and Mancinelli 2001). Among them, high temperature represents one of the main challenges encountered by prokaryotic organisms.

Number of thermophilic strains have been described among cyanobacteria. *Thermosynechococcus elongatus* and *Thermosynechococcus vulcanus* exhibit autotrophic growth optimally at 55 and 57°C resp. (Yamaoka et al. 1978, Inoue et al. 2000). Photosystem II isolated from *Thermosynechococcus vulcanus* was for its good thermal stability used for crystallographic structural analyses which elucidated its 3D protein structure (Umena et al. 2011). The maximal growth temperature of 74°C found in cyanobacterium *Synechococcus cf. lividus* Copeland (1936) is considered to be the upper limit for oxygenic photosynthesis (Pierson and Castenholz 1995, Ward and Castenholz 2000, Madigan and Jung 2009). Thermophilic species are known also among anoxygenic phototrophs. Here, the highest growth temperature of 70°C was found in green nonsulfur photosynthetic bacterium *Chloroflexus aurantiacus* (Pierson and Castenholz 1974, Madigan 2003).

Despite of the fact that cyanobacteria, green nonsulfur and purple phototrophic bacteria share homologous phaeophytin-quinone type reaction centers (so called type 2; Blankenship 1992, Blankenship 2010), purple phototrophic bacteria seem to lack truly thermophilic species. Among them, the purple sulfur bacterium *Thermochromatium tepidum* was proven to live at so far known the highest growth temperature with an optimum of 48 – 50°C (Madigan 1986). Some mildly thermophilic purple nonsulfur bacteria (optimal growth ~40°C) have been isolated from microbial mats in hot springs (e.g. *Rhodopseudomonas* sp. strain GI, *Rhodopseudomonas cryptolactis*, *Rhodospirillum centenum*; Madigan and Jung 2009).

Thermophilic adaptation is a very complex phenomenon affecting almost all parts

of the cellular apparatus. The transmembrane proteins of mesophilic and thermophilic organisms have been at large compared to find the factors contributing to their stability at elevated temperatures. In the amino acid sequences, the Arg and Tyr (Kumar et al. 2000), Gly, Ala, Ser, and Val (Meruelo et al. 2012), Asp, Glu, Ala, Gly and Ser (Schneider et al. 2002) were more preferred in thermophilic structures, whereas cysteine residues were found to decrease by about 70% (Schneider et al. 2002). Salt bridges and side-chain hydrogen bonds, further increased packing density correlating with increased contact density observed in hyperthermophilic archaea are common motifs in thermophilic proteins (Kumar et al. 2000, Berezovsky and Shakhnovich 2005).

So far most of the studies with thermophilic purple bacteria focused on the stability and function of the photosynthetic reaction centers in *Thermochromatium tepidum*. Using crystal structure data, Nogi et al. (2000) suggested that enhanced thermal stability of *Thermochromatium* reaction centers might be facilitated by arginine residues interacting with the periplasmic membrane. This hypothesis was not confirmed by subsequent study using *Rhodobacter sphaeroides* mutants where introduction of arginines did not affect the overall stability of the reaction centers (Watson et al. 2005). Later, Kibayashi et al. (2005) suggested that the *Thermochromatium* reaction center is stabilized mainly through its interaction with the inner light harvesting complex LH1. Recently, Kimura et al. 2009 and Jakob-Grun et al. 2012 pointed to the further stabilization of the *Thermochromatium* light-harvesting-reaction center core complex by calcium ions which reduce the RC-LHI lipid dynamics. However, a real understanding of thermal stability in purple reaction centers is missing.

Extensive research of thermal stability of photosynthetic system was done on thermophilic cyanobacteria. Here, Shlyk-Kerner et al. (2006) identified two amino acid residues of the transmembrane D1 protein in the PSII reaction center, which show consistent changes between mesophilic, thermotolerant and thermophilic algae and cyanobacteria. While mesophilic species contain D1-209 and D1-212 residues occupied by serine, thermophilic organisms possess more bulky amino acids alanine or cysteine. The identified amino acids are located at the point of the closest contact of the D1 and D2 subunits and they are involved in the interhelical hydrogen bond network

stabilizing the reaction center. The crucial role of the identified aminoacid residues was confirmed by side-directed mutation of mesophilic cyanobacterium *Synechocystis* sp. PCC6803 where the exchange of the serine for alanine or cysteine led to the engineering of mutants with more thermostable reaction centers (Shlyk-Kerner et al 2006).

Since the purple bacteria reaction center and Photosystem II reaction center are to a large extent structurally homologous (Deisenhofer et al. 1985, Nogi and Miki 2001, Allen and Williams 2011) we decided to test whether purple reaction centers employ similar mechanism to increase their thermal stability as it was described in case of PSII reaction centers. To verify this hypothesis we studied the thermal stability of the primary charge separation and forward electron transport rate (FETR) by kinetic fluorometry in representatives of different taxonomical and ecological groups of twenty phototrophic bacteria. In addition we employed molecular dynamics simulations to investigate the molecular foundations for the reaction center thermal stability.

4.3 Methods

4.3.1 Microbial cultures

The culture conditions are summarized in Table 4.1. Culture media were prepared according to the protocol following given publications. The aeration of the aerobically growing cultures was provided by shaking the 150 ml Erlenmeyer flasks enclosed with a cotton stopper. The anaerobic strains were cultivated in a 100 mL glass with a screw cap. An illumination of $100 \mu\text{mol photons m}^{-2} \text{ s}^{-1}$ was applied in a 12h light/12h dark regime.

4.3.2 Fluorescence measurement

Infra-red fluorescence measurements were performed using a kinetic fluorometer FL-3000 (Photon Systems Instruments Ltd., Brno, Czech Republic) equipped with a Superhead optics populated with an array of blue-green 505 nm Luxeon Rebel diodes, and a silicon photodiode registering the infra-red bacteriochlorophyll signal $> 850 \text{ nm}$. The fluorescence measurements were conducted at increments of 2.5°C in the range

from 5°C to 90°C controlled by a TR-2000 thermoregulator. The 2.3 mL of bacterial culture was first cooled down to 10°C and then linearly warmed in the dark to the chosen temperature over a period of 10 min. Then, the bacterial photosynthetic reaction centers were saturated by a 140 μs -long square-wave pulse of light with an intensity of $\sim 0.1 \text{ mol photon m}^{-2} \text{ s}^{-1}$. The yield of primary photochemistry was calculated as $F_V/F_M = (F_M - F_0)/F_M$, where F_0 is the fluorescence yield at time 1 μs , and F_M is the maximal fluorescence yield obtained after 100 μs . The fluorescence relaxation (Figure 4.1) was detected by 124 logarithmically spaced probing flashlets placed after the saturating pulse. Normalized fluorescence decays were fitted with three exponential-decay curves by least square numerical fitting. The fluorescence relaxation was fitted using three-exponential kinetics $f(t) = \alpha_1 \exp(-k_1 t) + \alpha_2 \exp(-k_2 t) + \alpha_3 \exp(-k_3 t)$, where $f(t)$ is the fluorescence response at time t , k_1 , k_2 , k_3 represent the rate constant of electron transport and α_1 , α_2 , α_3 their corresponding amplitudes (after Kolber et al., 1998).

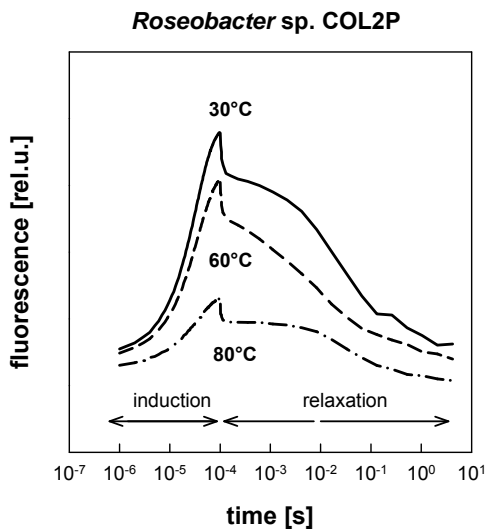


Figure 4.1 The fluorescence induction and relaxation curves of *Roseobacter* sp. COL2P measured by infra-red kinetic fluorometer. The fluorescence changes were recorded at the target temperature of 30°C (black circles), 60°C (white circles), and 80°C (semi-filled circles).

4.3.3 Sequence alignment

The *pufL* and *pufM* sequences were obtained from the GenBank database (NCBI) and aligned using ClustalX 2.0.10. The part of the sequences corresponding to D helices was manually selected and the sequence identity was calculated using ClustalX 2.0.10. For comparison, the D1 and D2 protein sequences of six oxygenic organisms including

higher plants (*Anabaena variabilis*, *Arabidopsis thaliana*, *Chlorella vulgaris*, *Cynophora paradoxa*, *Emiliana huxleyi*, *Nicotina tabacum*, *Synechocystis* PCC6803, *Thalassiosira pseudonana*, *Thermosynechococcus elongatus*, and *Trichodesmium erythraeum*) were aligned.

4.3.4 Molecular dynamics simulations

The three dimensional structures of the reaction centers of *Blastochloris viridis* (PDB ID: 2PRC), *Rhodobacter sphaeroides* (PDB ID: 3I4D), *Thermochromatium tepidum* (PDB ID: 1EYS), *Thermosynechococcus vulcanus* (PDB ID: 3ARC) were obtained from the protein database <http://www.pdb.org/pdb/home/home.do> (Figure 4.2). Structures of the D helices of the L, M or D1, D2 subunits of the reaction centers that do not have their structure solved were created by homology modeling and *in silico* mutagenesis of the *Rhodobacter sphaeroides* and *Thermosynechococcus vulcanus* model structures respectively as described in Dinamarca et al. (2011). Their sequences of transmembrane segments are listed in the Table S4.1. The models of reaction centers were placed in the periodic boundary simulation boxes that extended 1.5 nm on each side in the membrane plane and 1 nm along the perpendicular axis from the largest dimension of the protein. The models of the D helices were placed in cubic periodic boundary simulation boxes that were 1 nm larger than the peptides along all three axes. Hydrogen atoms were added according to basic chemistry rules and a pH of 7.3 was selected. In the whole reaction center molecular dynamics simulation the artificial phosphatidylcholine membrane was added, compressed and energy minimized. All boxes were then filled with TIP3P water and sodium atoms were iteratively placed at the coordinates with the lowest electrostatic potential until the cell was neutral. Molecular dynamics simulations were run with YASARA (www.yasara.org), using a multiple time step of 1.25 fs for intra-molecular and 2.5 fs for intermolecular forces.

Table 4.1 The growth characteristics of investigated phototrophic bacteria.

Species	Functional group	Phylogenetic group	Environment	Growth temp. (°C)		References	
				optimal	Cultivation temp.		
<i>Blastochloris viridis</i> DSM134	purple nonsulfur	α2	freshwater	25 – 30	25	Brenner et al. 2005b	
<i>Congregibacter litoralis</i> KT71	AAP	γ	Marine (North Sea)	9 – 33	25	Spring et al. 2009	
<i>Dinoroseobacter shibae</i> DFL12	AAP	α3	marine dinoflagellates	15 – 38	25	Biebl et al. 2005	
<i>Erythro bacter</i> sp. NAP1	AAP	α4	marine	33	5, 9, 18, 25, 28, 25	Koblížek et al. 2003	
<i>Porphyrobacter donghaensis</i> SW132	AAP	α4	marine (East Korean Sea)	< 50	30 – 37	Yoon et al. 2004	
<i>Porphyrobacter tepidarius</i> OT3	AAP	α4	hot spring (Japan)	< 50	40 – 48	Hanada et al. 1997	
<i>Rhodobaca barguzinensis</i> alga-05	purple nonsulfur	α3	mats of soda lake (East. Siberia)	10 – 45	20 – 35	Boldareva et al. 2008	
<i>Rhodobacter sphaeroides</i> 2.4.1.	purple nonsulfur	α3	freshwater	30 – 34	25	Brenner et al. 2005b; Cohen-Bazire et al. 1957	
<i>Rhodoferrax antarcticus</i> ATCC700587	purple nonsulfur	β	microbial mat (Antarctica)	0 – 25	15 – 18	Madigan et al. 2000	
<i>Rhodospirillum rubrum</i> DSM 467	purple nonsulfur	α1	freshwater habitats	30 – 35	25	Brenner et al. 2005b	
<i>Roseinatronobacter thiooxidans</i> ALG1	AAP	α3	alkaline soda lakes (Kenya)	30	25	Boldareva et al. 2008; Sorokin et al. 2000	
<i>Roseisalinus antarcticus</i> EL88	AAP	α3	freshwater lake (East Antarctica).	3 – 34	16 – 26	18 – 20	Labrenz et al. 2005
<i>Roseobacter</i> sp. COL2P	AAP	α3	marine		25	Koblížek et al. 2010	

Table 4.1 (continued)

Species	Functional group	Phylogen. group	Environment	Growth temp. (°C)	Growth optima temp. (°C)	Cultivation temp. (°C)	References
<i>Roseococcus suduntuyensis</i> Da	AAP	α1	sediments of soda lake (East Siberia)	10 – 50	23 – 28	25	Boldareva et al. 2008; Boldareva et al. 2009
<i>Rubrivivax gelatinosus</i> DSM1709	AAP	β	freshwater and mats		30	25	Adams and Ghiorse 1986; Brenner et al. 2005b
<i>Thermochromatium tepidum</i> MC	purple sulfur	γ	hot spring (Yellowstone, USA)	34 – 57	48 – 50	45	Brenner et al. 2005a; Madigan 1986
<i>Thiocapsa rocepersicina</i> BBS	purple sulfur	γ	freshwater	20 – 35	24 – 28	25	Brenner et al. 2005a
<i>Chloroflexus aurantiacus</i> DSM635-8	green nonsulfur		hot springs	< 70	52 – 60	55	Hanada and Pierson 2006; Malik 1996
<i>Synechocystis</i> sp. PCC6803	cyanobacteria		freshwater	25 – 40	30	30	Dinamarca et al. 2011; Inoue et al. 2001
<i>Thermosynechococcus elongatus</i> BP-1	cyanobacteria		hot spring (Japan)	< 60	57	55	Dinamarca et al. 2011; Yamaoka et al. 1978

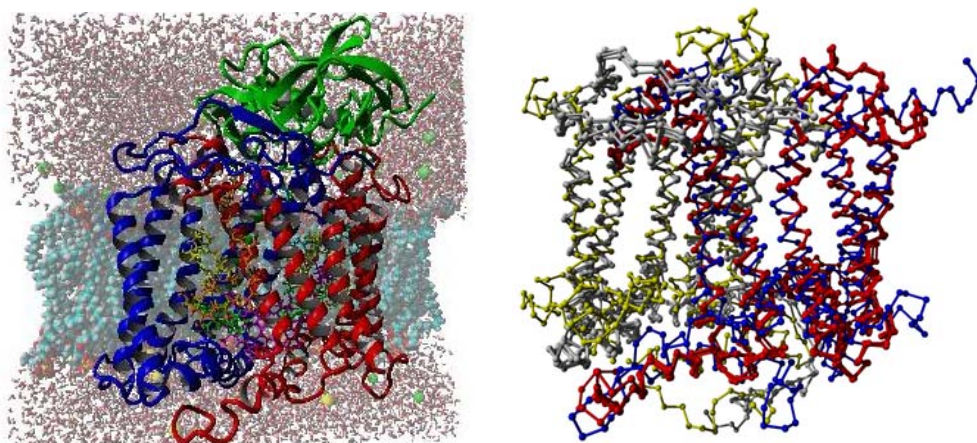


Figure 4.2 Reaction center of *Rhodobacter sphaeroides* (left). The model shows the reaction center embedded within the native phosphatidylcholine membrane surrounded by water molecules. The L, M and H subunit is shown in red, blue and green respectively. The white arrow follows the electron transfer from the special pair of bacteriochlorophylls (magenta) to accessory bacteriochlorophyll (green), bacteriopheophytin (yellow) and ubiquinone (orange). The phytol chains of the bacteriochlorophylls (bacteriopheophytins) in the depicted electron path of the photosystem were removed for clarity. Structural alignment of C α atoms of the reaction center core proteins (right). The L subunits of the *Blastochloris viridis*, *Rhodobacter sphaeroides* and *Thermochromatium tepidum* are shown in red, D1 protein of *Thermosynechococcus vulcanus* in blue; the respective M subunits are shown in gray while D2 protein of *Thermosynechococcus vulcanus* is yellow.

To remove bumps and to correct the covalent geometry, the structures were energy-minimized with the Yamber3 force field, using a 10 Å force cutoff and the Particle Mesh Ewald algorithm to treat long-range electrostatic interactions. After removal of conformational stress by a short steepest descent minimization, the procedure was continued by simulated annealing (time step 2 fs, atom velocities scaled down by 0.9 every 10th step) until convergence was reached, i.e., the energy improved by less than 0.012 kcal mol⁻¹ during 200 steps. The simulations were then run at 300 K at a constant pressure (NPT ensemble) to account for volume changes due to fluctuations of peptides in the solution. The simulations were run for a total time of 20 ns. Molecular graphics were created with YASARA (www.yasara.org) and POVray (www.povray.org).

4.4 Results

4.4.1 Thermal stability measurements

The thermal stability of photosynthetic reaction centers was studied in twenty strains of phototrophic Proteobacteria (Table 1). Phylogenetically, the selected strains included various subgroups of Alpha-, Beta-, and Gammaproteobacteria originating from different habitats including freshwater, saline lakes and marine environments. The studied organisms represented a wide range of temperature preference. Fourteen of them were mesophilic, four (moderately) thermophilic, and two facultative psychrophilic (psychrotolerant). For an outgroup comparison we used the green nonsulfur bacterium *Chloroflexus aurantiacus*, mesophilic and thermophilic cyanobacteria *Synechocystis* sp. PCC6803 and *Thermosynechococcus elongatus*.

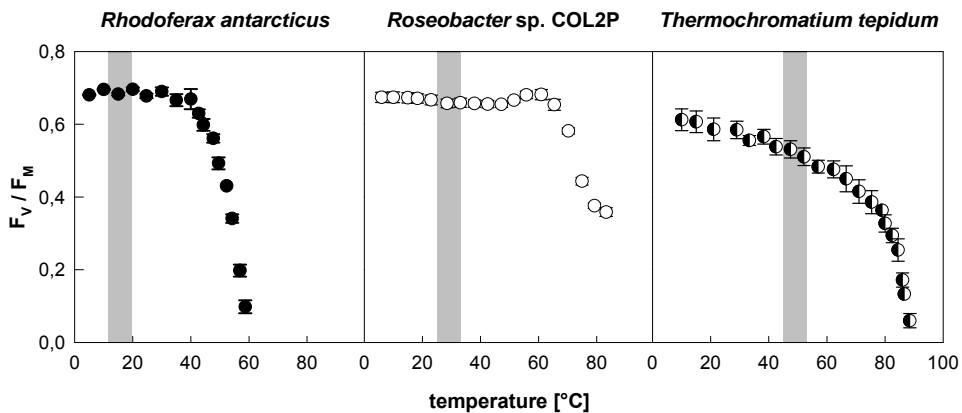


Figure 4.3 The dependence of efficiency of primary photochemistry (F_v/F_M) on temperature measured by infra-red kinetic fluorometry. The optimal growth temperature of the psychrophilic (*Rhodoflex antarcticus*), mesophilic (*Roseobacter* sp. COL2P) and thermophilic (*Thermochromatium tepidum*) purple bacterial strains are marked by the hatched columns. The thermal dependence of F_v/F_M in the remaining bacteria showed a similar trend.

The infra-red kinetic fluorometry measurements of photochemical yields (F_v/F_M) and forward electron transport rates (FETR) were performed in a temperature range between 5 to 80°C. The fluorometric measurements revealed similar trends in all investigated bacterial strains (Figure 4.3). Up to the temperature of at least 50°C, the

bacterial reaction centers were fully functional maintaining high F_V/F_M values (0.51 – 0.72 for given bacterial strain). At higher temperatures the F_V/F_M values steadily declined reflecting the gradual loss of the reaction centers functionality. Break-down temperature between 60 – 70°C was found in most of the studied strains, the lowest one was recorded for *Rhodospirillum rubrum* (Table 2). The reaction centers of three studied thermophilic nonsulfur bacteria retained functionality at temperatures > 80°C. The photosystems II in both mesophilic and thermophilic cyanobacteria showed lower thermal stability compared to their purple-bacterial counterparts.

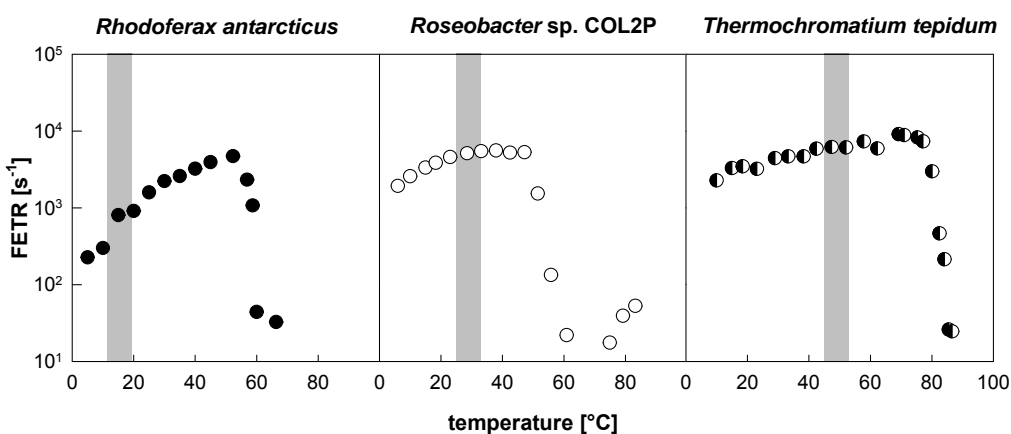


Figure 4.4 The dependence of forward electron transport rate (FETR) on temperature estimated by kinetic fluorometry in a psychrophilic (*Rhodospirillum rubrum*), mesophilic (*Roseobacter sp. COL2P*) and thermophilic (*Thermochromatium tepidum*) purple bacterial strain. The optimal growth temperature range of given bacterium is depicted by the striped columns. FETR was fastest at the temperature of 40 – 50°C in the studied mesophilic and psychrophilic purple bacterial strains regardless on their optimal growth requirements.

Further, the function of the photosynthetic reaction centers was investigated in terms of temperature stability of their forward electron transport. The forward electron transport rate rose with the increasing temperature reaching a plateau at about 5000 s⁻¹ followed by a steep decline (Figure 4.4). For example, in *Rhodospirillum rubrum*, *Roseobacter sp. COL2P* and *Thermochromatium tepidum*, the highest values of FETR reached 4980, 5410, and 9120 s⁻¹ respectively. The highest FETR was measured at temperatures > 40°C for all studied species (Table 2). In the thermophilic strains, a sustained functionality of the reaction centre marked by an undeclining FETR was

observed up to 60 – 80°C. The temperature of optimal FETR (the temperature of the highest FETR value) and the upper limit for the optimal charge separation (high F_V/F_M value) were positively correlated with their optimal growth conditions ($R = 0.762$, $p < 0.001$, $n = 17$; $R = 0.803$, $p < 0.001$, $n = 16$ resp.).

Table 4.2 Summary of photosynthetic response of the studied bacterial strains at an elevated temperature. The listed temperatures reflect the following variables: t (break-down) = temperature where the F_V/F_M value decreased to the half of its maximal value; t (optimal FETR) = the temperature of the highest FETR value (¹ strain cultivated at 25°C; ²Dinamarca et al. 2011).

species	t (break-down) (°C)	t (FETR) (°C)
<i>Blastochloris viridis</i>	72 ± 0.8	43 ± 0.9
<i>Congregibacter litoralis</i>	72 ± 0.7	50 ± 0.9
<i>Dinoroseobacter shibae</i>	68 ± 0.8	47
<i>Erythrobacter</i> sp. NAP1 ¹)	80 ± 0.5	43 ± 1.1
<i>Porphyrobacter donghaensis</i>	76 ± 0.2	48
<i>Porphyrobacter tepidarium</i>	84 ± 0.3	51 ± 0.3
<i>Rhodobaca barguzinensis</i>	80 ± 0.3	43
<i>Rhodobacter sphaeroides</i>	78 ± 0.3	38
<i>Rhodoferax antarcticus</i>	53 ± 1.1	50 ± 2.0
<i>Rhodospirillum rubrum</i>	71	48
<i>Roseinatronobacter thiooxidans</i>	76 ± 0.8	47
<i>Roseisalinus antarcticus</i>	74 ± 0.4	48
<i>Roseobacter</i> sp. COL2P	77 ± 0.1	47 ± 0.5
<i>Roseococcus suduntuyensis</i>	70 ± 1.1	52
<i>Rubrivivax gelatinosus</i>	74 ± 0.3	58 ± 0.7
<i>Thermochromatium tepidum</i>	86 ± 1.3	75 ± 0.9
<i>Thiocapsa roseopersicina</i>	68	–
<i>Chloroflexus aurantiacus</i>	> 85	77
<i>Synechocystis</i> sp. PCC6803 ²)	43	46
<i>Thermosynechococcus elongatus</i> ²)	60	75

A control measurement of influence of cultivating conditions was done on the strain of *Erythrobacter* sp. NAP1 grown at 5, 9, 18, 25, 28, and 35°C. The break-down temperature and FETR did not differ among cultures grown on different temperatures. The FETR measurements revealed that the electron transport was disrupted at temperatures at least ten degrees lower than those of the upper limit for primary

photochemical reactions (Figure 4.4). In all investigated bacteria, both the primary photochemistry and forward electron transport were fully functional at the temperatures above 40°C, some 10–30°C above their preferred living conditions (Figure 4.5).

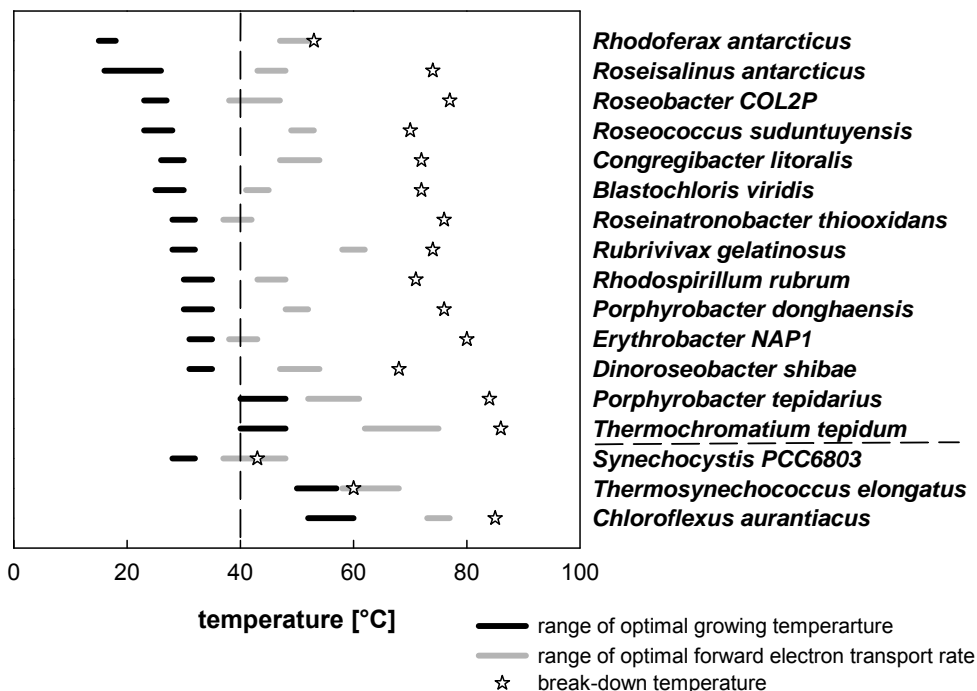


Figure 4.5 Comparison of the ranges of optimal growth temperature (black line), optimal forward electron transport rate (grey line) and upper limit of optimal charge separation (white star; the lower thermal limit was 5°C in all studied strains). The strains are ordered with their increasing optimal growth temperature. The primary photochemistry was functional 10–30°C above the optimal living condition of given bacterium. The optimal electron transport rate operated at least up to 40°C in all strains.

4.4.2 Molecular dynamics simulations

In search for the molecular mechanism behind the thermal stability of the bacterial reaction centers, the amino acid sequences of the L(D1) and M(D2) protein subunits of eighteen studied bacteria were aligned and examined (Table S4.1). The sequences of the reaction centre proteins largely differ among the studied phototrophic strains, with the *pufL* and *pufM* identities $67 \pm 11\%$ and $56 \pm 13\%$ resp. The identity of the D helices

of the corresponding reaction core proteins (Asn170-X198 for *pufL*; His195-Leu223 for D1; ProX200-Val(Leu)226 for *pufM*; Pro195-Thr221 for D2) reached $63 \pm 17\%$ in *pufL*, and $76 \pm 19\%$ in *pufM* respectively. In opposite, the D1 and D2 protein sequences were largely conserved ($96.3 \pm 3.5\%$ for D1, $96 \pm 3.0\%$ for D2). Yet, the differences in the primary protein sequence itself seemed to provide neither any clues for the high thermal stability of the reaction centers nor the differences in the said stability among the studied strains. Namely, the sequence was highly conserved only at the sites that are responsible for cofactor binding while the rest of the helix is populated by small amino acids that are often permuted with ones with similar properties – Gly for Ala, Ala for Ser, Val for Ile, Leu for Ile, or Val for Leu. Surprisingly, aminoacids at the centre of the transmembrane helix are more frequently mutated although to aminoacids of a similar kind e.g. Ser into Thr or Cys.

To gain further understanding of the structural basis for the thermal stability of the purple photosynthetic reaction centers, molecular dynamics of the pairs of D helices (L and M, D1 and D2) was analyzed first in the simplified model in a buffered aqueous environment for 20 ns. Out of the eighteen structures, only a half exhibited satisfying stability measured by the root mean square deviation (RMSD) of the atoms on the course of the simulation ($\text{RMSD} < 3$) (Figure S4.1). A sharp contrast in stability of the models was demonstrated in two control cyanobacterial structures. While the mesophilic *Synechocystis* sp. PCC6803 had $\text{RMSD} = 4.66 \pm 0.12 \text{ \AA}$, the thermophilic *Thermosynechococcus vulcanus* had $\text{RMSD} = 2.96 \pm 0.13 \text{ \AA}$.

Although the overall amino acid sequences of examined anoxygenic bacteria were not conserved, the *in silico* computation of all of the stable models revealed one to three interhelical hydrogen bonds formed between D helices of PufL and PufM proteins with the distance of $1.9 - 2.3 \text{ \AA}$ and energy of $9.7 - 22.3 \text{ kJ.mol}^{-1}$ (Table S4.3). The amino acid of the L subunit at the position 183 acted as a donor in an interhelical hydrogen bond to an amino acid of the M subunit at either the 213 or 212 positions. Likewise, the L-184Thr or L-184Cys residue became a frequent acceptor of an interhelical hydrogen bond from M-Ser212. Homologous interhelical bonds were analyzed in the two modeled structures of control cyanobacterial proteins D1 and D2,

as described in Dinamarca et al. (2011). The computed van der Waals contact varied largely among mesophilic and thermophilic modeled bacteria without any clear pattern (Figure 4.7, Table S4.2).

To assess the role of the intra- and intermolecular hydrogen bonds, geometries of the interacting transmembrane helices and their interactions with lipids in the thermal stabilization of the whole reaction centers were modeled within a phosphatidylcholine membrane surrounded by an aqueous phase. Four high resolution models of purple bacterial reaction centers *Blastochloris viridis*, *Rhodobacter sphaeroides*, and *Thermochromatium tepidum* and of cyanobacterial PSII *Thermosynechococcus vulcanus* were modeled for 20 ns. Although the whole simulated structures had their RMSD $< 2 \text{ \AA}$, their inner reaction center cores represented by the pairs of interacting D helices had always RMSD $< 0.6 \pm 0.05 \text{ \AA}$. In the reaction center models of *Blastochloris viridis* and *Rhodobacter sphaeroides*, the L-Asn183 residue became hydrogen bond donor to amino acid residues of the M protein subunit in the same way as in the simplified model of interacting D helices (Table 4.3). The bond length was in both cases $2.2 \pm 0.1 \text{ \AA}$ and the bond energy ranged from 12 and 17 kJ mol^{-1} resp. In the model of reaction center of *Thermochromatium tepidum* no statistically relevant interhelical hydrogen bonds were found, just as in the D helix model. When computed for cyanobacterium *Thermosynechococcus vulcanus*, the hydrogen bond network was identical to that predicted earlier for the D helix model (Dinamarca et al. 2011). The intrahelical hydrogen bond network was present in the reaction center models of purple bacteria. Together 22 – 26 intrahelical hydrogen bonds of 441 – 539 kJ mol^{-1} formed in the D helices of their L and M subunits (Table 4.4). The van der Waals contact between the D helices of the L and M subunits was significantly higher in the reaction centre of *Thermochromatium tepidum* that also exhibited the highest thermal stability. The van der Waals contact in the least thermally stable reaction centre of *Blastochloris viridis* and *Rhodobacter sphaeroides* was smaller by as much as 20 and 10 \AA^2 respectively. The *in silico* computed van der Waals contacts were positively correlated with the temperatures where the F_V/F_M decreased to the half of its maximal value (Figure 4.6).

Table 4.3 The parameters of L(D1)/M(D2) interhelical interactions in the whole reaction center model.

INTERHELICAL HYDROGEN BONDS					
	position of H-bond	distance (Å)	energy (kJ mol ⁻¹)	probability (%)	
<i>Blastochloris viridis</i>	L(ASN)183 → M(CYS)210	2.23 ± 0.12	11.9 ± 4.5	49.0	
<i>Rhodobacter sphaeroides</i>	L(ASN)183 → M(SER)212	2.21 ± 0.13	17.2 ± 5.5	65.0	
<i>Thermochromatium tepidum</i>	L(ASN)191 → M(SER)211	2.39 ± 0.15	9.9 ± 4.4	0.5	
<i>Thermosynechococcus vulcanus</i>	D1(GLY)208←D2(CYS)211	2.25	9.2	2.0	

Table 4.4 The parameters of L(D1)/M(D2) intrahelical interactions based on molecule dynamics simulation models of whole reaction center (X → Y means X donates a hydrogen bond to Y).

	HELIX GEOMETRY			INTRAHELICAL H-BONDS			
	volume (Å ³)		van der Waals contact (Å ²)	number of H-bonds		energy (kJ mol ⁻¹)	
	L(D1)	M(D2)		L	M	L	M
<i>Blastochloris viridis</i>	2947	2729	68.3	22.9	24.2	474.6	517.6
<i>Rhodobacter sphaeroides</i>	3026	2859	80.3	26.0	22.0	509.7	440.8
<i>Thermochromatium tepidum</i>	3139	2943	90.6	25.4	24.8	523.1	530.9
<i>Thermosynechococcus vulcanus</i>	2423	2235	69.3	25.9	25.4	538.5	524.9

Thermosynechococcus vulcanus had the widest angle ($66.2 \pm 0.4 - 68.3 \pm 0.4^\circ$), smallest helix volume and hence van der Waals contact as well, while exhibiting the lowest temperature for half inhibition of the primary charge separation.

As the photosynthetic reaction centers are membrane bound complexes, a range of hydrophobic but also electrostatic interactions are formed between various parts of lipids of the photosynthetic membrane and amino acids of α -helical parts of proteins. These interactions are pronounced due to the exclusion of water that would otherwise mask them. Overall 11 to 21 hydrogen bonds were formed between the hydrophilic parts of the lipids and the amino acids of the L and M membrane protein subunits in the examined reaction centers of *Blastochloris viridis*, *Rhodobacter sphaeroides*, *Thermochromatium tepidum*, and *Thermosynechococcus vulcanus* (Table S4.4). That is significantly more than in *Thermochromatium tepidum* where only 9 hydrogen bonds

were formed on average between the L and M proteins of reaction center and lipid molecules. The Arg84, Asn68 and Met85 were the most abundant hydrogen bond donors in L subunit while Arg104, Leu108 and Thr57 in the M subunit.

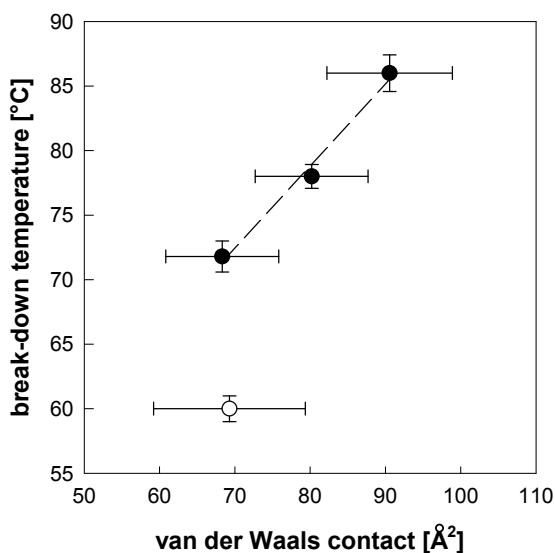


Figure 4.6 The linear correlation ($y = 1.55x - 42.35$; $R^2 = 0.987$) of van der Waals contact between D helices of L and M protein subunits of *Rhodobacter sphaeroides*, *Blastochloris viridis*, *Thermochromatium tepidum* (closed symbols), *Thermosynechococcus sp.* (open symbols) and temperature where the F_V/F_M value decreased to the half of its maximal value. The contact areas are computed based on the up-to-date resolved structures of bacterial reaction centers. Error bars represent the standard deviation of the mean of van der Waals contact during the 15 to 20 ns of simulations (x-axis) and the standard error (y-axis).

4.5 Discussion

We have found an unexpected thermal stability of primary charge separation in the reaction centers of purple anoxygenic bacteria. All of the examined psychrophilic, mesophilic and thermophilic strains showed unprecedented functional stability of their reaction centre up to temperatures of 40°C, moreover the mesophilic and thermophilic strains preserved the full capacity for the primary photochemical reactions at temperatures higher than 60°C. The photosynthetic reaction centres of psychrophilic and mesophilic bacterial strains revealed thermal stability far above the physiological limits of a whole bacterial cell. Nevertheless, the upper living temperatures of purple bacteria are below the upper limits of Chloroflexi.

reaction centre thermal stability.

Although the purple bacteria reaction centers do not lack the available amino acid residues with the potential to form networks of weak interhelical hydrogen bonds akin to the PSII, nearly half of the modeled structures including the whole reaction centers did not show sufficient abundances of such bonds. Only five models of interacting D helices showed probability of binding larger than 0.4 (Figure S4.2). The probability of binding between L-Asn183 and M-Cys210 (*Blastochloris*) or M-Ser212 (*Rhodobacter*) was 0.49 and 0.65 respectively in the models of reaction centres while the model of *Thermochromatium* reaction centre revealed negligible binding. Stabilization of the L-M protein pair by interhelical hydrogen bonds as means for stabilization of the bacterial reaction centres at high temperatures can be thus ruled out as the main and/or one of the main factors. The absence of a functional hydrogen bond network between the L and M subunits may be one of the reasons that limit the evolution of truly thermophilic reaction centers in purple bacteria. The question arises whether the introduction of those small amino acids and/or engaging the available – large but strong hydrogen bonding amino acids overly stabilize the reaction center and would compromise the electron transfer steps that require protein flexibility? A partial answer may be obtained from oxygenic photosynthesis where weak hydrogen bonds determine to a large extent the stability of photosystem II. In our recent study we have shown that the mutation of the D1-Gly208 residue in *Synechocystis* sp. PCC6803 into larger Ala, Ser or Thr residue leads to intensification of interhelical hydrogen bonds between the D1 and D2 proteins that in turn compromise the efficacy of the primary electron transfer steps. Introduction of any larger amino acids and/or those capable of stronger hydrogen bonding leads to a lethal phenotype. Our *in silico* modeling and direct measurements of the unbinding forces between the D helices of D1 and D2 proteins using dynamic force microscopy confirmed the aforementioned predictions in structures representing both impaired and lethal mutants (Shlyk et al., unpublished results).

Nogi et al. (2000) speculated, that the increased abundance of Arg residues at the membrane surface of *Thermochromatium tepidum* model structure may indicate a higher probability of lipid-protein interactions in this thermophilic bacterial centre

contrasting with the mesophilic *Blastochloris viridis*. Our MD simulations of whole reaction centre within artificial membrane did not confirm this prediction. Instead, the reaction centre of *Thermochromatium tepidum* formed on average only 9 hydrogen bonds between L and M protein subunits and the PC molecules of the membrane per simulation snapshot while the *Blastochloris viridis* formed 12 and *Rhodobacter sphaeroides* even 21 of such bonds. Surprisingly, the MD simulation of PSII model of *Thermosynechococcus vulcanus* revealed formation of 60 protein-lipid hydrogen bonds on average per simulation snapshot, out of these whole 46 were facilitated by the D1 and D2 proteins only.

The kinetic requirements of the thermotolerant reaction center of *Thermochromatium tepidum* appear to put an upper limit to the frequency of the interhelical hydrogen bonds together with protein-lipid hydrogen bonds while maximizing the L-M van der Waals contact, and helix packing with aid of intrahelical hydrogen bonds in their D helices. It seems though that hydrophobic and even more the van der Waals interactions dominate in magnitude the stabilizing factors in this reaction center yet apparently have their limits too in respect to the preservation of both the efficient photochemical reactions and structural integrity at elevated temperatures.

Despite the lack of conclusive evidence for the unique molecular mechanism, the purple bacterial reaction centers positively showed thermal stability beyond the preferred physiological boundary of recent purple bacterial cells. We have decided to put forth this fact in support of the theory that the early Archean environment that provided the nurturing ground for the first photoautotrophic bacteria was progressively warmer than today's oceans (Knaut and Lowe 2003, Hren et al. 2009; Blake et al. 2010). It seems that the photosynthetic reaction centres of purple bacteria adopted the "structure-based" mechanism of acquiring thermostability as defined by Berezovsky and Shakhnovich (2005). Unlike in oxygen evolving PSII that had made use of specific and strong interhelical interactions to increase its thermostability (Dinamarca et al. 2011) via the "sequence-based" mechanisms, the purple bacterial reaction centres did not liberate themselves from the structural limitations imposed at the very start of their evolution being dictated by the thermodynamic restrictions of folding under elevated

temperature. Thus it seems plausible that it is the van der Waals interactions between the adjacent highly packed transmembrane helices that play a key role in the optimization of the reaction centres' thermal stability. Further investigations may confirm that the purple bacteria have indeed evolved from genuinely thermotolerant bacteria harboring thermotolerant photosynthesis yet followed an evolutionary path that led them to lose the capacity to photosynthesize at extreme temperatures. Unlike the PSII, that stemmed from the joint ancestor to undertake a very different path that led them to evolve and colonize the oxygen containing world.

Acknowledgements This research was also supported by GA AVČR project IAA608170901, GAČR project P501/10/0221 and project Algatech (CZ.1.05/2.1.00/03.0110). The authors are indebted Dr. Matthias Labrenz, Dr. Hanno Biebl, Prof. Vladimir Gorlenko, Deborah Jung, and Prof. Michael T. Madigan for their generous gift of phototrophic strains; further to Katya Boldareva, Alexander Dulebo Dzmityr Hauruseu and Jason Dean for their kind help with conducting the experiments.

4.6 References

- Adams LF, Ghiorse WC (1986) Physiology and ultrastructure of *Leptothrix discophora* SS-1. *Arch Microbiol* 145: 126-135
- Berezovsky IN, Shakhnovich EI (2005) Physics and evolution of thermophilic adaptation. *Proc Natl Acad Sci USA* 102: 12742-12747
- Biebl H, Allgaier M, Tindall BJ, Koblizek M, Lünsdorf H, Pukall R, Wagner-Döbler I (2005) *Dinoroseobacter shibae* gen. nov., sp. nov., a new aerobic phototrophic bacterium isolated from dinoflagellates. *Int J Syst Evol Microbiol* 55: 1089-1096
- Björn LO, Govindjee (2009) The evolution of photosynthesis and chloroplasts. *Curr Sci* 96: 1466-1474
- Blake RE, Chang SJ, Lepland A (2010) Phosphate oxygen isotopic evidence for a temperate and biologically active Archean ocean. *Nature* 464: 1029-1033
- Blankenship RE (1992) Origin and early evolution of photosynthesis. *Photosynth Res* 33: 91-111

- Blankenship RE (2002) *Molecular mechanisms of photosynthesis*. Blackwell Science Ltd., Oxford, pp. 220-257
- Blankenship RE (2010) Early Evolution of Photosynthesis. *Plant Physiol* 154: 434-438
- Boldareva EN, Akimov VN, Boychenko VA, Sadnichuk IN, Moskalenko AA, Makhneva ZK, Gorlenko VM (2008) *Rhodobaca barguzinensis* sp. nov., a new alkaliphilic purple nonsulfur bacterium isolated from a soda lake of the Barguzin Valley (Buryat Republic, Eastern Siberia). *Microbiology* 77: 206-218
- Boldareva EN, Moskalenko AA, Makhneva ZK, Tourova TP, Kolganova TV, Gorlenko VM (2009) *Rubribacterium polymorphum* gen. nov., sp. nov., a novel alkaliphilic nonsulfur purple bacterium from an Eastern Siberian Soda Lake. *Microbiology* 78: 732-740
- Brenner DJ, Krieg NR, Staley J (2005a) *The Proteobacteria, Bergey's Manual of Systematic Bacteriology*. Second edition, Volume Two, Part B, Springer, New York, pp. 24-25, 27
- Brenner DJ, Krieg NR, Staley J (2005b) *The Proteobacteria, Bergey's Manual of Systematic Bacteriology*. Second edition, Volume Two, Part C, Springer, New York, pp. 4-6, 166-167, 749-750
- Cohen-Bazire G, Sistrom RW, Stanier RY (1957) Kinetic studies of pigment synthesis by nonsulfur purple bacteria. *J Cell Comp Physiol* 49: 25-68.
- Dinamarca J, Shlyk-Kerner O, Kaftan D, Goldberg E, Dulebo A, Gidekel M, Gutierrez A, Scherz A (2011) Double mutation in photosystem II reaction centers and elevated CO₂ grant thermotolerance to mesophilic cyanobacterium. *PlosOne* 6: e28389-e28389
- Hanada S, Kawase Y, Hiraishi A, Takaichi S, Marsuura K, Shimada K, Nagashima KVP (1997) *Porphyrobacter tepidarius* sp. nov., a moderately thermophilic aerobic photosynthetic bacterium isolated from a hot spring. *Int J Syst Bact* 47: 408-419
- Hanada S, Pierson BK (2006) *The family Chloroflexaceae* in Dworkin M, Falkow S (eds.) *Prokaryotes: A Handbook on the Biology of Bacteria*. Volume 7, Springer, pp. 815-842
- Hren MT, Tice MM, Chamberlain CP (2009) Oxygen and hydrogen isotope evidence

- for temperate climate 3.42 billion years ago. *Nature* 462: 205-208
- Inoue N, Emi T, Yamane Y, Kashino Y, Koike H, Satoh K (2000) Effect of high-temperature treatments on a thermophilic cyanobacterium *Synechococcus vulcanus*. *Plant Cell Physiol* 41: 515-522
- Inoue N, Taira Y, Emi T, Yamane Y, Kashino Y, Koike H, Satoh K (2001) Acclimation to the growth temperature and the high-temperature effects on photosystem II and plasma membranes in a mesophilic cyanobacterium, *Synechocystis* sp. PCC6803. *Plant Cell Physiol* 42: 1140-1148
- Jacob-Grun S, Radeck J, Braun P (2012) Ca²⁺-binding reduces conformational flexibility of RC1-LH1 core complex from thermophile *Thermochromatium tepidum*. *Photosynth Res* 111: 139-147
- Knauth LP, Lowe DR (2003) High Archean climatic temperature inferred from oxygen isotope geochemistry of cherts in the 3.5 Ga Swaziland Supergroup, South Africa. *Geol Soc Am Bull* 115: 566-580
- Koblížek M, Bějá O, Bidigare RR, Christensen S, Benitez-Nelson B, Vetricani C, Kolber MK, Falkowski PG, Kolber ZS (2003) Isolation and characterization of *Erythrobacter* sp. strains from the upper ocean. *Arch Microbiol* 180: 327-338
- Koblížek M, Mlčoušová J, Kolber, Z, Kopecký J (2010) On the photosynthetic properties of marine bacterium COL2P belonging to *Roseobacter* clade. *Arch Microbiol* 192: 41-49
- Kolber ZS, Prášil O, Falkowski PG (1998) Measurements of variable chlorophyll fluorescence using fast repetition rate techniques: defining methodology and experimental protocols. *Biochim Biophys Acta* 1367: 88-106
- Kumar S, Tsai CJ, Nussinov R (2000) Factors enhancing protein stability. *Prot Eng* 13: 179-191
- Labrenz M, Lawson PA, Tindall BJ, Collins MD, Hirsch P (2005) *Roseisalinus antarcticus* gen. nov., sp. nov., a novel aerobic bacteriochlorophyll a-producing α -proteobacterium isolated from hypersaline Ekho Lake, Antarctica. *Int J Syst Evol Microbiol* 55: 41-47
- Madigan MT (1986) *Chromatium tepidum* sp. nov., a thermophilic photosynthetic bacterium of the family *Chromatiaceae*. *Int J Syst Bacteriol* 36: 222-227

- Madigan MT (2003) Anoxygenic phototrophic bacteria from extreme environments. *Photosynth Res* 76: 157-171
- Madigan MT, Jung DO (2009) *An Overview of Purple Bacteria: Systematics, Physiology, and Habitats* in Hunter CN, Daldal F, Thurnauer MC, Beatty JT (eds.) *The Purple Phototrophic Bacteria*. Springer Science, pp. 1-15
- Madigan MT, Jung DO, Woese CR, Achenbach LA (2000) *Rhodoferox antarcticus* sp. nov., a moderately psychrophilic purple nonsulfur bacterium isolated from an Antarctic microbial mat. *Arch Microbiol* 173: 269-277
- Malik KA (1996) A modified medium and method for the cultivation of *Chloroflexus*. *J Microbiol Meth* 27: 147-150
- Meruelo AD, Han SK, Kim S, Bowie JU (2012) Structural differences between thermophilic and mesophilic membrane proteins. *Protein Sci* 21: 1746-1753
- Nisbet EG, Sleep NH (2001) The habitat and nature of early life. *Nature* 409: 1083-1091
- Nogi T, Fathir I, Kobayashi M, Nozawa T, Miki K (2000) Crystal structures of photosynthetic reaction centre and high-potential iron-sulfur protein from *Thermochromatium tepidum*: Thermostability and electron transfer. *Proc Natl Acad Sci USA* 97: 13561-13566
- Nold SC, Kocczynski ED, Ward DM (1996) Cultivation of aerobic chemoorganotrophic proteobacteria and gram-positive bacteria from a hot spring microbial mat. *Appl Environ Microbiol* 62: 3917-3921
- Olson JM (2006) Photosynthesis in the Archean era. *Photosynth Res* 88: 109-117
- Pierson BK, Castenholz RW (1995) *Taxonomy and Physiology of Filamentous Anoxygenic Phototrophs* in Blankenship RE, Madigan MT, Bauer CE (eds.) *Anoxygenic Photosynthetic Bacteria*. Kluwer Academic Publishers, Netherlands, pp. 31-47
- Rothschild LJ, Mancinelli R (2000) Life in extreme environments. *Nature* 409: 1092-1101
- Schneider D, Liu Y, Gerstein M, Engelman DM (2002) Thermostability of membrane protein helix-helix interaction elucidated by statistical analysis. *FEBS Lett* 532: 231-236

- Shlyk-Kerner O, Samish I, Kaftan D, Holland N, Maruthi Sai PS, Kless H, Scherz (2006) A Protein flexibility acclimatizes photosynthetic energy conversion to the ambient temperature. *Nature* 442: 827-830
- Sorokin DY, Tourova TP, Kuenen JG (2000) A new facultatively autotrophic hydrogen- and sulfur-oxidizing bacterium from an alkaline environment. *Extremophiles* 4:237-245
- Spring S, Lünsdorf H, Fuchs BM, Tindall BJ (2009) The photosynthetic apparatus and its regulation in the aerobic gammaproteobacterium *Congregibacter litoralis* gen. nov., sp. nov. *PLoS ONE* 4:e4866
- Tobler DJ, Benning LG (2011) Bacterial diversity in five Icelandic geothermal waters: temperature and sinter growth rate effects. *Extremophiles* 15: 473-485
- Umena Y, Kawasami K, Shen JR, Kamiya N (2011) Crystal structure of oxygen-evolving photosystem II at a resolution of 1.9 Å. *Nature* 473: 55-61
- Ward DM, Castenholz RW (2000) *Cyanobacteria in geothermal habitats* in Whitton BA, Potts M (eds.) *The ecology of cyanobacteria. Their diversity in time and space*. Kluwer Academic Publishers, Dordrecht, pp. 37-59
- Yamaoka T, Satoh K, Katoh S (1978) Photosynthetic Activities of a Thermophilic Blue-Green-Alga. *Plant Cell Physiol* 19: 943-954
- Yoon J, Lee M, Oh T (2004) *Porphyrobacter donghaensis* sp. nov., isolated from sea water of the East Sea in Korea. *Int J Syst Evol Microbiol* 54: 2231-2235

4.7 Supplements

Table S4.1 Multiple sequence alignment of partial *pufL* (170-198 aminoacid position in *Rhodobacter sphaeroides*) and *pufM* (200-226 aminoacid position) protein sequences corresponding to the transmembrane segments of D helix. Corresponding part of D1 and D2 proteins of cyanobacteria are shown for comparison. Aminoacids potentially forming the interhelical hydrogen bond are marked in bold.

species	pufL / D1	pufM / D2
<i>Blastochloris viridis</i>	NPGHMSSVSFLFANAMALGLHGGLIILSVA	PWHGFSIGFAYGCGLLFAAHGATILAV
<i>Congregibacter litoralis</i>	NPAHMLAVTFFF TTTTL ALSMHGSLILAVT	PFHMLSIAFLYGSTLLFAMHGATILAV
<i>Dinoroseobacter shibae</i>	NPAHMIAVTFFF TTTTL ALALHGALVLSAA	PFHALSIVFLYGSVLLFAMHGATILAV
<i>Erythrobacter</i> sp. NAP1	NPVHMLAITFFF TNCL ALALHGGLVLSAV	PFHALSIVFLYGSVAVLFAMHGATILAV
<i>Porphyrobacter tepidarius</i>	NPVHMLAITFFF TNCL ALALHGGLVLSAV	PFHALSIVFLYGSVAVLFAMHGATILAV
<i>Rhodobaca barguzinensis</i>	NPAHMIAVTFFF TTTTL ALALHGALVLSAA	PFHALSIAFLYGSALLFAMHGATILAV
<i>Rhodobacter sphaeroides</i>	NPAHMIASFFF TNAL ALALHGALVLSAA	PFHGLSIAFLYGSALLFAMHGATILAV
<i>Rhodoferax antarcticus</i>	NPAHMLAITFFF GGTTF ALSLHSSLIVSAS	PFHALSIAFLYGS TL IFAMHGATILAV
<i>Rhodospirillum rubrum</i>	npahmlgitlff ttctcl alalhgslil saa	PFHMLSIAFLYGSALLSAMHGATILAV
<i>Roseisalinus antarcticus</i>	NPAHMIAITFFF TTCF ALALHGSLVLSAV	PFHALSIAFLYGSALLFAMHGATILAV
<i>Roseococcus sudutuyensis</i>	NPAHMIAVTFFF TTTTL ALSLHASLVLSAAI	PFHALSIVFLYGSVLLFAMHGATILAV
<i>Roseobacter</i> sp. COL2P	NPAHMLAVTFFF TTTTL ALALHGGLIILSAA	PFHCLSIIVFLYGS TL LLFAMHGATILAV
<i>Roseococcus sudutuyensis</i>	NPAHMIAVTFFF TTTTL ALSLHASLVLSAAI	PFHALSIVFLYGSVLLFAMHGATILAV
<i>Rubrivivax gelatinosus</i>	NPAHMLAITFFF TTTTL AMSMHGGLIILSAA	PFHALSIAFLYGAT TL LLFAMHGATILAV
<i>Thermochromatium tepidum</i>	NPAHMLAISFFF TNCL ALSMHGSLIILSVT	PFHMLSIAFLYGSALLFAMHGATILSV
<i>Thiocapsa roseopersicina</i>	NPAHMLAITFFF TTTTL ALAMHGSLIILSVT	PFHMLSIAFLYGSALLFAMHGATILAV
<i>Chloroflexus aurantiacus</i>	NPFFHAIGITGLFA STW LLACHGSLIILSAA	PFHMLSIF FL LLGS TL LLAMHAGTIWAL
<i>Synechocystis</i> sp. PCC 6803	HPFHMLGVAGVFGGALFAAMH GS LVTS SL	PFHMMGVAG IL GGALLCAI HG ATVENT
<i>Thermosynechococcus elongatus</i>	HPFHQLGVAGVFGGALFCAMHGS LV TS SL	PFHMMGVAG VL GGALLCAI HG ATVENT

Table S4.2 The parameters of L(D1)/M(D2) intrahelical interactions based on molecule dynamics simulation models of a simplified model. Although the van der Waals contact area largely varied among the strains, it was positively correlated with both the temperature of the optimal FETR and growth temperature.

species	HELIX GEOMETRY			
	volume (\AA^3)		van der Waals contact	helix angle
	L (D1)	M (D2)	(\AA^2)	($^\circ$)
<i>Blastochloris viridis</i>	2969	2805	71	60.0
<i>Congregibacter litoralis</i>	3139	2983	152	34.3
<i>Dinoroseobacter shibae</i>	3048	2965	118	47.7
<i>Erythrobacter</i> sp. NAP1	3125	2915	129	47.8
<i>Porphyrobacter tepidarius</i>	3129	2936	96	50.9
<i>Rhodobaca barguzinensis</i>	3045	2897	106	114.6
<i>Rhodobacter sphaeroides</i>	3033	2880	174	51.7
<i>Rhodoferax antarcticus</i>	3105	2924	143	50.2
<i>Rhodospirillum rubrum</i>	3040	2883	115	33.7
<i>Roseisalinus antarcticus</i>	3134	2905	153	38.9
<i>Roseobacter</i> sp. COL2P	3046	2982	138	46.9
<i>Roseococcus suduntuyensis</i>	3130	2974	156	41.1
<i>Rubrivivax gelatinous</i>	3088	2916	159	45.3
<i>Thermochromatium tepidum</i>	3266	2965	80	64.1
<i>Thiocapsa roseopersicina</i>	3157	2956	123	44.9
<i>Chloroflexus aurantiacus</i>	3011	3061	103	35.7
<i>Synechocystis</i> sp. PCC6803	2953	2689	136	56.6
<i>Thermosynechococcus vulcanus</i>	2950	2672	120	58.1

Table S4.2 (continued)

species	INTRAHELICAL HYDROGEN BONDS			
	number of H-bonds		energy (kJ mol ⁻¹)	
	L	M	L	M
<i>Blastochloris viridis</i>	24.2±2.1	22.6±1.5	462.8±48.7	433.7±38.4
<i>Congregibacter litoralis</i>	27.2±1.9	20.9±1.8	530.5±44.9	397.6±41.5
<i>Dinoroseobacter shibae</i>	24.6±1.9	21.3±1.9	470.9±42.6	402.7±44.8
<i>Erythrobacter</i> sp. NAP1	25.8±1.9	21.7±1.8	496.3±45.4	405.7±42.5
<i>Porphyrobacter tepidarius</i>	24.1±2.3	18.6±2.3	441.7±52.8	326.6±50.2
<i>Rhodobaca barguzinensis</i>	27.7±1.8	21.9±2.0	540.5±50.2	404.9±51.7
<i>Rhodobacter sphaeroides</i>	22.8±1.9	21.5±1.9	425.3±46.4	386.2±42.7
<i>Rhodoferax antarcticus</i>	24.9±2.3	22.2±1.7	464.7±52.6	417.9±34.7
<i>Rhodospirillum rubrum</i>	26.3±2.6	19.8±1.9	494.5±56.1	383.5±40.5
<i>Roseisalinus antarcticus</i>	24.9±2.4	18.1±2.0	480.3±52.9	323.4±37.2
<i>Roseobacter</i> sp. COL2P	24.5±2.1	21.4±2.0	472.1±51.8	390.6±43.8
<i>Roseococcus suduntuyensis</i>	25.1±2.4	18.3±1.8	492.1±59.0	318.5±37.1
<i>Rubrivivax gelatinous</i>	24.8±1.9	21.4±1.7	471.3±48.6	404.4±38.5
<i>Thermochromatium tepidum</i>	24.7±2.1	21.2±2.2	479.0±51.1	414.5±47.8
<i>Thiocapsa roseopersicina</i>	27.9±1.9	21.7±1.9	541.3±48.9	400.7±45.1
<i>Chloroflexus aurantiacus</i>	25.0±1.7	19.8±2.4	483.5±53.1	358.1±54.7
<i>Synechocystis</i> sp. PCC6803	21.9±2.0	21.8±2.0	404.7±47.0	416.8±46.9
<i>Thermosynechococcus vulcanus</i>	24.1±2.1	20.6±1.4	451.9±49.3	389.0±34.5

Table S4.3 The parameters of interhelical hydrogen bonds between short segments of L- and M-subunits helixes based on molecule dynamics simulation models of simplified model (X → Y means X donates a H-bond to Y).

species	INTERHELICAL HYDROGEN BONDS			
	position of H-bond	distance (Å)	energy (kJ mol ⁻¹)	probability (%)
<i>Blastochloris viridis</i>	none			0
<i>Congregibacter litoralis</i>	L (THR) 184 ← M (SER) 212	2.05	16.2	22.0
	L (PHE) 180 ← M (SER) 212	2.22	12.4	11.2
	L (THR) 184 → M (SER) 212	2.10	20.0	9.2
<i>Dinoroseobacter shibae</i>	none			0
<i>Erythrobacter sp. NAP1</i>	L (ASN) 183 → M (ALA) 213	2.24	14.4	9.6
<i>Porphyrobacter tepidarius</i>	L (ASN) 183 → M (SER) 212	2.23	11.1	15.6
	L (CYS) 184 ← M (SER) 212	2.26	14.4	2.4
<i>Rhodobaca barguzinensis</i>	L (THR) 184 ← M (SER) 212	1.91	21.9	42.8
<i>Rhodobacter sphaeroides</i>	L (ASN) 183 → M (ALA) 212	2.24	10.9	8.0
<i>Rhodoferax antarcticus</i>	L (THR) 183 → M (THR) 213	1.98	19.6	94.0
<i>Rhodospirillum rubrum</i>	none			0
<i>Roseisalinus antarcticus</i>	L (CYS) 184 ← M (SER) 212	2.26	14.9	1.2
<i>Roseobacter sp. COL2P</i>	L (THR) 183 → M (THR) 213	2.02	18.6	74.0
	L (THR) 184 ← M (SER) 212	1.88	22.3	56.0
<i>Roseococcus suduntuyensis</i>	L (THR) 184 ← M (SER) 212	2.02	17.3	26.0
<i>Rubrivivax gelatinous</i>	L (THR) 183 → M (THR) 213	1.94	21.8	95.6
<i>Thermochromatium tepidum</i>	L (HIS) 181 ← M (TYR) 209	2.22	9.7	3.2
<i>Thiocapsa roseopersicina</i>	L (HIS) 171 ← M (TYR) 210	1.92	20.7	0.4
<i>Chloroflexus aurantiacus</i>	L (SER) 183 → M (THR) 213	1.95	21.9	45.8
	L (THR) 184 ← M (SER) 212	2.02	17.8	36.1
<i>Synechocystis sp. PCC6803</i>	D1 (GLY) 208 ← D2 (CYS) 211	2.33	8.7	0.4
	D1 (SER) 209 → D2 (ILE) 204	1.85	22.5	99.6
	D1 (SER) 212 → D2 (GLY) 207	1.82	22.8	94.0
<i>Thermosynechococcus vulcanus</i>	D1 (GLN) 199 → D2 (HIS) 197	2.22	15.5	21.6
	D1 (CYS) 212 → D2 (GLY) 207	2.01	18.0	18.4
	D1 (HIS) 215 → D2 (HIS) 214	2.40	6.38	0.4

Table S4.4 The interactions of lipids within phosphatidylcholine membrane surrounded by aqueous phase of the whole reaction center model. The number of lipid interactions were computed by the molecular dynamics simulations. In total, 9 to 21 H-bonds were formed between the hydrophilic parts of membrane lipids and the L and M protein subunits.

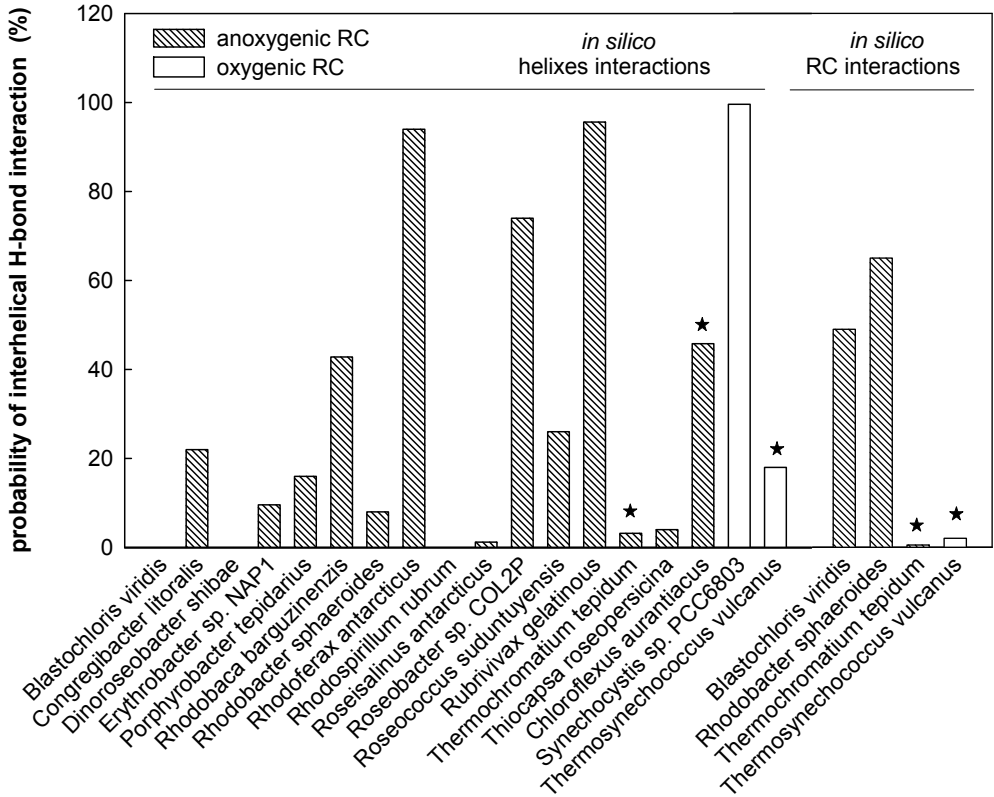
PROTEIN-LIPID HYDROGEN BOND INTERACTIONS					
<i>Blastochloris viridis</i>		<i>Rhodobacter sphaeroides</i>		<i>Thermochromatium tepidum</i>	
L-helix residues		L-helix residues		L- helix residues	
donor	count (%)	donor	donor	count (%)	donor
Ala 77	62	Ala1	Ala 77	62	Ala1
Arg257	76	His116	Arg257	76	His116
Gln55	70		Gln55	70	
Leu75	100	Leu80	Leu75	100	Leu80
Ser54	76	Lys202	Ser54	76	Lys202
Tyr51	0	Trp151	Tyr51	0	Trp151
		Tyr115			Tyr115
M - helix residues		M - helix residues		M- helix residues	
donor	count (%)	donor	donor	count (%)	donor
Leu82	8	Ala1	Leu82	8	Ala1
Ser35	100	Arg253	Ser35	100	Arg253
Trp37	53		Trp37	53	
Trp112	58	Asn25	Trp112	58	Asn25
Tyr132	21	Asn28	Tyr132	21	Asn28
		Asn81			Asn81
		Gln4			Gln4
		Gln138			Gln138
		Glu2			Glu2
		Gly31			Gly31
		Ile6			Ile6
		Leu38			Leu38
		Phe7			Phe7
		Thr37			Thr37
		Trp41			Trp41
		Tyr51			Tyr51
		Tyr3			Tyr3

Table S4.4 (continued)

PROTEIN-LIPID HYDROGEN BOND INTERACTIONS			
<i>Thermosynechococcus vulcanus</i>			
D1- helix residues (%)			
donor	count (%)	distance (Å)	energy (kJ mol ⁻¹)
Ala11	1	2.01	15.25
Asp12	70	2.14±0.15	18.26±5.80
Arg16	1	2.28±0.01	10.51±4.33
Leu28	30	2.15±0.12	12.09±4.10
Phe93	96	1.94±0.16	21.31±3.87
Ser232	85	1.84±0.15	22.25±3.37
Asn234	68	2.07±0.14	17.11±5.49
Tyr262	1	1.98	12
Asn267	38	2.11±0.15	38.0
Ser270	24	1.96±0.10	10.63±3.47
Ser305	53	1.95±0.15	17.41±5.92
D2- helix residues			
donor	count (%)	distance (Å)	energy (kJ mol ⁻¹)
Trp21	4	2.02±0.19	17.09±6.21
Arg26	78	2.07±0.16	17.21±5.44
Tyr67	39	1.84±0.15	1.84±0.15
Phe73	100	2.04±0.13	2.04±0.13
His87	100	1.93±0.13	21.78±4.57
Asp100	83	1.87±0.19	18.00±5.93
Phe101	78	2.20±0.14	18.52±5.71
Arg139	2	2.22±0.13	13.96±5.42
Tyr141	100	1.79±0.12	24.23±1.85
Ser165	9	1.99±0.17	18.06±6.64
Asn220	10	2.22±0.11	12.31±4.98
Ser230	3	2.19±0.13	2.19±0.13
Arg233	11	2.22±0.10	11.21±5.38
Ser262	100	1.85±0.14	22.09±4.14
Asn263	100	1.98±0.13	22.76±3.74
Trp266	100	1.97±0.14	22.41±3.75

Figure S4.2

The probability of forming interhelical bonds between pairs of D helices (L(D1) and M(D2)) obtained computed by molecular dynamics simulations. One to three hydrogen bonds were formed between the two helices. The probability is generally less in thermophilic strains (marked by an asterisk).



5. Effect of Post-mining Waters on Cyanobacterial Photosynthesis

This chapter is based on the manuscript:

Effect of post-mining waters on cyanobacterial photosynthesis

Hana Medová^{1,2}, Ivo Přikryl³, Eliška Zapomělová⁴, Libor Pechar^{3,5}

Water Environment Research, submitted

5.1 Summary

New water bodies have been created in a post-mining area of the brown coal basin Sokolov, Czech Republic. In a former open-cast brown coal quarry Medard, a new lake of a planned area of 500 ha and a retention volume 119 mil. m³ was established. The pit has been filling with post-mining waters of acid mine drainages (AMD), and water from the surrounding catchment spoil heaps and a local river. The effect of post-mining acidic and high-conductivity water on selected cyanobacteria and the possibility of cyanobacterial water bloom in the newly formed Lake Medard was considered and studied in this paper by means of chlorophyll fluorometry.

Actual PSII quantum yield $\Delta F/F_m'$ and relative electron transport rate $rETR$ were used to test the viability of *Dolichospermum* and *Microcystis* strains and study the immediate response of cyanobacterial photosystem II after the exposure to discharge water from small spoil-heap localities and post-mining Lake Medard where the pH range was 2.5 – 8.4 and conductivity 290 – 1,400 mS m⁻¹. A relatively low amount of the acidic spoil-heap water reduced cyanobacterial photosynthetic activity. The *Dolichospermum* strains were about ten times more sensitive than *Microcystis viridis*.

¹Institute of Microbiology CAS, Třeboň, Czech Republic

²University of South Bohemia, Faculty of Science, České Budějovice, Czech Republic

³ENKI, pbc., Třeboň, Czech Republic

⁴Biological Centre CAS, Institute of Hydrobiology, České Budějovice, Czech Republic

⁵Faculty of Agriculture, University of South Bohemia, České Budějovice, Czech Republic

The high concentration of dissolved ions appeared to have less effect on cyanobacterial PSII. Only the samples from the bottom water layers of Lake Medard caused a significant decrease in the $\Delta F/F_m'$ value of *Dolichospermum* spp.

The response of cyanobacteria to spoil-heap waters appeared to be species-specific and can promote selection of those resistant to post-mining environments. The actual water chemistry of the upper layers of Lake Medard did not prove to effectively prevent any cyanobacterial bloom.

5.2 Introduction

The Sokolov brown coal basin belongs to the Czech-German brown coal triangle, together with the Most brown coal basin (Czech Republic), Lausitzer Region (Saxony and Brandenburg, Germany), and Central German Region (Saxony-Anhalt, Germany). It is situated in the Karlovy Vary Region, West Bohemia (Czech Republic). After 1950, large open-cast surface mines were opened here.

Mining activities worldwide cause extensive changes in terrain and water regime. The opening of open-cast quarries results in the damaging of landscapes by the excavation of large volumes of overburden rocks and establishing new locations. The consequences are the change in surface and underground water regimes, and shifts in water chemistry to low pH and a higher amount of dissolved ions (Nixdorf et al. 2001; Schultze et al. 2010; the comparison of physio-chemical characteristics of AMD-affected water and common Central European surface water is summarized in Table S5.1). Exposure of overburden rocks rich in pyrite and non-pyrite sulfide minerals to both oxygen and water results in acidic and sulfate rich environments. Overall, mining and extraction mobilizes $\sim 150 \times 10^{12}$ g of sulfur per year, contributing $\sim 50\%$ to the net river transport of sulphate to the ocean, which is about half of the sulfate input into the ocean (Edwards 2000).

5.2.1 Microorganisms in post-mining areas

Harsh conditions in AMD waters lead to low diversity and often lower biomass (Nixdorf 1998). Planktonic biodiversity in acidic mining lakes is determined by the

water chemistry, whereas algal biomass is related to the degree of eutrophication (Das 2009). Low pH itself does not reduce photosynthetic activity. Minimum primary production is most likely due to metal stress or a lack of soluble reactive phosphate concentration. Phosphorus may be absorbed onto the surfaces of precipitates of iron and aluminium and buried in the sediment (Schultze et al. 2010). The nitrogen abundance is often sufficient due the fact that nitrification is facilitated in an acidic milieu (Nixdorf et al. 2001). Other limiting factors such as light intensity, H₂S concentration, phosphorus and carbon availability. In an acidic pH, all forms of DIC are in the form of dissolved CO₂ (Gross 2000). The lower availability of DIC for microorganisms is counterbalanced by the high exchange rate between the dissolved and atmospheric CO₂ under acidic conditions.

The common taxa reported from AMD are cosmopolitan green algae *Euglena* and *Klebsormidium* (Novis and Harding 2007). They are frequently dominant where they occur. In German pit lakes, *Chrysophytes* and *Chlamydomonas* are locally common (Nixdorf et al. 1998). *Ochromonas* sp., *Chlamydomonas acidophilis* and *Lepocinclis buetschlii* have been found in phytoplankton in the acidic post-mining Lake Langau (Austria) with a pH as low as 2.6 (Moser and Weisse 2011). The resistance of many algae to AMD is thought to be due to their ability to complex metals outside the cells, preventing entry into the cytoplasm (Novis and Harding 2007). In contrast, cyanobacteria are very poorly represented in AMD.

5.2.2 Sokolov post-mining area

The Medard quarry located north-west of the town of Sokolov was mined between 1923-2002. According to the restoration strategy, the remaining pit has been filled with water from different sources since 2008: with discharge water from small catchment spoil heaps, seepages of AMD water through the bottom of the lake, as well as water from the local river Ohře which is a possible source of cyanobacterial inoculum. The established volume of these water sources are 3, 40, and 76 mil. m³ respectively. Therefore, the final ratio of discharge spoil-heap and AMD water in the lake should reach 36%. The planned dimensions of the newly formed lake should be reached by

April 2014 (total area of the lake: 500 ha; length: 4,000 m; width: 1,500 m; maximum depth: 50 m; and retention volume: 119 mil. m³). The newly established lake is intended to function as a local water reservoir and recreational area. The oligotrophic status with the lack of cyanobacterial bloom is necessary to fulfil its managed functions and to provide an acceptable water quality.

Cyanobacteria are very sensitive to low pH and react quickly to the presence of discharge water. They are particularly suitable for use in bioassays of AMD-affected waters (Regel et al. 2002). Therefore, we measured the PSII chlorophyll *a-in vivo* fluorescence to test the immediate response of cyanobacteria to the exposure to spoil-heap and Lake Medard water. We used chlorophyll fluorometry to assess the effect of acidic and high-conductivity water on cyanobacteria in order to find out whether the possible toxicity of discharge spoil-heap water might prevent the cyanobacterial bloom in newly established Lake Medard.

5.3 Material & Methods

5.3.1 Sampling sites description

The Sokolov brown coal basin altitude ranges between 450 – 700 m a. s. l., its mean precipitation is about 650 mm, and its mean annual temperature is 6.5°C (Abakumov and Frouz 2009).

Seven aquatic localities situated in the Sokolov region were chosen for our study (Table 5.1). Their areas were 0.02 – 3.4 ha and their depths did not exceed 2.5 m. Four of them (Červená Ema, Lítov M1, Lítov M4, Lomnice-retention) were extremely acidic with a pH of 2.7 – 3.6, whereas the localities Eva and Muší contained high amounts of dissolved ions (conductivity up to 1,400 mS m⁻¹, Table 5.2). Only a few planktonic species were described here. *Euglena mutabilis* (Euglenophyceae), *Chlamydomonas*, *Phacus*, *Strombomonas*, and *Trachelomonas* sp. were found in acidic localities (Skácelová 2006). Chlorophyta and pennate diatoms were observed in the high-conductivity locality, Eva.

The water reservoir Skalka, situated 15 km upstream from Lake Medard, is assumed to influence the Medard water quality. Seasonal cyanobacterial water blooms are regularly reported here. In the summer season 2011, up to 1×10^5 cell per mL of *Microcystis aeruginosa* were monitored in the River Ohře 1 km upstream from Lake Medard.

Table 5.2 General characteristics of studied localities (date of sampling: *29th July 2009 †27th July 2010 ‡27th July 2011).

Locality	Latitude (N)	Longitude (E)	Max. depth (m)	Area (ha)
Lítov M1	50° 09'22"	12°31'45"	3.0	3.4
Lítov M4	50° 09'49"	12°31'22"	1.5	0.56
Lomnice – retention	50°12'48"	12°38'47"	5.0	3.0
Červená Ema	50°13'56"	12°39'05"	0.3	0.025
Eva	50°13'21"	12°38'56"	2.5	0.05
Medard	50°11'05"	12°36'59"	15.0 [*] 17.0 [†] 30 [‡]	35.0 [*] , 55.0 [†] 229 [‡]
Muší	50°13'53"	12°38'37"	2.5	0.03
Skalka	50° 04'72"	12°21'20"	12.2	378

The aquatic chemistry of Lake Medard is documented in Table S5.3 and Figure 5.1. Three layers evolved in the lake based on the measured temperature, pH, oxygen, and conductivity profile. The water samples from the upper layers (0 – 10 m in 2009; 0 – 15 in 2010 and 2011) and bottom water layers (10 – 15 m in 2009 and 2010; 20 – 30 m in 2011; i.e. 5 – 10 m above the bottom of the lake) were chosen for the fluorometric measurements and described in this paper. The pH did not go below 5.9 throughout the water column during the last three years of filling with water. On the bottom, an anoxic zone with a conductivity exceeding 600 mS m^{-1} evolved. The water status remained ultraoligotrophic during the summer 2011 (chlorophyll *a* concentration $1.8 \mu\text{g L}^{-1}$, TP $< 0.04 \text{ mg L}^{-1}$, water transparency 2.20 m). From phytoplanktonic species, the dominant groups were Chrysophyceae (*Chrysococcus* sp.), further diatoms, Cryptophyceae (*Cryptomonas* sp.), and Chlorophyta in total abundance of 1700 individuals per mL. No cyanobacterial cells were found under the light microscope.

5.3.2 Sampling

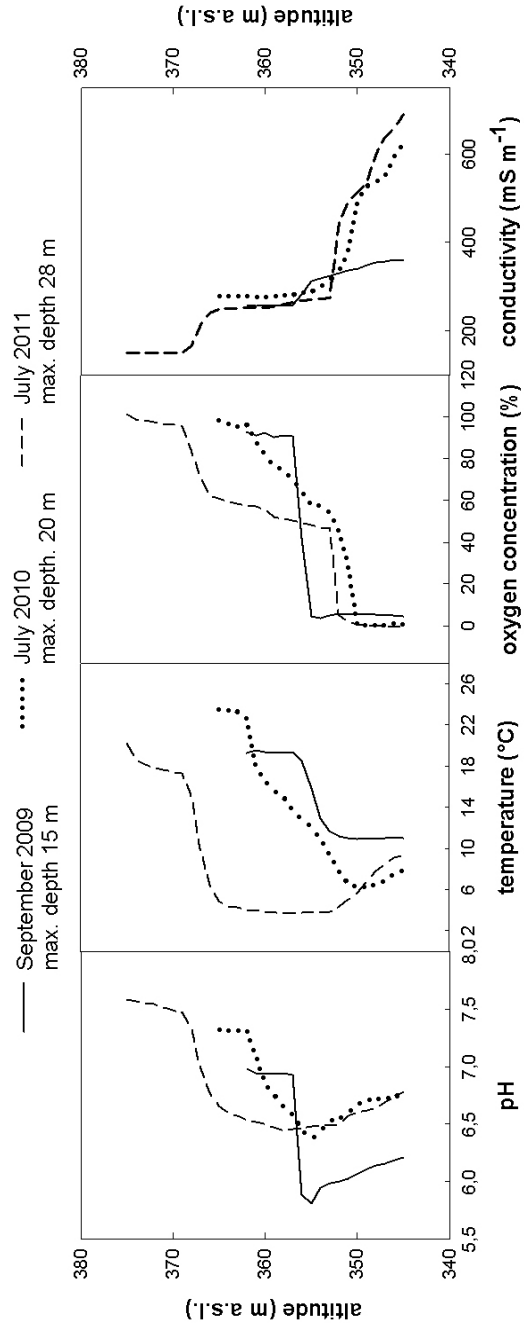
The sampling of the Sokolov spoil-heap localities was conducted in 2008 - 2011. Lake Medard has been regularly monitored in three deep profiles from spring 2009. The laboratory experiments done with the samples taken in the summer high-season (September 2009, July 2010, and July 2011) are described in this paper. The summer water bloom from the Skalka water reservoir was sampled in July 2010.

In the field, water pH, conductivity, and temperature were measured in surface layers of spoil-heap localities using a Hanna Combo pH&EC pH-meter (Hanna Instruments, Germany). The deep profile characteristics (pH, oxygen, temperature, conductivity) were obtained using a YSI 6600 sonde (YSI Environmental, Ohio, U.S.A.). A Secchi disc with a diameter of 20 cm was used to estimate the water transparency. The fluorescence measurements were achieved using a portable fluorometer AquaPen AP100 (PSI Ltd. Brno, Czech Republic). Water samples were transferred into a two-liter plastic bottle and stored at 8°C. The following day, the water pH, conductivity, alkalinity, nutrients, and anion concentration were evaluated in the laboratory. For cation analysis, 100 mL of the samples were frozen and analyzed within one month using a Varian SpectrAA-640 spectrophotometer.

5.3.3 Algal cultures

Laboratory cultures were cultivated in the Institute of Hydrobiology, AS CR, České Budějovice. All *Dolichospermum* (formerly *Anabaena*) and *Microcystis* strains used in our measurements were isolated from Czech ponds and dam reservoirs between the years 2000 – 2004. The specific strains measured were: *Dolichospermum planctonicum* 03-02 Apl (Lipno, 2003), *Dolichospermum mendotae* 04-33, *Dolichospermum compactum* 00-01, and *Dolichospermum mendotae* 04-10, *Dolichospermum circinalis* 12-Lip09/VI, and *Dolichospermum mendotae* 04-27. Further *Microcystis aeruginosa* 13-Lip09/VI, and *Microcystis aeruginosa* 18-Lip 09/VIII were also used.

Figure 5.1 The summer deep profiles of Lake Medard measured in the high summer season in September 2009, July 2010, and July 2011. Three distinctive zones with different water characteristics evolved in the lake. The upper layer (0 – 10 m in 2009, 0 – 15 m in 2010, and 2011) and the bottom layer (10 – 15 m in 2009, and 2010, 20 – 30 m in 2011, t.m. 5 – 10 m above the bottom of the lake) are discussed in this paper. The maximum depth of the lake increased from 15 to 30 m during the sampling dates



All laboratory strains were cultivated in WC medium (Guillard and Lorenzen 1972) with the pH ranging from 7 – 8. The strains were maintained at 21 °C on the 16 h light/8 h dark cycle and irradiance of 50 $\mu\text{mol photons m}^{-2} \text{s}^{-1}$.

The wild population of *Microcystis viridis* was collected during its summer bloom on the Skalka dam reservoir using a 20 μm plankton net. In the laboratory, the dense sample was transferred to a glass conic vessel, where the upper part of the buoyant population with cyanobacterium was gently collected and resuspended into GF/C filtered water of Skalka reservoir. After inspection under the optical microscope only *Microcystis viridis* cells were observed.

5.3.4 Chlorophyll *a*-in vivo fluorescence measurement

The chlorophyll *a* fluorescence changes were recorded by a portable fluorometer AquaPen AP 100 (PSI Ltd. Brno, Czech Republic). The AquaPen AP 100 was equipped with a blue (455 nm) light-emitting diode for chlorophyll *a* fluorescence measurement in algae and a red (630 nm) light-emitting diode for the detection of fluorescence changes in cyanobacteria. The measuring chamber is designed for using common spectroscopic cuvettes with a volume of 3 mL.

In the laboratory, a dilution series was done on the collected discharge water from the studied localities using dark-adapted *Dolichospermum* and *Microcystis* strains, and *Microcystis viridis* population. Therefore, a 40x diluted discharge water sample consisted of one part sample water and 39 parts culture inoculated medium (vol/vol).

After 15 min of dark adaptation, all samples were illuminated in a glass measuring chamber with a volume of 45 mL and regulated at 20°C. A halogen light source was used with an intensity of 300 $\mu\text{mol photons m}^{-2} \text{s}^{-1}$ in the measuring chamber (photometer Li-Cor, Li 190SA, Nebraska, U.S.A.). The light intensity used was selected according to the PI-curve measurements by Tesařová (2011) and was chosen to induce photosynthesis without damaging the cyanobacterial photosystems. From the irradiance response curves (Falkowski and Raven 2007), the parameters E_{opt} (saturation irradiance) and P_{max} (light-saturated rate, maximal photosynthetic capacity) of studied cyanobacterial culture were calculated as $E_{\text{opt}} 382 \pm 83 \mu\text{mol m}^{-2} \text{s}^{-1}$ (mean \pm SD, min –

max 237 – 503 $\mu\text{mol m}^{-2} \text{s}^{-1}$), P_{max} 7.12 ± 3.49 $\text{mg O}_2 \text{ mg chl}a \text{ h}^{-1}$ (2.26 – 12.66 $\text{mg O}_2 \text{ mg chl}a \text{ h}^{-1}$).

The experiment duration was as follows: 15 minutes of dark adaptation; 60 minutes with an irradiance of 300 $\mu\text{mol photons m}^{-2} \text{s}^{-1}$; 60 minutes of dark relaxation. The chlorophyll fluorescence was recorded in 0 (initial, dark-adapted value), 6, 15, 30, 45, 60 minutes of irradiation, and after 60 min of dark relaxation.

Before the laboratory experiments, the culture's density was adjusted to the $F_0 = 8,000$. The fluorescence parameters F_0 , F_v/F_m , and light curves (LC) were measured. The duration of the LC protocol was 360 s. Each actinic light exposure (E) (0, 20, 50, 100, 300, 500 $\mu\text{mol photons m}^{-2} \text{s}^{-1}$) lasted for 60 s. Relative electron transport rate ($r\text{ETR}$) was calculated from the fluorescence light curves measurements as:

$$r\text{ETR} = \Delta F/F_m' \times E \times a.$$

where $\Delta F/F_m'$ (Masojidek, 2011; sometimes referred as $\phi\text{PSII}'$) is the actual PSII photochemical yield, E is the actinic light intensity and a an experimental factor. The final amount of PAR in the sample is dependent on the optical cellular properties of the cells (Blache et al. 2011). Thus, the $r\text{ETR}$ value were corrected by an experimental factor a , which reflects the cell shading.

5.3.5 Statistical analysis

Statistical analysis was performed using the program Statistica 9.1 (StatSoft, Inc., 2008-2010). The following analyses were done: one-way ANOVA with fixed effects analysis; the Tukey's HSD (Honestly Significant Difference) post-hoc test and the Dunnett's post-hoc test with a probability level of $\alpha = 0.95$. The Tukey's test calculates a new critical value that can be used to evaluate whether differences between any two pairs of means are significant. The Dunnett's test was used to compare the treatment groups to the control group.

5.4 Results

5.4.1 Measurements of PSII photochemistry – spoil-heap localities

The non-treated dark-adapted wild population of *Microcystis viridis* generally showed a greater F_v/F_m value (0.51) compared to the pure *Dolichospermum* (0.41) or *Microcystis* culture (0.41).

The PSII of the *Dolichospermum compactum* and *D. mendotae* was affected by small amounts of acidic spoil-heap water (Table 5.). The most inhibiting for *Dolichospermum* spp. was the sample from the most acidic locality (Lítov M1; pH 2.7, conductivity 310 mS m⁻¹) where under the 40× dilution, *D. compactum* proved to have no photosynthetic activity (F_v/F_m was zero). The *Dolichospermum* strains retained their PSII photosynthetic ability in concentrations of no more than 40× diluted mixture in the case of Červená Ema water (pH 3.1, conductivity 560 mS m⁻¹), 20× diluted sample from Lítov M4 (pH 3.0, conductivity 300 mS m⁻¹), and Lomnice-retention (pH 3.0, conductivity 290 mS m⁻¹). The water samples from locality Eva (pH 7.15, conductivity 547 mS m⁻¹), and Muší (pH 8.44, conductivity 1,130 mS m⁻¹) influenced the photosynthesis of *Dolichospermum* negligibly, even in instances with high amounts of studied water in the culture (2 – 10× dilution).

In the presence of water from spoil-heap localities, *Microcystis viridis* retained photosynthetic ability in volumes of spoil-heap water five to ten times higher than was the case of *Dolichospermum* strains (Table 5.2). In water samples from the three most acidic localities, the $\Delta F/F_m'$ value decreased to 0.03 – 0.35 (7 – 66%) in 4× diluted spoil-heap water after 60 min of irradiance of 300 $\mu\text{mol photons m}^{-2} \text{s}^{-1}$. The 2× diluted sample from Eva and Muší did not prove to have any additional negative effect, other than the light inhibition of the control *Microcystis* population (fall of F_v/F_m only to 0.39 (81%) and 0.33 (69%)).

The $r\text{ETR}$ curves measured after one hour of 300 $\mu\text{mol photons m}^{-2} \text{s}^{-1}$ light exposure followed the results of measurements of variable fluorescence (Figure 5.2). The *Dolichospermum* strains were 5 – 10 times more sensitive to the acidic spoil-heap water samples than *Microcystis viridis*. The highest tolerated concentrations of samples

from the most acidic localities, which did not have any pronounced effect on $rETR$ of *Dolichospermum* spp., spanned from 20 – 80× dilutions. Samples with a high conductivity did not have any noticeable effect on tested cyanobacteria. Overall, the relative electron transport rate was slower in the case of *Dolichospermum* than in *Microcystis viridis*.

Table 5.2 The maximum photochemical yield (F_v/F_m) and actual PSII quantum yield $\Delta F/F_m'$ of *Dolichospermum compactum*, *Dolichospermum mendotae* and *Microcystis viridis* in mixture with water samples from the studied localities, before and after one hour of irradiation of 300 $\mu\text{mol photons m}^{-2} \text{s}^{-1}$. The spoil-heap water was diluted with cyanobacterial culture using the ratios listed here. The concentrations show the highest tolerated concentrations before inhibition and the lowest concentrations inducing inhibition. The percentual decrease of $\Delta F/F_m'$ value at time 60 min compared to the values at time 0 min is added here. The pH value refers to the final mixture.

Locality	Dilution	pH	F_v/F_m (0 min)	$\Delta F/F_m'$ (60 min)	Decrease of $\Delta F/F_m'$ (%)
<i>Dolichospermum</i> spp. (control)	0×	7.08	0.40 – 0.48	0.19 – 0.30	52 – 25
Lítov M1	80×	4.40	0.44	0.19	57
	40×	4.10	0.47	0	100
Červená Ema	40×	4.64	0.47	0.23	51
	20×	4.34	0.43	0	100
Lítov M4	20×	4.11	0.48	0.31	35
	10×	3.81	0.49	0	100
Lomnice-retention	20×	4.28	0.48	0.32	34
	10×	3.98	0.39	0	100
Eva	10×	7.11	0.38	0.16	58
Muší	10×	7.12	0.43	0.18	58
	2×	7.36	0.47	0.30	36
<i>Microcystis viridis</i> (control)	0×	8.79	0.52	0.44	15
Lítov M1	10×	3.74	0.45	0.19	58
	4×	3.34	0.46	0.03	93
Červená Ema	7×	4.08	0.51	0.26	49
	4×	3.86	0.36	0.11	69
Lítov M4	4×	3.34	0.43	0.35	19
	2×	3.04	0.39	0.08	79
Eva	2×	7.09	0.47	0.33	30
	1.5×	7.01	0.50	0.30	40
Muší	2×	7.33	0.48	0.39	19
	2×	7.36	0.47	0.30	36

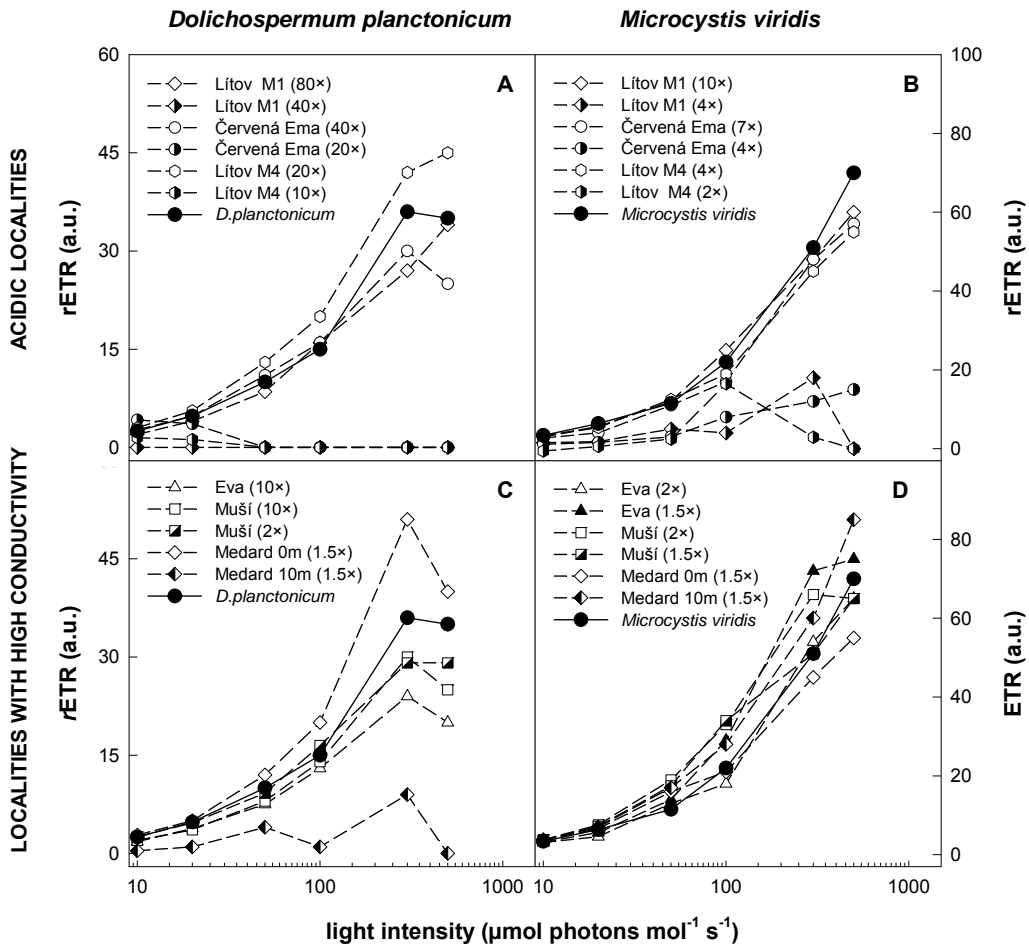


Figure 5.2 Effect of spoil-heap water samples on cyanobacterial PSII. The figure shows relative electron transport rate ($r\text{ETR}$) of cyanobacteria after one hour of irradiation of $300 \text{ mol m}^{-2} \text{ s}^{-1}$ in absence (black circles) or presence (other symbols) of water from spoil-heap localities. The $r\text{ETR}$ curves of non-treated cyanobacterium were used as a control. The left panels describe $r\text{ETR}$ s of *Dolichospermum planctonicum*, the right ones the $r\text{ETR}$ s of the wild population of *Microcystis viridis* from the water dam Skalka (B, D). The photosynthesis of *Dolichospermum* culture or wild population of *Microcystis viridis* was either influenced or stopped at varying volume dilutions of culture-inoculated medium in spoil-heap water samples. Panels A and B show the influences of water samples from acidic localities (pH 2.5 – 3), panels C and D from neutral localities with high conductivity ($250 - 1,100 \text{ mS m}^{-1}$).

Table 5.3 The maximal photochemical yield (F_v/F_m) and actual PSII quantum yield $\Delta F/F_m'$ of mixtures of Lake Medard water samples diluted with the *Dolichospermum* and *Microcystis* spp. before and after one hour of irradiation of $300 \mu\text{mol photons m}^{-2} \text{s}^{-1}$ (value \pm S.D., $n = 3$).

	Dilution	pH	F_v/F_m (0 min)	$\Delta F/F_m'$ (60 min)
<i>Dolichospermum planctonicum</i>	control	7.08	0.40 \pm 0.01	0.29 \pm 0.01
0 – 5 m	1.5 \times	6.97	0.45 \pm 0.02	0.30 \pm 0.02
10 – 15 m	1.5 \times	6.17	0.47 \pm 0.01	0.09 \pm 0.01
<i>Dolichospermum circinalis</i>	control	7.50	0.46 \pm 0.02	0.36 \pm 0.02
0 – 10 m	1.5 \times	7.45	0.49 \pm 0.02	0.39 \pm 0.02
20 – 30 m	1.5 \times	6.68	0.48 \pm 0.02	0.02 \pm 0.01
<i>Microcystis aeruginosa</i>	control	7.10	0.41 \pm 0.02	0.24 \pm 0.01
0 – 10 m	1.5 \times	7.26	0.43 \pm 0.02	0.28 \pm 0.02
20 – 28 m	1.5 \times	6.89	0.47 \pm 0.02	0.39 \pm 0.02
<i>Microcystis viridis</i>	control	8.79	0.51 \pm 0.02	0.39 \pm 0.02
0 – 5 m	1.5 \times	6.95	0.55 \pm 0.02	0.41 \pm 0.02
10 – 17 m	1.5 \times	6.74	0.56 \pm 0.02	0.43 \pm 0.02

5.4.2 Measurement of PSII photochemistry – Medard water samples

The response of PSII photosynthetic activity of the *Dolichospermum planctonicum* and *Dolichospermum circinalis* was measured after the exposure to the samples from the upper and bottom water layers of the lake from different sampling days (Table 5.3, Figure 5.3). After 60 min of irradiance of $300 \mu\text{mol photons m}^{-2} \text{s}^{-1}$, only the decline caused by photoinhibition of PSII per se was observed in 1.5 \times dilution of the upper layers of Lake Medard.. The samples from Medard bottom layers rapidly caused the change in $\Delta F/F_m'$ of *Dolichospermum* spp. That change in $\Delta F/F_m'$ of *Dolichospermum* spp. exposed to the samples from bottom layers (averaged pH 6.5, conductivity 352 mS m^{-1}) was significantly different from the response to samples of upper layers, which was confirmed by using a post-hoc Tukey's HSD test and a Dunnett's test (Table 5.4).

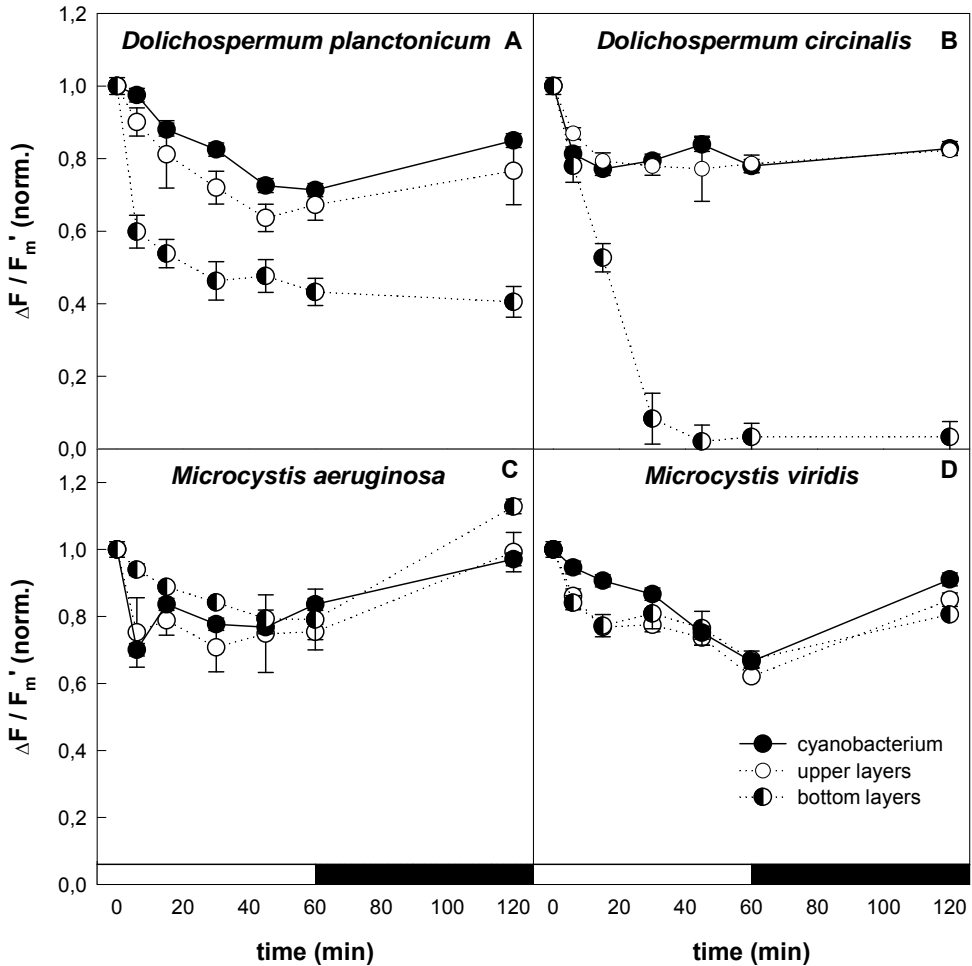


Figure 5.3 Maximum photochemical and actual PSII quantum yield (F_v/F_m and $\Delta F/F_m'$) of cyanobacteria in 1.5 \times dilution of Medard water samples after 60 min of irradiation of 300 $\mu\text{mol photons m}^{-2}\text{s}^{-1}$ and followed by 60 min of relaxation in darkness. The samples from upper/bottom water layers of Lake Medard are marked by open/semi-filled circles (means \pm standard deviations). The black symbols represent the non-treated cyanobacteria as the control. The changes in photochemistry of *Dolichospermum planctonicum* (A), *Dolichospermum circinalis* (B), and *Microcystis aeruginosa* (C) culture, and the wild population of *Microcystis viridis* (D) were recorded. Only in the case of the *Dolichospermum* strains was the cyanobacterial photosystem II negatively influenced by the samples from the lake bottom water layers. Lake Medard was sampled in July 2011 (A, C), and July 2010 (B, D).

The normalized $\Delta F/F_m'$ value of *Microcystis viridis* or *Microcystis aeruginosa* exposed to the Medard water did not show any difference when compared to the non-treated cyanobacterial cells as a control (Table 5.3, Figure 5.3). No significant differences between treatments of upper layers and bottom layers water samples were proved by the ANOVA analysis (Table 5.4).

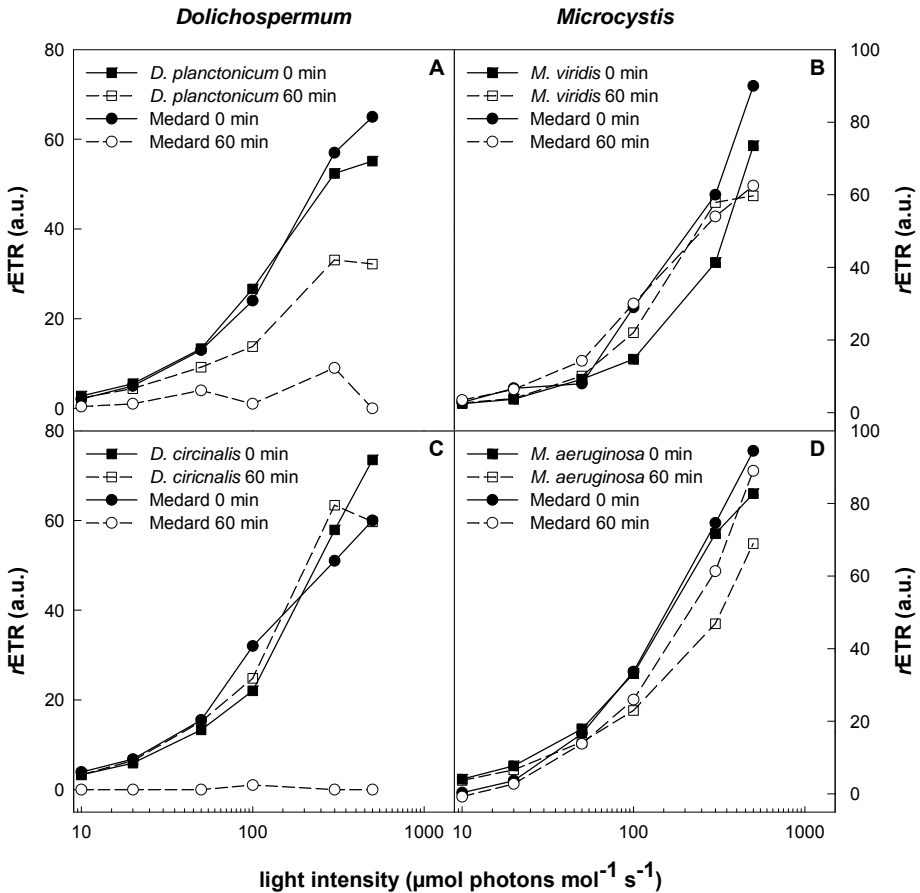


Figure 5.4 Effect of Lake Medard water samples on cyanobacterial photosynthesis. Figure shows relative electron transport rate ($rETR$) of cyanobacteria before (at time 0 min, black symbols) and after (at time 60 min, white symbols) one hour of irradiation of $300 \mu\text{mol m}^{-2} \text{s}^{-1}$ in absence (squares) or presence (circles) of bottom layer water samples of Lake Medard. The $rETR$ curves of non-treated cyanobacterium (squares) were used as a control. The left panels describe $rETR$ s of *Dolichospermum* culture (A, C), the right ones the $rETR$ s of wild population of *Microcystis viridis* and *Microcystis aeruginosa* (B, D). The photosynthesis of *Dolichospermum* spp. was either influenced or stopped after treatment with bottom water layers samples.

Table 5.4 The effect on cyanobacterial photochemistry of different water layers of Lake Medard was statistically evaluated. The one-way ANOVA was run in the program Statistica 9.1 (StatSoft, Inc. 2010).

The treated cyanobacterium	<i>p</i>	df	F
<i>Dolichospermum planctonicum</i>	<0.001	4	32.64
<i>Dolichospermum circinalis</i>	<0.001	5	15.61
<i>Microcystis aeruginosa</i>	0.111	5	1.98
<i>Microcystis viridis</i>	0.3838	4	1.09

The *r*ETR curves of cyanobacterial cells exposed to the Medard water samples showed similar trends to the PSII photochemical yield measurements (Figure 5.4). When treated by bottom layer samples, both strains of *Dolichospermum planctonicum* and *Dolichospermum circinalis* slowed their electron transport rate to zero after 60 min of irradiance. By contrast, the *r*ETR curves of *Microcystis aeruginosa* and *Microcystis viridis* did not change their trend compared to the *Microcystis* control curves.

The summarized results from all conducted laboratory experiments are plotted in Figure 5.5. The cyanobacterial PSII was functional in a broader pH range in the case of *Microcystis* cells (pH > 3) than in the case of *Dolichospermum* strains (pH > 4). The two lowered values of $\Delta F/F_m'$ by pH 6.19 and 6.68 reflect the response of *Dolichospermum* spp. to the bottom layers of Lake Medard. The amount of dissolved ions does not have any clear effect on cyanobacterial PSII.

5.4.3 Photosynthetic activity of natural green algae populations

The photosynthetic abilities of wild populations of green algae *Euglena mutabilis* (Euglenophyceae), *Mougeotia* sp. (Zygnematophyceae) and *Spirogyra* sp. (Zygnematophyceae) that occurred naturally in the studied localities were tested (Table 5.5). The wild population of alga *Euglena mutabilis* dominated shallow parts of the acidic localities Lítov M1, Lítov M4, and Červená Ema. Any cyanobacterial cells naturally living in small spoil-heap localities were not found during the sampling in 2009 – 2011.

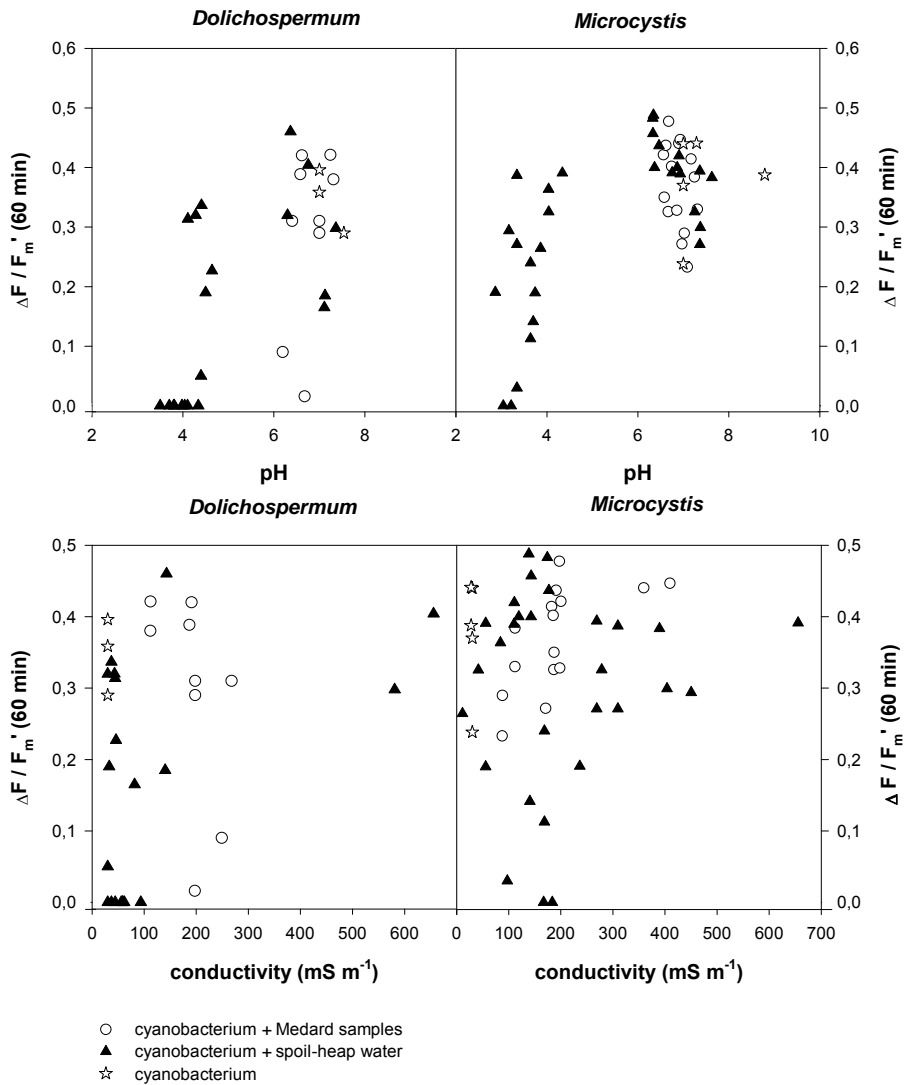


Figure 5.5 The relationship of cyanobacterial photochemical activity on pH (upper panel) and conductivity (lower panel). Black triangles represent the mixture of spoil-heap water from small localities, the white circles the mixture of water samples from different water layers of Lake Medard. The pH and conductivity values plotted here reflect the actual values of the final mixture of the studied water samples and cyanobacterium. The semi-filled squares indicate the $\Delta F / F_m'$ value of non-treated cyanobacteria as a control. The *Dolichospermum* and *Microcystis* strains were used for our measurements. For clarity, the standard deviations were left out.

The effect of light inhibition on *Euglena mutabilis* was imperceptible (F_v/F_m value of the dark-adapted cells 0.64 – 0.68, $\Delta F/F_m'$ after one hour of irradiation 0.60 – 0.64, 89 – 97% of the initial F_v/F_m value). The alga *Mougeotia* sp. was photoinhibited by high light when compared to the *Dolichospermum* and *Microcystis* strains. Its dark-adapted F_v/F_m value sank from 0.62 to 0.33 (52%) after one hour of irradiation, but returned to the initial value after 60 min of relaxation in darkness.

Table 5.5 The averaged value (n = number of experiments) of the maximal photochemical yield (F_v/F_m) and actual PSII quantum yield $\Delta F/F_m'$ of green-algae populations naturally occurring in sampled spoil-heap localities before and after one hour of irradiation of $300 \mu\text{mol m}^{-2} \text{s}^{-1}$. The sampling was done in years 2010-2011.

Locality	Species	F_v/F_m (0 min)	$\Delta F/F_m'$ (60 min)	Decline of $\Delta F/F_m'$ (%)	n
Červená Ema	<i>Euglena mutabilis</i>	0.65	0.56	13	4
Lítov M1	<i>Euglena mutabilis</i>	0.67	0.58	14	3
Lítov M4	<i>Euglena mutabilis</i>	0.68	0.59	13	1
Eva	<i>Spirogyra</i> sp.	0.66	0.50	24	1
Muší	<i>Mougeotia</i> sp.	0.61	0.43	30	3

5.5 Discussion

The physiological response of cyanobacteria to low pH was studied marginally. The now classic publication of Kratz and Myers (1955) states that cyanobacteria have preferences for alkaline conditions; their conclusion was based on ecological observation. Similarly Brock (1973) pointed out that the cyanobacterial growth optimum lies between pH 7.5 – 10. He studied 22 lakes in the Yellowstone National Park with pH ranging from 1.9 – 8.6; no cyanobacteria were found at a pH lower than 4 – 5, although eukaryotic algae were present.

In studies of the effect of AMD on stream biota as well as studies of the effect of acidification in lakes. Regel (2002) reported the restriction or absence of cyanobacteria in waters with pH 5, while various species of green algae are able to thrive when pH is lower than 4. No cyanobacteria were found in the acidic post-mining lake Langau (Austria) with pH 2.6 (Moser and Weisse 2011). Similarly, in our survey in 2009-2011

no cyanobacteria were present in spoil-heap localities with pH 2.5 – 3.6. Contrary to the above mentioned findings, an acidic Lusatian lake (Germany, pH 2.9) was inhabited by two populations of filamentous cyanobacteria *Oscillatoria/Limnothrix* and *Spirulina* spp. (Steinberg 1998). The filamentous cyanobacteria are considered to be acid-tolerant rather than acidophilic.

In the laboratory studies, the oxygen evolution and dry weight of *Anabaena* strain PCC7120 exposed to a pH of 5.4 – 7.5 was measured (Giraldez-Ruiz et al. 1997). Photosynthesis appeared to be more affected than the growth was under acidic conditions (photosynthesis in the cultures grown at pH 5.4 was highly impaired after only 1 day of exposure to this low pH). Further, the culture of *Synechocystis* sp. strain PCC 6308 did not grow when stressed at pH 4.4 and lower. Pre-stressing the cells at pH 5.1 did not enable them to grow when stressed below pH 4.4 (Huang, 2002). In our laboratory experiments, the *Microcystis* cells were able to thrive in a pH range as low as 3, whereas the low pH limit of *Dolichospermum* strains were around 4. The *Dolichospermum* spp. had less endurance to spoil-heap as well as Lake Medard water samples than *Microcystis* spp. The viability of cyanobacteria in low pH conditions seemed to be species-specific. We suggest that colonial *Microcystis* cells could endure higher dissolved ion concentrations than *Dolichospermum* (Wu 2007). Further, the presence of a multilayered polypeptide mucilaginous sheath encircling the colony increases its resistance to unfavorable environmental conditions by preventing the penetration of hydrogen ions and dissolved metals inside the *Microcystis* colonies (Kolmakov 2006, Obelholster 2010).

The potential toxicity of spoil-heap substrate for the soil algae community was tested by Frouz et al. (2011). The low pH and associated solubility of Al and Fe content were the major factors correlated with the toxicity of post-mining sites. That is in accordance with our observations, that the low pH conditions inhibited the cyanobacterial photosynthesis, whereas water with higher amounts of dissolved ions did not significantly influence the cyanobacterial PSII.

The maximal photochemical yield of non-stressed *Dolichospermum* and *Microcystis* strains showed lower dark-adapted values (0.40 – 0.48) than the natural

population of *Microcystis viridis* (0.52). The wild-type strain of *Synechococcus* under acclimated growth had a F_v/F_m of 0.4 – 0.6 (Campbell 1998). In healthy microalgal culture, F_v/F_m typically ranges from 0.6 for cyanobacteria (Masojídek 2011) and varies significantly during the diurnal cycle, depending on the irradiance regime and treatment which determines the physiological status. In outdoor cultures, F_v/F_m exhibits a diurnal depression that is roughly symmetric with the irradiance intensity (Masojídek 2001, 2011). Under prolonged supra-optimal irradiance, light induces a depression in the maximum quantum yield of PSII photochemistry (F_v/F_m) (photoinhibition of photosynthesis). A decrease of about 20% at mid-day maximum irradiance can be considered physiological. In our laboratory experiment, a drop of 50 – 85% in $\Delta F/F_m'$ of the cyanobacterial culture was observed after 60 min of illumination. The photoinhibition light effect on cyanobacterial PSII was more pronounced for *Microcystis* cells compared to *Dolichospermum*. Nevertheless, the $\Delta F/F_m'$ values returned to the initial F_v/F_m values following dark relaxation.

The benthic alga *Euglena mutabilis* (Euglenophyceae) dominated the acidic spoil-heap localities on all sampling dates. It occurred naturally in studied spoil-heap localities with a pH as low as 2.5, and conductivity as high as 590 mS m⁻¹. It prefers living in habitats with shallow water. The dark-adapted F_v/F_m value of *E. mutabilis* reached 0.55 – 0.71. One-hour exposure to continuous light did not change its actual photochemical yield. The maximum reported value of F_v/F_m for green algae is approx. 0.65 – 0.70, but can be significantly lower if the cells are stressed (Falkowski and Raven 2007). Thus, *E. mutabilis* would appear to be well-adapted to thrive in extreme living conditions like low pH, a high amount of dissolved ions, and high light intensities.

The dominance of *E. mutabilis* in waters with pH 2.69 – 3.57 followed its experimentally known physiological preferences. In the laboratory conditions, the growth of *E. mutabilis* is maximal between 3.4 and 5.4, although its total range of growth was from pH 2.1 to pH 7.7 (von Dach 1943). The success of *E. mutabilis* in AMD systems may be due to a recent acquisition of heavy metal tolerance rather than a species-specific ability to cope with low pH (Novis and Harding 2007). Moreover, the

nutrient supply from sediment may favor it in nutrient-poor acidic waters.

Microcystis aeruginosa and *Selenastrum capricornutum* have been used in rapid tests of AMD water pollution in a South Australian stream (Regel 2002). The algal bioassays were based on esterase activity converting fluorescein diacetate to fluorescein. The range of response between AMD-affected and other sites tended to be greater for *Microcystis aeruginosa* than for *Selenastrum capricornutum*.

To conclude, the low pH of spoil-heap water inhibited the cyanobacterial photosystem II and appeared to be potentially toxic for them. The chemistry of surface water layers of Lake Medard seemed to be non-toxic for cyanobacteria, thus they may proliferate in the littoral and surface zones. The perennial stratification of the lake does not enable the dissolved ions from meta- and hypolimnion to be washed out, which might suppress the undesirable cyanobacterial bloom.

Acknowledgements Supported by project No. 2B08006 of the Ministry of Education, Youth and Sport of the Czech Republic, and project No. Qh82078 of Research, Development and Innovation program of the Ministry of Agriculture of the Czech Republic. We would like to thank to Ing. Miroslav Kosík and Ing. Adam Truszik for help with sampling. We are indebted to Ing. Jana Šulcová, Ing. Iva Chmelová (ENKI p.b.c., Třeboň, Czech Republic) and Ing. Adam Truszik (Faculty of Agriculture, South Bohemia University, České Budějovice, Czech Republic) for the chemical analysis.

5.6 References

- Abakumov EV, Frouz J (2009) Evolution of the Soil Humus Status on the Calcareous Neogene Clay Dumps of the Sokolov Quarry Complex in the Czech Republic. *Euroasian Soil Science* 42: 718-724
- Blache U, Jakob T, Su W, Wilhelm C (2011) The impact of cell-specific absorption properties on the correlation of electron transport rates measured by chlorophyll fluorescence and photosynthetic oxygen production in planktonic algae. *Plant Physiol Biochem* 49:801-808
- Brock TD (1973). Lower pH limit for the existence of blue-green algae: evolutionary and ecological implications. *Science* 179, 480-483

- Campbell D, Hurry V, Clarke AK, Gustafsson P, Öquist G (1998) Chlorophyll Fluorescence Analysis of Cyanobacterial Photosynthesis and Acclimation. *Microbiol Mol Biol Rev* 62(3): 667-683
- von Dach H (1943) The effect of pH on pure cultures of *Euglena mutabilis*. *The Ohio Journal of Science* 43: 47-48
- Das BK, Roy A, Koshorreck M, Mandal SM, Wendt-Potthoff K, Bhattacharya J (2009) Occurrence and role of algae and fungi in acid mine drainage environment with special reference to metals and sulfate immobilization. *Water Res* 43: 883-894
- Edwards KJ, Bond PL, Gihring TM, Banfield JF (2000) An archeal iron-oxidizing extreme acidophile important in acid mine drainage. *Science* 287: 1796-1799
- Falkowski PG, Raven JA (2007) *Aquatic Photosynthesis*. Princeton University Press, pp. 112-113
- Frouz J, Hřčková K, Lána J, Křišťůfek V, Mudrák O, Lukešová A, Mihaljevič M (2011) Can laboratory toxicity tests explain the pattern of field communities of algae, plants, and invertebrates along a toxicity gradient of post-mining sites? *App Soil Ecol* 51: 114-121
- Fyson A, Nixdorf B, Kalin M (2006) The acidic lignite pit lakes of Germany – Microcosm experiments on acidity removal through controlled eutrophication. *Ecol Engineering* 28: 288-295
- Giraldez-Ruiz N, Mateo P, Bonilla I, Fernandez-Piñas F (1997) The relationship between intracellular pH, growth characteristics and calcium in the Cyanobacterium *Anabaena* sp. strain PCC7120 exposed to low pH. *New Phytol* 137: 599-605
- Guillard RRL, Lorenzen CJ (1972) Yellow-green algae with chlorophyllide C. *J Phycol* 8: 10-14
- Huang JJ, Kolodny NH, Redfearn JT, Allen MM (2002) The acid stress response of Cyanobacterium *Synechocystis* sp. strain PCC 6308. *Arch Microbiol* 177: 486-493
- Kolmakov VI (2006) Methods for prevention of mass development of the cyanobacterium *Microcystis aeruginosa* Kutz emend. Elenk. in aquatic systems.

- Microbiology* 75: 115-118
- Kratz WA, Myers I (1955) Photosynthesis and respiration of three blue-green algae. *Plant Physiol* 30, 275-280
- Malý J, Klem K, Lukavská A, Masojídek J (2005) Degradation and movement in soil of the herbicide isoproturon analyzed by a photosystem II-based biosensor. *J Environ Qual* 34: 1780-1788
- Masojídek J, Grobbelaar JU, Pechar L, Koblížek M (2001) Photosystem II electron transport rates and oxygen production in natural waterblooms of freshwater cyanobacteria during a diel cycle. *J Plankton Res* 23: 57-66
- Masojídek J, Vonshak A, Torzillo G (2011) *Chlorophyll fluorescence applications in microalgal mass cultures* in DJ, Prášil O, Borowitzka MA (eds.) *Chlorophyll a fluorescence in aquatic sciences: methods and applications*. Springer, pp. 277-292
- Moser M, Weisse T (2011) The most acidified Austrian lake in comparison to a neutralized mining lake. *Limnologica* 41(4): 303-315
- Nixdorf B, Mischke U, Leßmann D (1998) Chrysophytes and chlamydomonads: pioneer colonists in extremely acidic mining lakes (pH<3) in Lusatia (Germany). *Hydrobiologia* 369/370: 315-327
- Nixdorf B, Hemm M, Schlundt A, Kapfer M, Krumbeck H (2001) *Braunkohlentagebaueen in Deutschland. Umweltforschungsplan des Bundesministeriums für Umwelt, Naturschutz und Reaktorsicherheit Forschungsbericht*. 298 22 240 UBA-FB 000146
- Novis PM and Harding JS (2007) *Extreme acidophiles: freshwater algae associated with acid mine drainage* in Seckbach J (ed.) *Algae and cyanobacteria in extreme environments*. Springer, pp.445-463
- Obelholster PJ (2010) Responses of phytoplankton upon exposure to a mixture of acid mine drainage and high levels of nutrient pollution in Lake Loskop, South Africa. *Ecotox Environ Safe* 73: 326-335
- Payne RA (2000) *Spirulina* as bioremediation agent: Interaction with metals and involvement of carbonic anhydrase. M.Sc. thesis, Rhodes University

- Pitter P (2009) *Hydrochemie*. VŠCHT, Praha
- Regel RH, Ferris JM, Ganf GG, Brookes JD (2002) Algal esterase activity as a biomeasure of environmental degradation in a freshwater creek. *Aquat Toxicol* 59: 209-223
- Rose, PD, Boshoff GA, Van Hille RP, Wallace LC, Dunn KM, Duncun JR (1998) An integrated algal sulfate reducing high rate ponding process for the treatment of acid mine drainage wastewater. *Biodegradation* 9: 247-257
- Schultze M, Pokrandt KH, Hille W (2010) Pit lakes of the Central Germany lignite mining district: Creation, morphometry and water quality aspects. *Limnologica* 40: 148-155
- Skácelová O (2006) Cyanobacteria and algae inhabiting new biotops on spoil heaps (Sokolov coal-mining district). *Zprávy Čes Bot Společ* 41: 141-150
- Suggett DJ, Moore M, Geider RJ (2011) *Estimating aquatic productivity from active fluorescence measurement* in Suggett DJ, Prášil O, Borowitzka MA (eds.) *Chlorophyll a fluorescence in aquatic sciences: methods and applications*. Springer, pp. 104-127
- Steinberg CEW, Schäfer H, Beisker W (1998) Do Acid-tolerant Cyanobacteria exist? *Acta Hydrochim Hydrobiolog* 26: 13-19
- Tesařová B (2011) Photosynthetic characteristics of phytoplankton in eutrophic waters. Magister thesis, Charles University in Prague

5.7 Supplements

Table S5.1 The physio-chemical parameters of common surface waters and localities on spoil heaps.

	Common surface water ¹⁾	Eutrophic ponds ²⁾	Sokolov spoil heaps ³⁾	Permissible upper limits ¹⁾
pH	4.5 – 9.5 ⁴⁾	6.8 – 10.5	2.5 – 8.4	6.0 – 9.0
cond. (mS m ⁻¹)	5 – 50	11 – 44	202 – 1,400	160
Chl a (µg L ⁻¹)	2 – 40	2 – 524	0 – 23	10
Fe (mg L ⁻¹)	< 0.5	0.1 – 1.0	0.1 – 540	2.0
Mn (mg L ⁻¹)	0.01 – 0.14	0.02 – 0.21	0.05 – 25	0.50
As (µg L ⁻¹)	4 – 8	n.a.	15 – 23	50
Be (µg L ⁻¹)	0.2 – 1	n.a.	4 – 17	1
Al (µg L ⁻¹)	< 150	n.a.	29 – 705	200
Co (µg L ⁻¹)	0.1 – 3	n.a.	12 – 85	0.05
Ni (µg L ⁻¹)	< 20	n.a.	20 – 76	20
Zn (µg L ⁻¹)	5 – 200	0.02 – 0.09	10 – 295	0.2
sulphate (mg L ⁻¹)	70 – 120 ⁵⁾	0.1 – 56	101 – 9 300	300
chloride (mg L ⁻¹)	21 – 44 ⁵⁾	4 – 24	0.5 – 32	350
HCO ₃ ⁻ (mg L ⁻¹)	80 – 130	15 – 180	50 – 960	– ⁴⁾
NH ₄ -N (mg L ⁻¹)	< 1	0.01 – 2.57	0.01 – 3.10	2.5
NO ₂ -N (mg L ⁻¹)	0.1	0.01 – 0.24	0.01 – 0.09	0.05
NO ₃ -N (mg L ⁻¹)	4.5 – 10	0.01 – 2.59	0.02 – 2.57	11
PO ₄ -P (mg L ⁻¹)	0.03 – 0.30	0.01 – 0.26	0.01 – 0.19	0.40

¹⁾ after Pitter 2009

²⁾ minimum and maximum value from the survey of 50 ponds in Třeboň basin in June and July 2010 (Pechar, unpublished results)

³⁾ minimum and maximum value from analysis of studied spoil-heap localities in 2008-2011

⁴⁾ not established for drinking water

⁵⁾ the concentration in sea water: sulfate 2,700 mg L⁻¹, chloride 19 mg L⁻¹

Table S5.2 Summary of physical-chemical characteristics of studied spoil-heap localities sampled in 2008–2011. The average value ($n = 5 - 9$), the minimum and maximum value are shown here.

Locality	pH	Cond. mS m ⁻¹	Chl <i>a</i> µg L ⁻¹	NH ₄ -N mg L ⁻¹	NO ₂ -N mg L ⁻¹	NO ₃ -N mg L ⁻¹	TN mg L ⁻¹	PO ₄ -P mg L ⁻¹	TP mg L ⁻¹
Červená Ema	3.11	563	4.2	0.987	0.027	0.059	4.827	0.029	0.371
	2.69	357	0.8	0.514	0.003	0.017	0.952	0.015	0.073
	3.57	679	10.5	1.880	0.090	0.170	16.071	0.058	1.043
Eva	7.06	542	11.7	0.023	0.005	0.114	0.620	0.009	0.062
	6.95	527	3.2	0.002	0.002	0.042	0.589	0.004	0.059
	7.18	563	20.2	0.033	0.007	0.175	0.652	0.013	0.065
Lítov M1	2.72	307	9.3	1.141	0.095	0.098	2.593	0.011	0.377
	2.53	252	1.4	0.754	0.022	0.048	1.008	0.005	0.063
	2.99	364	23.1	1.504	0.567	0.214	8.536	0.024	1.287
Lítov M4	3.0	295	5.7	0.880	0.015	0.084	2.520	0.010	0.200
	2.7	202	2.0	0.008	0.004	0.020	1.203	0.006	0.037
	3.2	379	9.6	1.680	0.035	0.227	5.962	0.013	0.664
Lomnice- retention	2.98	294	-	1.546	0.035	0.288	2.252	0.037	0.074
	2.74	242	-	0.710	0.009	0.080	1.711	0.019	0.061
	3.15	326	-	1.940	0.071	0.630	2.990	0.053	0.098
Muší	8.18	1053	8.4	0.029	0.028	0.734	2.100	0.019	0.062
	7.63	510	1.9	0.002	0.005	0.044	1.101	0.001	0.008
	8.44	1400	19.6	0.077	0.066	2.568	3.813	0.035	0.084

Table S5.2 (continued)

Locality	Na mg L ⁻¹	K mg L ⁻¹	Mg mg L ⁻¹	Ca mg L ⁻¹	Fe mg L ⁻¹	Mn mg L ⁻¹	Zn mg L ⁻¹	HCO ₃ ⁻ mg L ⁻¹	SO ₄ ²⁻ mg L ⁻¹	Cl ⁻ mg L ⁻¹
Červená	475	23	330	300	316.9	20.2	0.5	0	4491.6	0.8
Ema	383	19	93	152	208.9	16.7	0.4	0	3057.8	0.5
	631	29	511	440	538.5	25.3	0.7	0	6954.8	1.0
Eva	481	18	302	290	16.9	3.1	0.3	914	3211.3	3.1
	149	9	232	75	0.2	0.1	0.0	887	2310.3	2.4
	614	23	370	416	48.6	9.4	1.1	933	3998.6	4.1
Lítov M1	22	3	124	119	85.6	13.4	1.7	0	2294.3	3.8
	12	2	92	59	0.7	8.2	1.0	0	1246.9	1.6
	31	4	174	206	145.1	19.7	2.4	0	4211.8	17.7
Lítov M4	70	10	208	122	50.1	12.1	1.4	0	1902.3	3.2
	51	6	130	91	15.0	8.0	0.7	0	898.1	1.7
	101	15	280	177	118.2	17.2	2.1	0	3581.3	7.6
Lomnice- retention	226	8	236	93	72.1	6.1	1.2	0	1750.0	11.6
	145	8	170	64	54.0	0.1	1.10	0	1510.0	7.6
	388	10	268	109	87.5	8.8	1.28	0	2070.0	13.9
Muší	2025	38	271	344	1.2	0.1	0.1	732	6546.7	1.0
	640	11	44	60	0.2	0.0	0.0	353	2295.0	0.0
	2671	63	834	651	3.2	0.3	0.1	958	9335.8	1.5

Table S5.3 The averaged physio-chemical characteristics of Lake Medard in years 2009-2011 (date of sampling: September 2009, July 2010, July 2011). Two water layers formed in the lake: the upper part: 0 – 10 m (in 2009), 0 – 15 m (in 2010, and 2011) and the bottom layer located 0 – 10 m above the bottom of the lake.

Layers	pH	Cond. mS m ⁻¹	Chl a µg L ⁻¹	SO ₄ ²⁻ g L ⁻¹	Cl ⁻ mg L ⁻¹	HCO ₃ ⁻ mg L ⁻¹	NH ₄ -N mg L ⁻¹	NO ₂ -N mg L ⁻¹	NO ₃ -N mg L ⁻¹	PO ₄ -P mg L ⁻¹	TN mg L ⁻¹	TP mg L ⁻¹
upper	7.01	225	1.5	1509	19	58	0.359	0.010	0.850	0.016	0.008	0.024
	6.62	149	1.0	1039	14	51	0.104	0.004	0.511	0.007	0.001	0.016
	7.49	264	1.8	2225	26	62	0.634	0.017	1.700	0.040	0.017	0.040
lower	6.49	352	1.6	2136	16	66	1.251	0.004	0.442	0.010	0.007	0.021
	5.92	255	0.2	1120	8	51	0.122	0.001	0.000	0.007	0.003	0.016
	6.78	530	4.4	3125	32	92	3.097	0.010	0.881	0.020	0.019	0.034

Table S5.3 (continued)

Layers	Na mg L ⁻¹	K mg L ⁻¹	Ca mg L ⁻¹	Mg mg L ⁻¹	Fe mg L ⁻¹	Mn mg L ⁻¹	As µg L ⁻¹	Be µg L ⁻¹	Al µg L ⁻¹	Co µg L ⁻¹	Ni µg L ⁻¹	Zn µg L ⁻¹
upper	218	10	226	83	0.24	1.37	<0.002	0.001	0.113	0.026	0.037	0.060
	119	8	146	55	0.11	0.84	<0.002	0.001	0.044	0.012	0.020	0.039
	269	11	256	94	0.36	2.04	<0.002	0.002	0.177	0.047	0.053	0.092
lower	521	13	323	117	22.47	2.48	0.019	0.006	0.251	0.086	0.058	0.127
	263	11	252	80	0.28	1.02	0.015	0.001	0.029	0.019	0.038	0.034
	755	16	446	169	54.00	3.39	0.023	0.017	0.705	0.185	0.076	0.295

6. Thesis Summary

This thesis deals with the distribution and physiological state of phototrophic extremophilic organisms in saline, alkalic, acidic, and polar environments along with the effect of raised temperature on photosynthetic apparatus.

The anoxygenic phototrophic bacteria were found in saline (salinity up to 300 g L⁻¹), alkalic (up to the pH of 10.4), and cold (with the lowest temperature of 5°C) lakes. Their abundance positively correlated with the concentration of chlorophyll *a* in highly mineralized steppe lakes, whereas in polar lakes, their presence was driven by temperature, total nitrogen, and chlorophyll *a* amount. They were abundant in both saline and alkalic environments. Unlike mineralization, low temperature seemed to limit the growth of (aerobic) anoxygenic bacteria in these environments.

Thermal adaptation of reaction centers was investigated in psychrophilic, mesophilic and thermophilic anoxygenic phototrophic bacteria. The anoxygenic reaction centers were stable and functional far above optimal growth conditions of studied strains. At elevated temperatures, the purple bacterial reaction center seemed to be stabilized by the tight packing of the transmembrane helices of L a M protein subunits. The observed thermal stability of the reaction centers may indicate that the early purple phototrophic bacteria evolved in a warmer-than-today environments.

Finally, a response of cyanobacterial cultures to post-mining waters was investigated in laboratory experiments. Photosystem II of the *Microcystis* and *Anabaena* strains were negatively influenced by a pH lower than 4 and 3.5 resp. The high concentration of dissolved ions did not affect the photosystem II function. However, the response of cyanobacteria was species-specific and the current characteristics of discharged post-mining waters differed from common central-european surface waters may not prevent the cyanobacterial bloom in newly formed water bodies.

Curriculum vitae

Mgr. Hana Medová

Address Institute of Microbiology AS CR, Opatovický mlýn, CZ-379 01 Třeboň, CR
E-mail hanka-medova@email.cz, medova@alga.cz
Mobile +420 606 458 523
Date of birth 3rd September 1982
Place of birth Sokolov, Czech Republic

Areas of competence

aquatic microbial ecology, microbial cultivation, water quality monitoring

Education

2007-2013 Ph.D. studies in Biophysics, Faculty of Science, University of South Bohemia in České Budějovice, Czech Republic
2002-2007 Master studies in inorganic chemistry, Department of Inorganic Chemistry, Faculty of Science, Charles University in Prague, Czech Republic

Professional experience

since 2007 Laboratory of Photosynthesis, Institute of Microbiology in Třeboň, Academy of Science, Czech Republic
2012 research assistant, University of Otago, Dunedin, New Zealand
2007-2012 Laboratory of ENKI, pbc., Třeboň, Czech Republic
July 2011 Field course of Polar Ecology, Svalbard, Spitsbegren
2003-2007 Laboratory of prof. Ivan Lukeš, Csc., Faculty of Science of Charles University in Prague, Czech Republic
2006 Laboratory of DKFZ (German Cancer Research Centrum) in Heidelberg, Germany

Publications

Prášil O, Bina D, Medová H, Řeháková K, Zapomělová E, Veselá J & Oren A (2009) Emission spectroscopy and kinetic fluorometry studies of phototrophic microbial communities along a salinity gradient in solar saltern evaporation ponds of Eilat, Israel. *AME*, 56(2): 285-296

Řeháková K, Zapomělová E, Prášil O, Veselá J, Medová H & Oren A (2009) Composition changes of phototrophic microbial communities along the salinity gradient in the solar saltern evaporation ponds of Eilat, Israel. *Hydrobiologica*, 636(1): 77-88

Suggett DJ, Stambler N, Prášil O, Kolber Z, Quigg A, Vázquez-Dominguez E, Zohary T, Berman T, Iluz D, Levitan O, Lawson T, Meeder E, Lazar B, Bar-Zeev E, Medová H, Bermann-Frank I (2009) Nitrogen and phosphorus limitation of oceanic microbial growth during spring in the Gulf of Aqaba. *Aquat Microbial Ecol* 56: 227-239

Medová H, Boldareva EN, Hrouzek P, Borzenko SV, Namsaraev ZB, Gorlenko VM, Namsaraev BB & Koblížek M (2011) High abundance of aerobic anoxygenic phototrophs in saline steppe lakes. *FEMS*, 76(2): 393-400

Medová H (2012) Kam v Čechách za extrémofilními řasami a sinicemi. *Vesmír*, 91: 229 (a scientific popularization article in Czech)

Publications in manuscript

Lew S, Koblížek M, Medová H, Owsiany P Seasonal changes of microbial communities in two shallow peat-bog lakes. *in preparation*

Medová H, Dulebo A, Boldareva EN, Kaftan D & Koblížek M (2012) The thermal stability of purple bacterial reaction centers. *in preparation*

Medová H, Příklad I & Pechar L (2012) Effect of post-mining waters on cyanobacterial photosynthesis. *Water Environ Res*, submitted

Conference presentations

- | | |
|---------------------|--|
| oral presentation | ASLO 2011 in San Juan, Puerto Rico
SAME12 2011 in Rostock, Germany
AAP workshop 2010 in Třeboň, Czech Republic
Limnological conference 2009, Třeboň, Czech Republic |
| poster presentation | ASLO 2009 in Nice, France
BioMicroWorld09 in Lisboa, Portugal |
| participation | conference of NZ Freshwater Science Society 2012, Dunedin, New Zealand
GAP workshop 2008 in Eilat, Israel |

© for non-published parts Hana Medová
hanka-medova@email.cz

Phototrophic microorganisms in extreme environments
Ph.D. Thesis Series, 2013, No. 1

All rights reserved
For non-commercial use only

Printed in the Czech Republic by Vlastimil Johanus
Edition of 20 copies

University of South Bohemia in České Budějovice
Faculty of Science
Branišovská 31
CZ-37005 České Budějovice, Czech Republic
Phone: +420 387 772 244
www.prf.jcu.cz, e-mail: sekret@prf.jcu.cz